UNIVERSITY OF CALIFORNIA SAN DIEGO

SAN DIEGO STATE UNIVERSITY

Cardiomyocyte Cell Cycle Revealed by FUCCI

A dissertation submitted in partial satisfaction of the requirements for the degree
Doctor of Philosophy

in

Biology

by

Roberto Alvarez Jr

Committee in charge:

University of California San Diego

Professor Asa Gustafsson
Professor Randall Hampton

San Diego State University

Professor Mark A. Sussman, Chair
Professor Roland Wolkowicz
Professor Robert Zeller

2018

The Dissertation of Roberto Alvarez Jr is approved, and it is acceptable in quality and form for publication on microfilm and electronically:

Chair

University of California San Diego

San Diego State University

2018

DEDICATION

I would like to dedicate this work to my family. My wife, Gabriela, for her continued support and gentle but firm coaxing throughout this journey. My two beautiful children, Sofia and Perla, I am thankful every day for the opportunity to be your father and a good role model. My parents, Roberto and Maria, they gave me a strong foundation from which to build upon, and my siblings; Meme, Hil, Q, Jaime and Al, for showing me the meaning of teamwork and the importance of surrounding yourself with people who push you to be better. It is because of their teachings that I persist. Thank you for being in my life.

TABLE OF CONTENTS

LIST OF ABBREVIATIONS

AKT	Protein Kinase B
αMHC	alpha myosin heavy chain
αSA	alpha sarcomeric actinin
ACM	adult cardiomyocyte
AzGr	azami green
BrdU	5'-bromo-deoxy-uridine
BZ	border zone
kit	tyrosine-protein kinase Kit or CD117
Cdk	cyclin dependent kinase
CM	cardiomyocyte
CPC	cardiac progenitor cell
cTnT	cardiac troponin T
cTnI	cardiac troponin I
dpc	days post coitum
dpi	days post injury
E2F	transcription factor
FUCCI	Fluorescent Ubiquitination-based Cell Cycle Indicators
FBS	fetal bovine serum
FVB/NJ	Friend leukemia virus B Strain
G1	Gap 1 (G1-phase)

G2	Gap 2 (G2-phase)
HRP	horse radish peroxidase
HS	horse serum
hCdt1	human Cdt1
hGem	human Geminin
IGF-1	Insulin growth factor 1
Iso	Isoproterenol
IZ	infarct zone
M	Mitosis (M-phase)
MI	myocardial injury
mKO	monomeric Kusabira Orange 2
P	postnatal day
PCR	polymerase chain reaction
pHH3	phosphorylated Histone H3
PIM1	proviral integration site Maloney leukemia virus
Rb	retinoblastoma
RZ	remote zone
S	Synthesis phase (S-phase)
SA-X	streptavidin (X= LS490, 700, etc.)
sm22α	smooth muscle 22 alpha
SMA	smooth muscle actin
TERT	Telomerase reverse transcriptase
Tyr	tyramide

Vinc	vinculin
vWF	von Wilebrand Factor
WGA	wheat germ agglutin
YAP1	Yes-associated protein-1

LIST OF FIGURES

LIST OF TABLES

ACKNOWLEDGEMENTS

First and foremost, I would like to acknowledge my mentor, Dr. Mark A. Sussman, for his continued support and guidance. The environment he has created in his lab has allowed me grow as a scientist. I am grateful for the opportunity provided me under his tutelage.

I would like to thank my committee members, Dr. Asa Gustafsson, Dr. Randy Hampton, Dr. Robert Zeller and Dr. Roland Wolkowicz. Their guidance, invaluable input, and expertise is greatly appreciated. I am honored to have them as part of my committee.

To all the lab personnel I have encountered along this journey, thank you for allowing me to be part of your group and thank you for the great conversations. Without your expertise and personalities, I would not have survived the long hours in lab. Dr. Natalie Gude, thank you for being my sounding board, I am forever indebted to you for your wisdom and your belief in me. Wang Nai-nai, thank you for all your help!

Chapter 2, in full, is prepared for submission. I would like to thank all the co-authors who contributed to this work; Bingyan J. Wang, Natalie Gude, Fareheh Firouzi, David Ebeid, and Mark Sussman. Thank you all for your participation. The dissertation author was the primary author and investigator of this manuscript.

VITA

1999	Bachelor of Science, Illinois Institute of Technology
2000-2001	Atomic Spectrophotometry Tech, Graphite Company
2001-2005	Research Associate, Transgenic and Targeted Mutagenesis Lab, Northwestern University, School of Medicine
2005-2018	Mouse Genomics Specialist II, Department of Biology, San Diego State University
2018	Doctor of Philosophy, University of California San Diego and San Diego State University

PUBLICATIONS

Alvarez Jr R, Wang BJ, Gude N, Farouzi F, Ebeid D, and Sussman MA. Title: TBD. (Prepared for submission, 2018)

Gude NA, Firouzi F, Broughton KM, Ilves K, Nguyen KP, Panye CR, Sacchi V, Monsanto MM, Casillas AR, Khalafalla FG, Wang BJ, Edeid D, **Alvarez R**, Dembitsky WP, Bailey BA, Berlo JH, Sussman MA. Cardiac c-Kit Biology Revealed by Inducible Transgenesis. (2018) Circulation Research. DOI: 10.1161/CIRCRESAHA.117.311828

Sacchi V, Wang BJ, Kubli D, Martinez AS, Jin JK, **Alvarez R Jr**, Hariharan N, Glembotski C, Uchida T, Malter JS, Yang Y, Gross P, Zhang C, Houser S, Rota M, Sussman MA. Peptidyl-Prolyl Isomerase 1 Regulates Ca_{2+} Handling by Modulating Sarco(Endo)Plasmic Reticulum Calcium ATPase and Na_{2+}/Ca_{2+} Exchanger 1 Protein Levels and Function. (2017) Journal of the American Heart Association. DOI: 10.1161/JAHA.117.006837

Khalafalla FG, Kayani W, Kassab A, Ilves K, Monsanto MM, **Alvarez R Jr**, Chavarria M, Norman B, Dembitsky WP, Sussman MA. Empowering human cardiac progenitor cells by $P2Y_{14}$ nucleotide receptor overexpression. (2017) J Physiol. DOI: 10.1113/JP274980

Khalafalla FG, Greene S, Khan H, Ilves K, Monsanto MM, **Alvarez R Jr**, Chavarria M, Nguyen J, Norman B, Dembitsky WP, Sussman MA. $P2Y_2$ Nucleotide Receptor Prompts Human Cardiac Progenitor Cell Activation by Modulating Hippo Signaling. (2017) Circ Res. DOI: 10.1161/CIRCRESAHA.117.310812

Liu N, Wang BJ, Broughton KM, **Alvarez R**, Siddiqi S, Loaiza R, Nguyen N, Quijada P, Gude N, Sussman MA. PIM1-minicircle as a therapeutic treatment for myocardial infarction. (2017) PLoS One. DOI: 10.1371/journal.pone.0173963.

Gude N, Joyo E, Toko H, Quijada P, Villanueva M, Hariharan N, Sacchi V, Truffa S, Joyo A, Voelkers M, **Alvarez R**, Sussman MA. Notch activation enhances lineage commitment and protective signaling in cardiac progenitor cells. (2015) Basic Res Cardiol. DOI: 10.1007/s00395-015-0488-3.

Quijada P, Salunga HT, Hariharan N, Cubillo JD, El-Sayed FG, Moshref M, Bala KM, Emathinger JM, Torre ADL, Ormachea L, **Alvarez Jr R**, Gude NA, Sussman MA. Cardiac Stem Cell Hybrids Enhance Myocardial Repair. (2015) DOI: 10.1161/CIRCRESAHA.115.306838 1

Wade F, Quijada P, Al-Haffar MKA, Awad SM, Kunhi M, Toko H, Marashly Q, Belhaj K, Zahid E, Al-Mohanna F, Stanford SM, **Alvarez R**, Liu Y, Colak D, Jordan MC, Roos KP, Assiri A, Al-Habeeb W, Sussman M, Bottini N and Poizat C. Deletion of Low Molecular Weight Protein Tyrosine Phosphatase (Acp1) Protects Against Stress-Induced Cardiomyopathy. (2015) Journal of Pathology. Jul 25. doi: 10.1002/path.4594

Samse K, Emathinger J, Hariharan N, Quijada P, Ilves K, Völkers M, Ormachea L, Torre ADL, Orogo A, **Alvarez R**, Din S, Mohsin S, Monsanto M, Fischer K, Dembitsky W, Gustafsson A, Sussman M. Functional Effect of Pim1 Depends upon Intracellular Localization in Human Cardiac Progenitor Cells. (2015) Journal of Biological Chemistry. May 29;290(22):13935-47.

Makau F, Morsi K, Gude N, **Alvarez R**, Sussman M and May-Newman KD. Viability of Titanium-Titanium Boride Composite as a Biomaterial. (2013) ISRN Biomaterials.

Khan M, Mohsin S, Avitabile D, Siddiqi S, Nguyen J, Wallach K, Quijada P, McGregor M, Gude N, **Alvarez R**, Tilley DG, Koch WJ, Sussman MA. β-Adrenergic regulation of cardiac progenitor cell death versus survival and proliferation. (2013) Circulation Research. Feb 1;112(3):476-86.

Bailey B, Fransioli J, Gude NA, **Alvarez Jr R**, Zhang X, Gustafsson AB, Sussman MA. Sca-1 knockout impairs myocardial and cardiac progenitor cell function. (2012) Circulation Research. Aug 31;111(6):750-60.

Sussman M, **Alvarez R**, Völkers M, Fischer K, Bailey B, Cottage CT, Din S, Gude N, Avitabile D, Sundararaman B, Quijada P, Mason M, Konstandin MH, Malhowski A, Cheng Z, Khan M, McGregor M. Myocardial AKT: the omnipresent nexus. (2011) Physiolical Reviews. July;91(3):1023-70.

Avitabile D, Bailey B, Cottage CT, Sundararaman B, Joyo A, McGregor M, Gude N, Truffa S, Zarrabi A, Konstandin M, Khan M, Mohsin S, Völkers M, Toko H, Mason M,

Cheng Z, Din S, **Alvarez Jr R**, Fischer K, Sussman MA. Nucleolar stress is an early response to myocardial damage involving nucleolar proteins nucleostemin and nucleophosmin. (2011) Proceedings of the National Academy of Sciences, U S A. April 12;108(15):6145-50.

Cheng Z, Völkers M, Din S, Avitabile D, Khan M, Gude N, Mohsin S, Bo T, Truffa S, **Alvarez R**, Mason M, Fischer KM, Konstandin MH, Zhang XK, Heller-Brown J, Sussman MA. Mitochondrial translocation of Nur77 mediates cardiomyocyte apoptosis. (2011) European Heart Journal. Jan 12.

Borillo GA, Mason M, Quijada P, Völkers M, Cottage C, McGregor M, Din S, Fischer K, Gude N, Avitabile D, Barlow S, **Alvarez R**, Truffa S, Whittaker R, Glassy MS, Gustafsson AB, Miyamoto S, Glembotski CC, Gottlieb RA, Heller-Brown J, Sussman MA. Pim-1 kinase protects mitochondrial integrity in cardiomyocytes. (2010) Circulation Research. April 16;106(7):1265-74.

Cottage CT, Bailey B, Fischer KM, Avitable D, Collins B, Tuck S, Quijada P, Gude N, **Alvarez R**, Muraski J, Sussman MA. Cardiac progenitor cell cycling stimulated by pim-1 kinase. (2010) Circulation Research, Mar 19;106(5):891-901.

Bailey B, Izarra A, **Alvarez R**, Fischer KM, Cottage CT, Quijada P, Díez-Juan A, Sussman MA. Cardiac stem cell genetic engineering using the alphaMHC promoter. (2009) Regenerative Medicine. 2009 Nov;4(6):823-33.

Muraski JA, Fischer KM, Wu W, Cottage CT, Quijada P, Mason M, Din S, Gude N, **Alvarez, Jr R**, Rota M, Kajstura J, Wang Z, Schaefer E, Chen X, MacDonnel S, Magnuson N, Houser SR, Anversa P, and Sussman MA**.** Pim-1 kinase antagonizes aspects of myocardial hypertrophy and compensation to pathological pressure overload. (2008) Proceedings of the National Academy of Sciences, Vol 105, pp. 13889-13894.

Gude NA, Emmanuel G, Wu W, Cottage CT, Fischer K, Quijada P, Muraski JA, **Alvarez R**, Rubio M, Schaefer E, Sussman MA. Activation of notch-mediated protective signaling in the myocardium. (2008) Circulation Research, Vol 102, pp. 1025-1035.

Fransioli J, Bailey B, Gude NA, Cottage CT, Muraski JA, Emmanuel G, Wu W, **Alvarez R**, Rubio M, Ottolenghi S, Schaefer E, Sussman MA. Evolution of the c-kit-positive cell response to pathological challenge in the myocardium. (2008) Stem Cells Vol. 26, pp. 1315-1324.

Muraski JA, Rota M, Misao Y, Fransioli J, Cottage C, Gude N, Esposito G, Delucchi F, Arcarese M, **Alvarez R**, Siddiqi S, Emmanuel GN, Wu W, Fischer K, Martindale JJ, Glembotski CC, Leri A, Kajstura J, Magnuson N, Berns A, Beretta RM, Houser SR,

Schaefer EM, Anversa P & Sussman MA. Pim-1 regulates cardiomyocyte survival downstream of Akt. (2007) Nature Medicine, Vol. 13, pp. 1467-1475.

Rota M, Kajstura J, Hosoda T, Bearzi C, Vitale S, Esposito G, Iaffaldano G, Padin-Iruegas ME, Gonzalez A, Rizzi R, Small N, Muraski J, **Alvarez R**, Chen X, Urbanek K, Bolli R, Houser SR, Leri A, Sussman MA, and Anversa P. Bone marrow cells adopt the cardiomyogenic fate in vivo. (2007) Proceedings of the National Academy of Sciences, Vol 104, pp. 17783-17788.

PROFESSIONAL PRESENTATIONS

Poster: Emerging Molecular and Cellular Insights into Heart Failure and Arrhythmias – The 13th La Jolla-International Cardiovascular Research Conference. La Jolla, California. 03/2011.

Poster: Basic Cardiovascular Sciences 2017 Scientific Sessions – American Heart Association. Portland, Oregon. 06/2017.

Poster: Alternative Muscle Club 5th Annual Meeting – University of California San Diego. La Jolla, California. 09/2017.

Poster: American Heart Association's Scientific Sessions 2017. Anaheim, California. 11/2017.

Poster: International Society for Heart Research 2018-North American Session. Halifax, Nova Scotia, Canada. 05/2018

ABSTRACT OF THE DISSERTATION

Cardiomyocyte Cell Cycle Revealed by FUCCI

by

Roberto Alvarez Jr

University of California San Diego, 2018

San Diego State University, 2018

Professor Mark A. Sussman, Chair

Rationale: Pre-existing cardiomyocytes and resident cardiac stem cells are limited in their capacity for substantial regeneration in postnatal endogenous mammalian myocardial repair. Evidence for adult cardiomyocyte proliferation remains inconclusive,

relying on proliferation markers that also present in hypertrophy or DNA repair. Unambiguous identification of myocyte cell cycle activity to demarcate *de novo* cardiomyogenesis within the injured myocardium has not been achieved using traditional markers of cellular proliferation. A powerful tool, Fluorescence Ubiquitination-based Cell Cycle Indicators (FUCCI) reporter system utilized to examine dynamic oscillations between G1 and S/G2/M phases of the cell cycle has yet to be exploited in a cardiomyocyte specific fashion. Targeted myocardial expression of FUCCI has the potential to delineate cardiomyocyte cell cycle entry and completion during postnatal development and following pathologic challenge.

Objective: Authenticate fidelity of proliferative markers as indicators of *de novo* cardiomyogenesis and subsequently delineate the post-mitotic status of postnatal cardiomyocytes.

Methods and Results: Cardiomyocyte specific FUCCI expression driven by the α-myosin heavy chain (αMHC) promoter was utilized in conjunction with traditional proliferation markers to identify cell cycle status of postnatal murine cardiomyocytes. Cardiomyocyte proliferation rapidly decreased after birth, with cell cycle arrest corresponding to G1/S rather than full mitotic exit at G0. Interestingly, cell cycle activity increased in cardiomyocytes of sham injured hearts, potentially in response to systemic insult. Proliferation markers commonly utilized to ascertain *de novo* cardiomyocyte formation failed to fully correspond with FUCCI cell cycle activity in

injured αMHC-FUCCI hearts. Moreover, rare cKit^{+} amplifying progenitors identified in early postnatal development confirmed contribution to cardiomyogenesis.

Conclusions: Proliferation markers used to identify *de novo* cardiomyogenesis failed to distinguish cycling cardiomyocytes after injury. Adult cardiomyocytes upregulated cell cycle activity in response to sham injury but failed to complete regenerative proliferation following cell cycle reentry. αMHC-FUCCI elucidated post-mitotic cardiomyocyte arrest at G1/S as opposed to G0 cell cycle exit previously reported in the literature. Finally, αMHC-FUCCI revealed cardiac progenitor cells remain a possible source of neonatal cardiomyogenesis within the myocardium.

CHAPTER 1

INTRODUCTION OF THE DISSERTATION

Cardiovascular Disease

Cardiovascular disease (CVD) is the leading cause of death in the world with origins ranging from genetics, ethnicity and age to lifestyle choices[1]. An average of 1 in 3 deaths in the US is attributed to CVD every year[1, 2]. The most prevalent form of coronary artery disease is myocardial infarction, commonly known as a heart attack, and accounts for over 45% of all CVD deaths affecting almost 800,000 people yearly[2]. A heart attack results from blockage of blood flow through the coronary artery that supplies nutrients and oxygen to the cells responsible for generating the contractile force necessary to pump blood throughout the body, resulting in death to the myocardial tissue directly distal to the blockage. The damage caused by heart attacks results in scar formation and a less efficient pump. Research efforts in the last decade have focused on stem cell-mediated and existing cardiomyocyte-induced regeneration to the area of damage in an effort to improve remodeling after a heart attack[3-8]. Ongoing debate persists regarding the extent of existing cardiomyocyte contribution to *de novo* cardiac formation following injury, in part due to the difficulty of assessing surviving cardiomyocyte contribution to *de novo* formation. Mature cardiomyocytes have been reported to fully exit the cell cycle within the first two weeks of birth in the mouse myocardium into a post-mitotic configuration incapable of cellular replication[9, 10]. The overall post-mitotic status of the myocardium renders *de novo* myocyte formation after injury from surviving cardiomyocytes a challenging endeavor. Current markers utilized to identify proliferating myocytes in a post-injury model can also mark cellular states such as hypertrophy or DNA repair that do not involve the formation of two daughter cells necessary to replace damaged or dead cardiomyocytes, diminishing their validity

and specificity as stand-alone markers of *de novo* cardiomyocyte formation[11-13]. Given these deficiencies, new tools to verify cellular proliferation are necessary to 1) validate current markers of cardiomyocyte cell cycle status and 2) accurately evaluate pre-existing, post-mitotic cardiomyocyte ability to reenter the cell cycle and contribute to *de novo* myocardial formation.

The post mitotic heart

The heart is traditionally considered a post-mitotic organ unable to replace damaged myocardium due to its remarkable resilience to proliferative stimuli and loss of myocyte cell division shortly after birth. Cardiomyocyte proliferation peaks between embryonic stage E10-12 and decreases sharply before birth in mice[9, 14, 15]. Estimates of myocyte turnover in the adult mammalian myocardium range from less than 1% up to 40% annually, dependent on calculation methods utilized[3, 15-19]. Variability in these published studies highlight the methodological challenge associated with studying proliferation in a heterogeneous, largely non-proliferative cell population. Furthermore, experiments utilizing tritiated (^{3}H) thymidine show only a 0.005% incidence of DNA synthesis during postnatal development that remain stable after induced injury[15]. These results demonstrate the intrinsic proliferative capacity in the mouse myocardium to be quite rare. Attempts to force myocyte cell cycle re-entry by cardiomyocyte directed overexpression of pro-proliferative mitotic and oncogenic proteins such as AKT, c-Myc, IGF and TERT fail to induce robust, sustained reentry into the cell cycle resulting in proliferation[6, 8, 20-22]. Cardiomyocyte specific overexpression of cell cycle genes is similarly unsuccessful in progressing cardiomyocytes through a full cell cycle event[5, 23, 24].

Eukaryotic Cell Cycle

Deciphering the cellular mechanisms inhibiting post-mitotic cardiomyocyte proliferation require fundamental understanding of the eukaryotic cell cycle of somatic cells. The cell cycle is a tightly orchestrated sequence of events that involve a multitude of proteins necessary to advance cells through a series of checkpoints spanning four distinct phases: Gap 1 (G1), Synthesis (S), Gap 2 (G2) and Mitosis (M). The resting phase of G1 is necessary for cell growth prior to initiation of cellular division. Cell size and content in the form of organelles and cytoplasm determine if a cell will divide or enter into a state of quiescence termed G0[23, 25, 26]. Once cells commit to cell cycle entry, duplication of cellular chromatin occurs in S-phase. The cellular decision to proceed to the next phase of the cell cycle is made based on final DNA integrity during the G2 checkpoint in the cell cycle where newly synthesized DNA is monitored for aberrations and repaired if necessary[26, 27]. Intact DNA integrity initiates M, the nuclear/cell division phase, typically resulting in the production of two daughter cells. Key regulators of the different phases of the cell cycle include, Cyclins D, E, A and B, cyclin dependent serine-threonine kinases (CDKs) 2, 4/6, 1 as illustrated in **Figure 1.1**, and cyclin dependent kinase inhibitors (CdkIs) p21, p27 and p16[26, 28, 29].

Cyclin D is expressed during G1 in response to cell growth stimuli[25, 30-32]. Binding of Cyclin D to Cdk4/6 drives partial phosphorylation of the retinoblastoma protein (Rb), a cell cycle repressor at the G1 checkpoint[25, 26, 30, 31, 33]. Partial phosphorylation of Rb by the CyclinD-Cdk4/6 complex results in release of the early transcription factor (E2F), necessary for production of Cyclin E; required for transition from G1 into S phase of the

cell cycle.[31, 34-36]. Cyclin E binds its catalytic partner Cdk2, the Cyclin E-Cdk2 complex further phosphorylates Rb and renders the hyper-phosphorylated form of Rb inactive for the remainder of the cell cycle[34, 35, 37]. In addition to freeing E2F for transcriptional activity, Cyclin E-Cdk2 complex initiates the pre-replication complex necessary for S-phase. Furthermore, this cyclin-cdk complex phosphorylates Cdk inhibitors p21 and p27 and marks them for degradation via the ubiquitin-proteasome system[36, 37]. E2F activity and p27 degradation allow for the upregulation of Cyclin A which binds cdk2 to form the CyclinA-Cdk2 complex to initiate DNA synthesis[27]. At the onset of S phase, competitive binding of Cyclin A to Cdk2 terminates the formation of pre-replication complexes[27, 38, 39]. Once threshold levels of cyclin A-Cdk2 necessary for DNA synthesis are reached, the cell begins the arduous process to make a duplicate copy of its chromatin[24, 27]. As S phase progresses, cyclin A binds Cdk1 to allow transition from S to G2 phase of the cell cycle[27, 38]. If DNA is damaged beyond repair in G2 the cell cycle can arrest and result in cellular senescence[40]. The G2/M checkpoint permits accumulation of the CyclinB-Cdk1 complex in the cytoplasm where it plays a role in reorganization of cellular contents[38, 39]. Inactive CyclinB-Cdk1 shuttled to the nucleus during G2 is exported immediately however, activation of the nuclear CyclinB-Cdk1 complex by Cdc25 phosphatases initiate M followed by breakdown of the nuclear envelope[38, 39]. Toward the end of M-phase, the remaining cyclins (A and B) are degraded by the anaphase promoting complex/cyclosome (APC/C) and cells undergo cytokinesis to produce two daughter cells, complete the current cycle and prepare for the next round of cellular division. Unlike most proliferative eukaryotic cells, cardiomyocytes may deviate from the canonical sequence of cell cycle events during postnatal maturation.

Cardiac Myocyte Cell Cycle

Most proliferative cells adhere to the canonical cell cycle, however post-mitotic cardiac myocytes exhibit atypical cellular features. The complex structure, multiple nuclei and a "tetraploid checkpoint" characteristic of adult cardiomyocytes render standard cell cycle analysis insufficient to address questions of cardiac myocyte proliferation[40]. For example, myocytes are proliferative during embryonic gestation when the number of cells dictate the size of the heart[40, 41]. The number of proliferative myocytes quickly diminish shortly after birth, and proliferative capacity is thought to be abolished by postnatal day 7, hence the term, "terminally differentiated" used to identify non-proliferative cells within an organ. Proliferation of adult mammalian cardiomyocytes has been postulated based on the ability of adult cardiac myocytes to re-enter the cell cycle and regenerate myocardium in zebrafish and other non-mammalian vertebrates[42]. Subsequent studies to analyze the proliferative capacity of P1-P7 neonatal mouse cardiac myocytes after cardiac cryo-injury, infarction and apical resection demonstrate reparative capacity similar to adult zebrafish[41, 43-47]. These reports of proliferation in neonatal and non-mammalian adult cardiomyocyte reports have sparked a frenzy of studies revisiting myocyte proliferation in the adult mammalian heart as a possible mechanism for cardiac repair[48-50]. As a result, and in conjunction with recent disclaimers against the reparative capacity of resident cardiac stem cells, it has been postulated that only existing myocytes give rise to new myocytes after acute injury. Approaches to measure cardiomyocyte proliferation utilized in the past have resurfaced and are being applied to demonstrate *de novo* cardiomyocyte formation. Defining new myocyte formation with markers of proliferation such as nuclear antigen Ki67, proliferating cell

nuclear antigen (PCNA), bromo-deoxy uridine (BrdU), and phosphorylated histone H3 (pHH3) has become a benchmark in this regard[3, 5, 8, 9, 48-52]. Studies show incorporation of one or two proliferative markers and claim unequivocal *de novo* adult cardiomyocyte formation. However, these same markers have been shown to be upregulated in response to injury or stress and call into question conclusions that post-mitotic cardiomyocytes actually undergo cell division.

Proliferative Markers in Response to Injury

Markers of proliferation include Ki67, PCNA, BrdU, pHH3 along with Aurora Kinase B (Aurora B) and Anillin have been successfully utilized to accurately identify proliferation events during canonical cell cycle activity due to their established presence in specific cell cycle phases[46, 53] **(Figure 1.2)**. Recent studies employ a combination of these markers as unequivocal identifiers of proliferation and *de novo* cardiac formation in the post-mitotic heart following injury[54, 55]. In the case of cardiomyocytes however, it is plausible that the presence of these markers indicate cellular stress instead of *de novo* myocyte[11-13]. Additionally, cardiomyocytes are capable of undergoing endocycle processes known as endomitosis and endoreduplication in response to stress[56, 57]. Endomitosis results in a binucleated cell which contains two nuclei with diploid (2n) DNA content within the same cytoplasm, a common feature of mature cardiomyocytes. Endoreduplication entails chromatin duplication without nuclear envelope breakdown (NEB) and result in nuclei with >2n DNA content. The ability of cardiomyocytes to engage in endomitosis and endoreduplication in addition to normal cell division **(Figure 1.3)** allow for the presence of PCNA, BrdU, pHH3, Aurora B and Anillin in response to injury[12, 19, 58]. *De novo* postnatal mammalian cardiomyocyte formation requires clearer

understanding of cardiomyocyte cell cycle status prior to intervention and manipulation. Fortunately, the field of cell cycle dynamics has experienced a mini-revolution in recent years producing powerful tools to report live readouts for specific stages of the cell cycle.

Cell Cycle Analysis Tools

Analysis of the cell cycle with the introduction of the Fluorescent Ubiquitination Cell Cycle Indicator (FUCCI) system is now possbile[59-65]. FUCCI is a powerful tool that exploits the dynamic relationship of human Chromatin licensing and DNA replication factor 1 (hCdt1) and human Geminin, an inhibitor of hCdt1 where both proteins are visualized using fluorescent probes. A truncated form of hCdt1 containing amino acids (aa) 30-120, lacking the Cul4 and Geminin binding regions, is fused to monomeric Kusabira Orange 2 to create the mKO2-hCdt1 (mKO) probe. The N terminal region of Geminin from aa 1-110, lacking the Cdt1 binding region, is fused to Azami Green to form the AzGr-Geminin (AzGr) probe[59]. These fluorescently labeled mKO and AzGr probes have been modified to ensure proper oscillation in G1 and S/G2/M of the cell cycle, respectively[59] **(Figure 1.4)**.

In G1, mKO is upregulated as hCdt1 is required for initiation of DNA synthesis when bound to the origin recognition complex (ORC), thus cells exhibit an orange fluorescence in the nucleus at this stage. The complex acts as a helicase to allow loading of DNA polymerase. Once DNA polymerase is bound, Cdt1 is released, the complex is dissociated and the cells begin to exit G1. At the onset of S phase, Cdt1 is degraded through ubiquitination proteolysis. Additionally, during the transition between G1 and S phase, there is an upregulation of AzG, the presence of both orange and green fluorescence give a yellow fluorescence appearance in nucleus of G1/S

transitioning cells. Geminin is upregulated in S phase and maintained at high levels through the end of M phase. Geminin serves as a secondary mechanism to limit Cdt1 strictly to the G1 phase thus a green fluorescence is observed in the nucleus of S/G2/M cells. At the end of M phase, Geminin is similarly degraded through ubiquitination proteolysis, green fluorescence disappears from the nucleus and allows for the accumulation of Cdt1 and orange fluorescence as the cells transition out of M and back into G0 or G1[66, 67]. Loss of Geminin coincides with accumulation of Cdt1 due to the loss of the licensing machinery during the G0/G1 stage of the cell cycle[32, 68]. Protein levels of Cdt1 and Geminin inversely oscillate during the G1 and S/G2/M phases, respectively, in a tightly regulated manner[67, 69, 70]. These two oscillating cell cycle proteins play a role in licensing replication origins, namely G1 and S/G2/M and serve as direct reporters of these cell cycle states visualized through orange and green fluorescence within the nucleus of expressing cells[59].

This system has been used *in vitro* to study the response of HeLa cells to hypoxia and cell cycle arrest[69, 71-74]. Additionally, neural tissue was studied *in vivo* using ubiquitously expressed FUCCI transgenes to investigate proliferation during development[32, 59]. Myocyte proliferation was studied in zebrafish and Drosophila expressing FUCCI[75,76]. FUCCI is quickly becoming the method of choice to study cell cycle dynamics in multi cellular organisms due to its proven fidelity as a cell cycle reporter[77-89]. Given its rising popularity to study cell cycle dynamics in different organisms and its fidelity to identify cell cycle activity, FUCCI can thus be exploited to monitor the cardiac cell cycle in a cell-type specific manner.

Promoter Selectivity

Cardiomyocyte specific expression of a variety of genes is possible with promoter specificity. The alpha myosin heavy chain (αMHC) promoter, first established by Dr. Robbins[90], consists of non-coding exons 1-3 and a 4.4 kilobase fragment upstream of exon 1 from the mouse chromosome. The promoter is well insulated and allows uniform expression regardless of insertion site within the chromosome[91]. As an established promoter widely used in the cardiac research community it is the ideal choice for this doctoral project.

The primary aim of this dissertation is to establish the cell cycle status of cardiac myocytes during development and following cardiac injury using a novel cardiomyocyte specific FUCCI reporter mouse model. In this system, the αMHC promoter will be utilized to express both FUCCI transgenes in order to study cell cycle oscillations in cardiac myocytes.

GOALS OF THE DISSERTATION

Overarching Theme: Cardiomyocyte withdrawal from the cell cycle and contribution of adult cardiomyocytes to *de novo* cardiomyocyte formation in response to injury remains unresolved. Novel tools are required to assess fidelity of proliferation markers, to unequivocally resolve *de novo* cardiomyogenesis, and to elucidate the “true” nature of

the post-mitotic heart by pinpointing cell cycle dynamics of postnatal cardiomyocytes during postnatal growth and after pathological injury.

Hypothesis: **A subset of adult cardiomyocytes retain the ability to reenter the cell cycle in response to acute injury, however, markers utilized to clearly identify *de novo* cardiac formation fail to unmistakably identify cell cycle activity after injury.** We intend to elucidate cardiomyocyte cell cycle dynamics by using a novel tool targeted to the heart. **Specific Aims** of the dissertation test the following postulates:

Specific Aims:

I. A subpopulation of adult cardiomyocytes retains the ability to enter the cell cycle in postnatal development.
   A. Generate the alpha-myosin heavy chain FUCCI (αMHC-FUCCI) mouse model.
   B. FUCCI myocytes actively cycle within the first two weeks of birth exiting the cell cycle shortly thereafter.

II. Adult cardiac myocytes near the border zone re-enter the cell cycle in response to injury.
   A. Border zone cardiomyocytes in FUCCI hearts reenter the S/G2/M phase and re-express Azami Green-hGeminin1 in response to myocardial infarction.
   B. Remote zone cardiomyocytes fail to reenter the cell cycle in response to myocardial infarction.
   C. Isoproterenol cardiotoxic injury induces cell cycle reentry of cardiomyocytes in response to global stress.

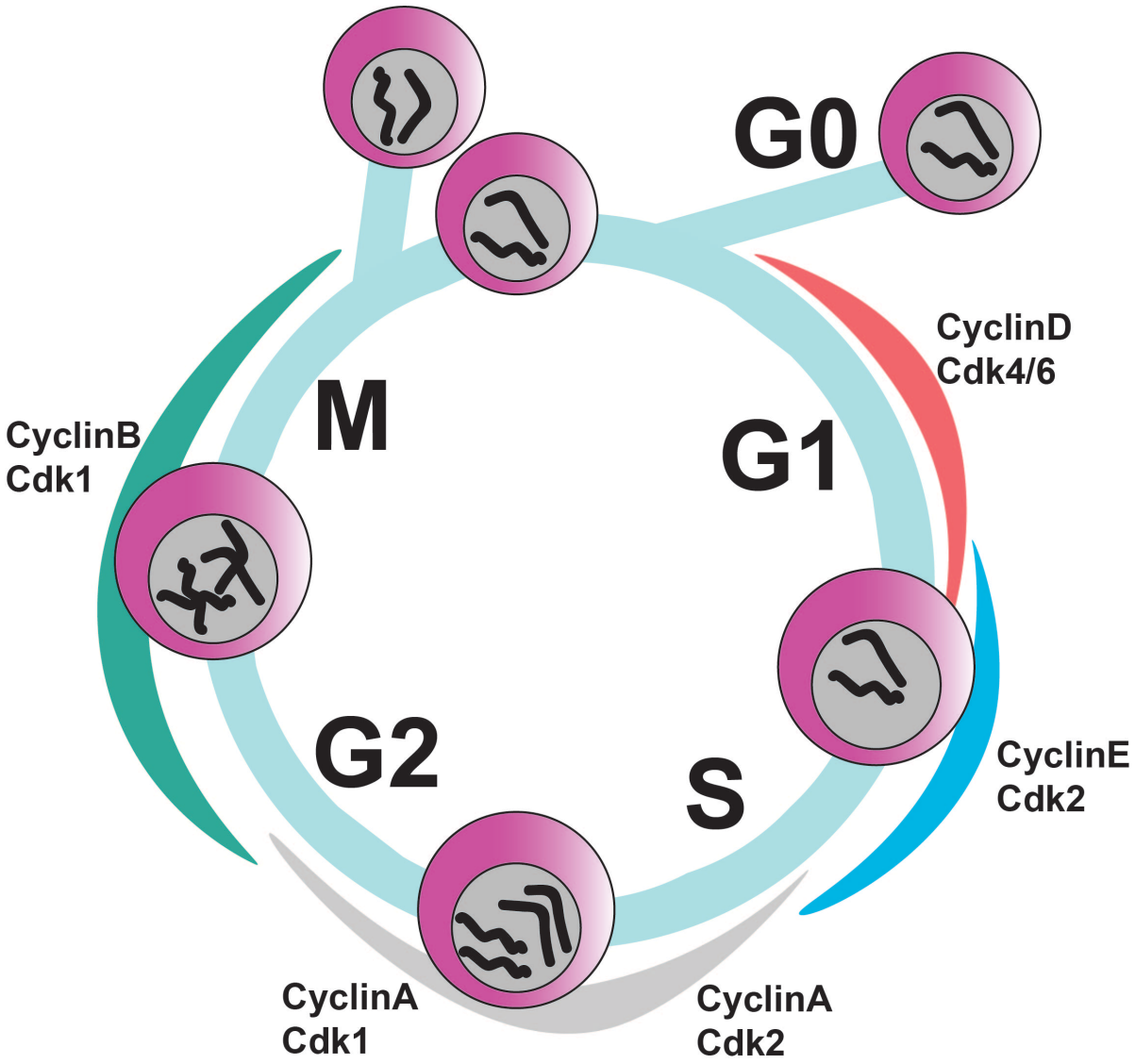

Figure 1.1. The Mammalian Cell Cycle. Gap1 (G1): Growth phase of a new cell. Cyclin D-Cdk4/6. G1-S: Transition from Growth (G1) to Synthesis (S). Cyclin E-Cdk2. Synthesis (S): DNA content is duplicated 2n→4n. Cyclin A-Cdk2. Gap 2 (G2): DNA integrity check. Cyclin A-Cdk1. Mitosis (M): Distribution of DNA and cytoplasmic contents to two daughter cells 4n→ 2n + 2n. CyclinB-Cdk1

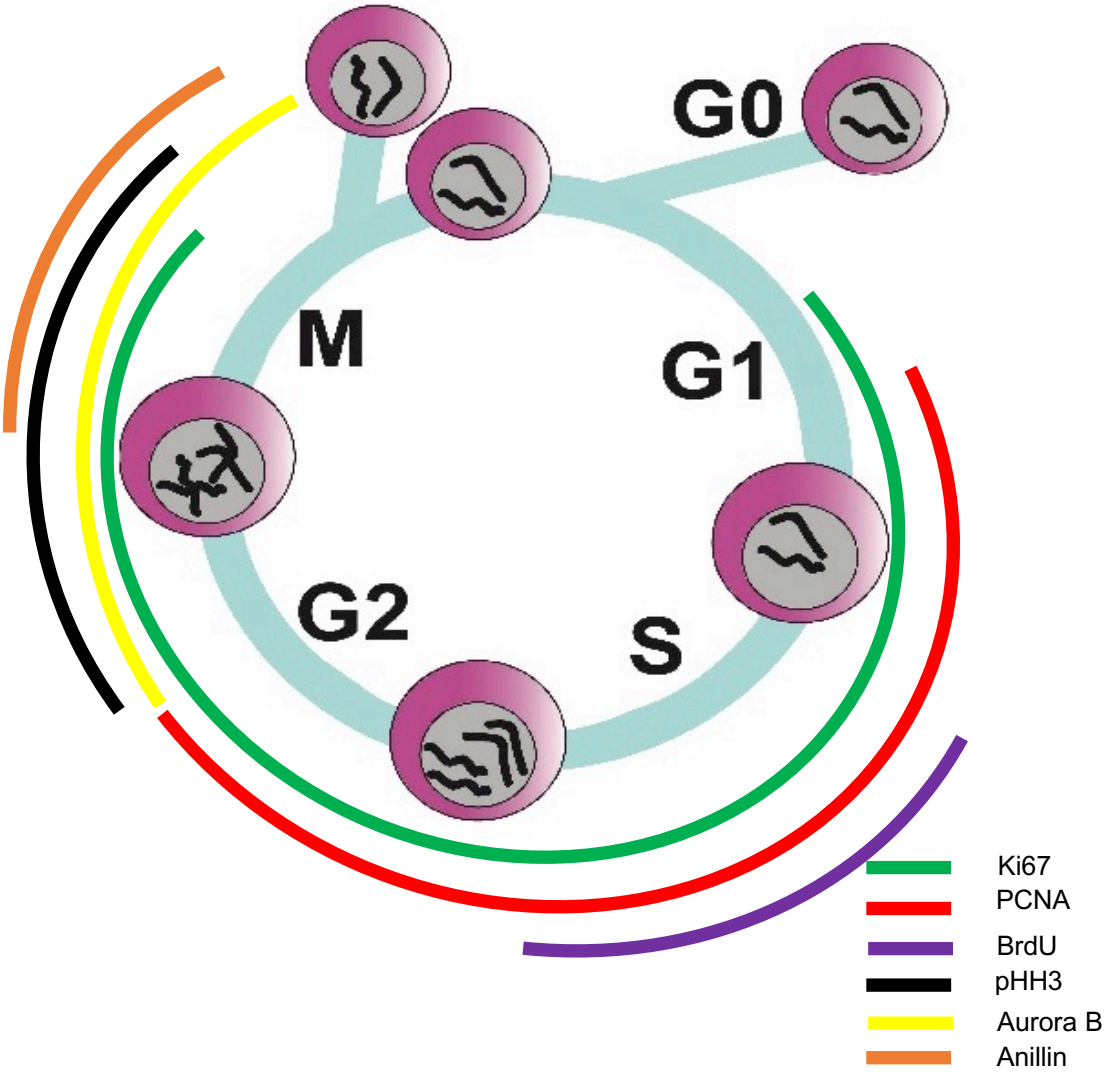

Figure 1.2. Markers of Division and Cell-Cycle Status. Nuclear antigen Ki67 is present from G1 to M phase (green). PCNA is presents between G1 and G2 phase in response to DNA synthesis (red). BrdU, a thymidine analog incorporates into DNA during synthesis (purple). pHH3 is responsible for chromatin condensation and is thus present during G2 through M phase (black). Aurora B in part phosphorylates pHH3 and plays a role in mitosis, present from G2 through M phase (yellow). Anillin plays a role in creating the cleavage furrow and begins to accumulate in late G2 through late M phase (orange).

A. Mitosis

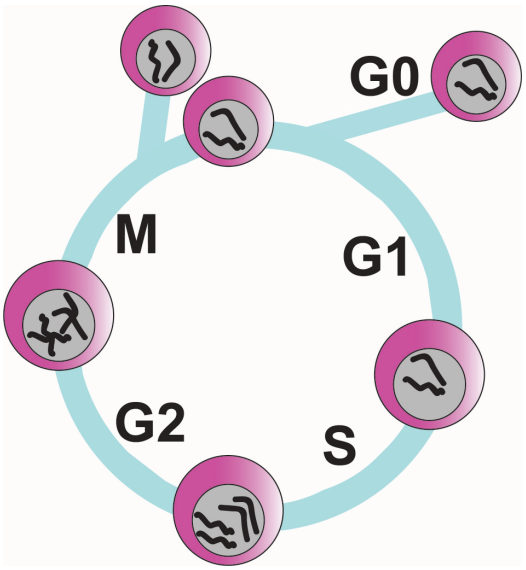

B. Endomitosis

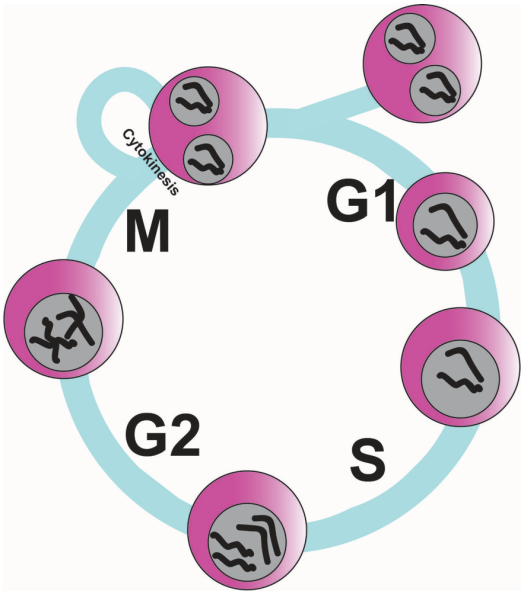

C. Endoreduplication

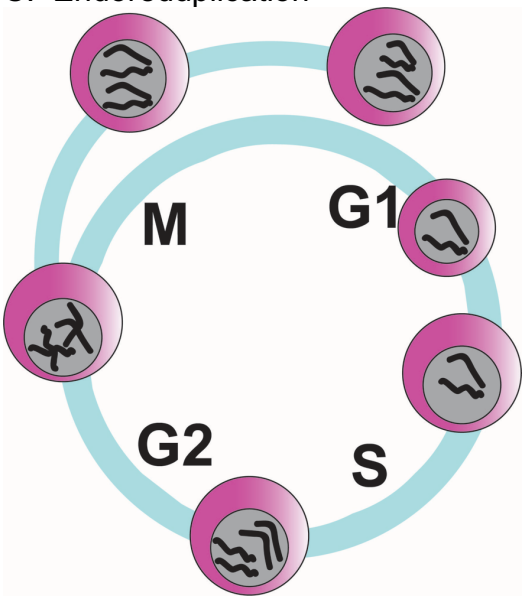

Figure 1.3. Cardiomyocyte Cell Cycle and endocycles. A) Mammalian cell division as shown in Figure 1.1. B) Endomitosis: Cells progress through G1, S, G2, and M however the final step, cytokinesis, is "skipped". Results in two nuclei, each with 2n DNA content within the same cell. C) Endoreduplication: Cells progress through S phase, duplicating DNA content (2n→4n). M phase is completely "skipped" resulting in a cell with 4n DNA content within the same nucleus.

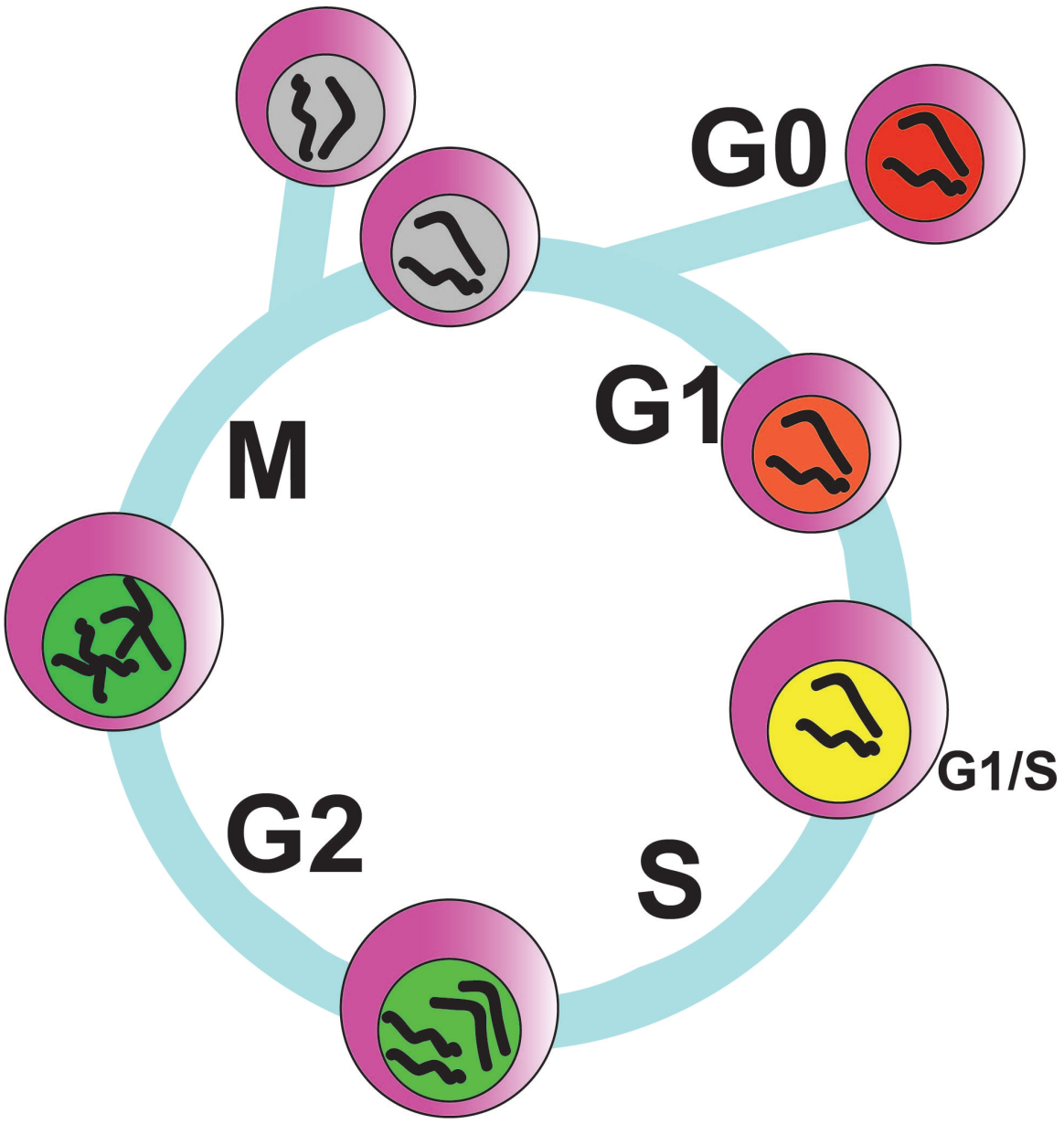

Figure 1.4. The Mammalian FUCCI Cell Cycle. Gap1 (G1): Peak mKO2-hCdt1 fluorescence (orange). G1-S: mKO2-hCdt1 fluorescence (orange) decreases as AzamiGreen-hGeminin fluorescence (green) increases, resulting in a yellow nucleus. Synthesis/Gap 2/Mitosis (S/G2/M): mKO2-hCdt1 is suppressed, AzamiGreen-hGeminin fluorescence (green) guards against aberrant DNA synthesis. AzamiGreen-hGeminin fluorescence (green) is degraded shortly after karyokinesis resulting in non-fluorescent nuclei until mKO2-hCdt1 can increase in quantity and intensity at G0/G1.

CHAPTER 2

VISUALIZING CARDIOMYOCYTE CELL CYCLE DYNAMICS WITH αMHC-FUCCI

INTRODUCTION

Estimates of cardiomyocyte turnover in the adult mammalian myocardium range from less than 1% to 40% annually dependent on calculation methods utilized[9, 17, 41, 52, 92]. A recent consensus statement in the field places the annual turnover potential closer to 1% and define the adult mammalian heart as a post-mitotic organ with extreme limited potential for proliferation and regeneration[47, 93-96]. Resilience to proliferative stimuli and significant *de novo* cardiac formation after birth contribute to adverse outcomes following injury[97]. Studies over the past decade place endogenous stem/progenitor cells expressing surface proteins tyrosine protein kinase kit (c-Kit), insulin gene enhancer (Isl-1), or stem cell antigen 1 (Sca-1) and/or cardiogenic markers like GATA-4 or Nkx2.5 as a potential source of proliferative cells capable of regenerating myocardial tissue lost after injury[7, 98-100]. Pre-existing adult cardiomyocyte activation and progression through the cell cycle resulting in two daughter cells has also been posited as a potential donor source[4, 54, 55, 97, 101, 102] yet attempts to stimulate post-mitotic cell cycle reentry after injury fail to induce profound effects necessary to be effective[8, 20, 103, 104]. Recent studies exploit markers of proliferation to identify new cardiomyocytes during the neonatal proliferative window and have been extrapolated as detectors of *de novo* cardiomyocytes following myocardial injury in adult mice[55, 94, 105,10, 23, 24, 26]. Clear and unambiguous identification of new cardiomyocytes remains elusive due to the alternate roles proliferation markers possess under stress conditions[11, 13] as a response to injury[27, 28]. Adding to the complexity is the lack of a well-defined cell cycle exit of cardiomyocytes in the post-mitotic heart. Clear demarcation of *de novo* cardiomyocyte formation and the perceived

mitotic-exit remains difficult to ascertain using current approaches[53, 106, 107]. Successfully identifying *de novo* cardiomyocyte formation and evidenced reentry into the cell cycle first requires a clearly identified exit that to date, has remained obscure in cardiomyocytes[10, 40, 108].

The proliferative window in postnatal (P) development diminishes within the first two weeks in the mouse heart[95], further corroborated by a decrease in cyclin and cyclin dependent kinase (CDK) downregulation necessary for cell cycle progression, coinciding within the same timeframe[14]. Comparisons between a proliferative neonatal heart and non-proliferative adult hearts to identify potential markers of proliferation have gained popularity in recent years[45, 47, 97, 105, 109]. Cell cycle markers like proliferating cell nuclear antigen (PCNA), Ki67, Aurora Kinase B, Anillin, phosphorylated histone H3 (pHH3) and finally, thymidine analogs like bromo-deoxy-uridine (BrdU) are employed to identify *de novo* cardiomyocyte formation. Analysis of both, exploited markers and the cardiomyocyte cell cycle progression to determine fidelity of current markers to clearly identify cell cycle progression after injury, prompted the use of powerful and accurate cell cycle analysis technology to better understand the cardiomyocyte cell cycle at the cellular level.

Fluorescence ubiquitination-based cell cycle indicators (FUCCI) was first introduced in 2008[59] to study cell cycle dynamics. FUCCI has revolutionized studies involving cell cycle analysis and has been utilized to study cell cycle dynamics from cell culture, Drosophila and fish to mammals[61, 71, 76, 110-112]. Monomeric Kusabira orange 2 (mKO) fused to a truncated human chromatin licensing factor 1 (hCdt1 30/120) present

in G1 phase of the cell cycle and its inverse partner monomeric Azami Green (AzG) fused to truncated human Geminin (hGeminin 1/110) present in S/G2/M distinctly delineate cells from G1 to M phase. The original FUCCI model attempted to elucidate cardiomyocyte cell cycle dynamics utilizing the ubiquitously expressed synthetic chicken β-actin-globin (CAG) promoter however, ubiquitous expression in all cell types within the myocardium made identification of cardiomyocyte specific expression difficult. Existing FUCCI mouse models[61, 111, 113, 114] still lack specificity to the cardiomyocyte population inciting the creation of a FUCCI mouse model using the alpha myosin heavy chain (αMHC) promoter[91, 115] to drive FUCCI probes in a cardiomyocyte specific manner, named αMHC-FUCCI.

αMHC-FUCCI faithfully oscillates between G1 and S/G2/M phase in a cardiomyocyte specific fashion in the postnatal heart. Cultured neonatal cardiomyocytes reveal myocyte division, binucleation and possible endoreduplication, showing robust and accurate FUCCI fluorophore oscillation within the system. Single positive cells (AzG^+ or mKO^+) and non-fluorescent cardiomyocytes, indicative of G0, peak at P2 and decrease thereafter. αMHC-FUCCI establishes the majority of cardiomyocytes are poised at the G1/S interface with levels reaching over 95% by P90, indicating arrest within the cell cycle and thus do not undergo a full mitotic exit. There is a small but statistically significant increase in single positive (AzG^+ or mKO^+) cells as a result of trauma to the heart that decreases by 21 days post myocardial infarction (MI) relative to homeostatic adult hearts. FUCCI cell cycle activity correlates with markers of proliferation like BrdU and pHH3 in development yet these same markers fail to correlate

with actively cycling FUCCI myocytes after injury. This study is the first to our knowledge to demonstrate cardiomyocytes do not undergo a full mitotic exit and instead identifies the G1/S interface as the point of seized cycling. A quantifiable sub-population of cardiomyocytes capable of reentering the cell cycle in response to injury confirms their existence but rendered insufficient to contribute to significant *de novo* cardiomyocyte formation. Markers commonly employed in identifying *de novo* cardiomyocyte formation did not correlate with observed FUCCI activity following injury raising speculation of their validity and accuracy for this purpose. Finally, FUCCI identifies a rare population of amplifying cardiac progenitors early in development that seem to disappear in conjunction with age.

METHODS

FUCCI Plasmids

FUCCI vector set was purchased from MBL international (Cat# VS0601). Transgenic plasmids for microinjection: mAG1-hGeminin 1/110 (AzGr) and mKO2-hCdt1 30/120 (mKO) were digested, blunted and subcloned into the pCR2.1 Topo Vector (Thermo Scientific Cat# K202020) to add NheI and KpnI sites at 3' and 5' end respectively. Topo clones were digested with NheI and KpnI in CutSmart Buffer 4 (New England Biolabs, B7204S) and directionally subcloned into the αMHC promoter plasmid. Clones were verified by digest using NotI enzyme to produce a 6.8 kilobase (kb) pair fragment containing the promoter-transgene-pA on a 1% agarose gel. Fragments were excised directly from the gel and purified using a Machery Nagel Nucleospin Gel and PCR Cleanup Kit (Cat# 740609.10) and cleaned according to Mouse Genomics Core specifications and diluted to 2ng/μl for microinjection.

Lentiviral plasmids: FUCCI vectors were digested with KpnI and HindIII, respectively and subcloned into the pShuttle Vector (Agilent Cat # 240006) to add BamHI and SalI sites at the 3' and 5' end. pShuttle-FUCCI vectors were released by BamHI-HF and SalI-HF in CutSmart Buffer 4 and directionally subcloned into pCCLsin.ppt.hPGK.GFP (a kind gift from Dr. Maurizio Capogrossi, Centro Cardiologico Fondazione I. Monzino-IRCCS) in place of GFP. Verified clones were amplified and lentivirus generated.

Transgenic Mouse Generation and Genotyping

αMHC-FUCCI linearized plasmids from above containing αMHC-AzGr-hGem-pA and αMHC-mKO2-hCdt1-pA where mixed at 1:1 molar ratio and injected into 0.5dpc embryos using Leica Micromanipulators with consistent positive air flow of 3 pounds per square inch (psi). Over 250 embryos were injected over 3 sessions and transplanted to a total of 6 pseudo pregnant females. A total of 28 pups were born and genotyped for the presence of the transgene at P14. AzG was detected by Forward Primer: 5' GGG TGC TCT CTT ACC TTC CTC ACC A and Reverse Primer: 5'- CCC TTG CCC TCG CCC TCG while mKO was detected by Forward Primer: 5' GGG TGC TCT CTT ACC TTC CTC ACC A and Reverse Primer: 5' GCA CTG ACT GAA GCG GAC CCA C respectively. A total of 4 potential founders were identified to have both of the injected transgenes and further bred for immunoblot analysis for protein expression.

Immunoblot Analysis

Hearts were excised and collected at postnatal day 0, 2, 7 and 10; postnatal week 2, 3, and 4; and postnatal month 3, 6, 9 and 12 for whole heart protein lysates. Whole hearts were weighed and snap frozen in liquid nitrogen and homogenized in Isolation Buffer + Inhibitors (containing 70 mM sucrose, 190 mM mannitol, 20 mM HEPES solution, and 0.2 mM EDTA in de-ionized water supplemented with protease and phosphatase inhibitor cocktails from Sigma-Aldrich). Bradford assay using a 0 - 2mg BSA protein standard curve was performed to calculate protein concentration. 15μg of protein was loaded per well in a 4-12% gradient Bis-Tris polyacrylamide minigel (Thermo Fishers) and run in 1x MOPS Buffer (Thermo Fisher) for 1.5 hours. Protein was transferred onto PVDF nitrocellulose membrane in 1x Transfer Buffer (Thermo Fisher)

for 1.5 hours, blocked in 1x Tris Buffered Solution-Tween (TBST) containing 8% (weight /volume, w/v) skim milk for one hour. Antibodies were diluted in TBST+8% milk as shown in Table 2. Primary antibodies were incubated overnight at 4°C. Secondary antibodies were incubated at room temperature for 1.5 hours prior to detection of signal. Immunoblots were processed with a LICOR Odyssey Clx to detect signal of 680 or 800 probes. Image Studio Software was utilized to quantitate signal intensity detected by LICOR for statistical calculations. Primary antibodies used to detect AzGr-hGeminin (Santa Cruz, SC74456), mKO2-hCdt1 (Cell Signaling Technology, D10F11), and Vinculin (Sigma, V9131). Secondary antibodies include, Donkey anti rabbit (DAR) 680 (LICOR, P/N 925-68073), DAM 800 (LICOR, P/N 925-32212) and DAM 680 (LICOR, P/N 925-68072).

Isolation of P2 Neonatal Mouse Ventricular Cardiomyocytes Cell Culture and Staining

Neonatal cardiomyocytes were isolated as previously described[116]. Briefly, postnatal day 2 hearts were excised, and atria removed. Hearts were placed in isolation media (containing 20mM Butanedione Monoxime (BDM), 0.0125% Trypsin in 1x Hank's Buffered Saline Solution (HBSS)) overnight at 4°C. The following day, ventricles were digested in digestion media (containing 20mM BDM, 7mg Collagenase/Dispase Enzyme (Sigma, 10269638001) in 10mL of Leibovitz's L-15 base media (Thermo Fisher, 11415-064)) at 37°C for 20 minutes. Hearts were triturated 10-20 times, allowed to settle and supernatant was passed through a 70um cell strainer. Digestion was repeated on

undigested tissue for an additional 5 to 10 minutes and passed through strainer. Dissociated cells were centrifuged, resuspended in plating media (65% Dulbecco's Modified Eagle Medium (DMEM, Thermo Fisher), 19% Media M-199(M199, Thermo Fisher), 10% horse serum (HS, Thermo Fisher), 5% fetal bovine serum (FBS, Thermo Fisher), and 1% pen-strep glutamine (100X PSG, Thermo Fisher)) onto uncoated 100mm tissue culture plate, incubated at 37°C, 5% CO2 for three hours to remove non-cardiomyocytes. Supernatant containing cardiomyocytes was plated onto laminin (Invitrogen) coated 35mm glass bottom tissue culture dishes at a concentration of 150,000 cells/mL in 37°C in 5% CO2 to allow attachment. After three days of incubation, CMs were rinsed three times with PBS and fixed in 1% paraformaldehyde (PFA) in 1x PBS for 15 minutes at room temperature. Fixed cells were washed, and permeabilized with 1x PBS containing 0.2M Glycine, 0.2% TritonX-100 for 15 minutes. Cardiomyocytes were rinsed and blocked in PBS + 10% HS. Primary antibodies were diluted in 1x PBS + 10% HS at concentrations found in Table 2.1 and applied overnight at 4°C. The following day, cardiomyocytes were washed with 1x PBS, fluorescently conjugated secondary antibodies incubated at room temperature for 1.5 hours. Cardiomyocytes were rinsed, and nuclei were counterstained with DAPI, for 15 minutes and scanned using Leica TCS SP8 confocal microscope. Primary antibodies used to label neonatal cardiomyocytes in vitro; α sarcomeric actinin (Sigma, A7811), Sytox Blue (Invitrogen, S34857), sm22α (Abcam, AB14106), Wheat germ agglutinin 680 (Invitrogen, W32465). Secondary antibodies used; DAR 405 (Jackson Immunoresearch), DAM 633 (Abcam). Antibody concentrations can be found in Table 2.1.

Isolation and Culture of Adult Cardiomyocytes and MG132 treatment

Adult cardiomyocytes were isolated from anesthetized mice using ketamine-xylazine solution, the chest opened, and the aortic arch was isolated. Curved forceps were used to push a 4-0 suture (Ethicon) underneath the arch. A small incision was made to the arch to insert a 22-guage cannula (Radnoti LLC). Perfusion buffer consisting of water supplemented with Sodium Chloride (113mM), Potassium Chloride (4.7 mM), Potassium Phosphate-Monobasic (0.6mM), Sodium Phosphate-Dibasic (0.6mM), Magnesium Sulfate-Heptahydrate (1.2mM), Sodium Bicarbonate (12mM), Potassium Bicarbonate (10mM), HEPES (10mM), Taurine (30mM), Glucose (30mM) and BDM (10mM) was used as a base. Digestion buffer, consisting of perfusion buffer supplemented with Collagenase II (460 Units/mL, Worthington Biochemical), was slowly perfused through the heart after suspending from a Radnoti EZ Myocyte/Langendorff Isolated Heart System within a 100 mL beaker warmed to 37°C using constant water flow for no more than 14 minutes. The heart was removed from the cannula and placed in a 100mm tissue culture dish containing perfusion buffer with collagenase II. The heart was removed from the cannula and transferred to a sterile hood and atria removed. Ventricles were teased with blunted forceps to dissociate the tissue and triturated slowly using a sterile transfer pipette. The cell suspension was transferred to a 15 mL conical tube and chunks were allowed to settle. Supernatant was passed through a 100 μm filter pre-wet with 10mL of Stop Buffer 1 solution consisting of perfusion buffer supplemented with 10% fetal bovine serum and Calcium Chloride (12.5μM). Remaining chunks of tissue were incubated with collagenase buffer, triturated and passaged

through fresh 100 μm filters 2 more times until all tissue was dissociated. All fractions were allowed to sit 30 minutes at room temperature to allow cardiomyocyte settling. The supernatant was aspirated and the fractions containing myocytes were pooled and washed in Stop Buffer 2 containing 5% FBS and Calcium Chloride (12.5μM). Resuspended myocytes were transferred to a T-75 flask and calcium add back was performed in a step wise fashion over a 30-minute interval. Rod-shaped cardiomyocytes were resuspended and used for staining, or culture. Cardiomyocytes used for staining were fixed in 1% PFA and immunostained as described in neonatal isolation methods section. Cardiomyocytes used for MG132 (Sigma, 10μM) experiments were resuspended in plating media, counted on a hemocytometer slide and plated at 150,000 cells/mL in 6 well plates coated with Laminin for two hours at 37°C to allow attachment. After incubation, cells were washed with plating media and switched to maintenance media. MG132 was introduced to the media and incubated for 12 hours prior to collection for immunoblot analysis. Primary antibodies used for staining; α-sarcomeric actinin (Sigma), endogenous Geminin for FVB myocytes (Santa Cruz, SC13015), Sytox Blue (Invitrogen, S34857). Secondary antibodies used for staining; DAM 633 (Abcam). Primary antibodies used for immunoblot; Vinculin (Sigma), ubiquitin (Abcam, Ab140601). Secondary antibodies used for immunoblot; DAM 680 (LICOR), DAR (LICOR, P/N 925-32213). Dilution for antibodies can be found in Table 2.1.

Histology and Immunofluorescence

Tissue samples used for histology were fixed in 1% PFA and embedded in Tissue-Tek optimal cutting temperature (OCT) Media after equilibration in 1x PBS containing 30% sucrose (w/v). Frozen sections were cut at 5-10 μm and fixed onto glass slides, incubated at room temperature for two hours prior to storage at -20°C. Sections were allowed to equilibrate at room temperature for 20 minutes, washed in 1x PBS, permeabilized with 0.2% TritonX 100/0.2M glycine and washed with 1x PBS. Sections were quenched in 1x PBS + 3% H2O2 (v/v) for 20 minutes and washed three times with 1x PBS. After quenching, samples were incubated with DNase Buffer (40mM Tris-HCl, 10mM NaCl, 6mM $MgCl_2$, 10mM $CaCl_2$, pH 7.9) for 5 minutes, treated with 500U/mL DNaseI in DNase Buffer for 15 minutes at RT and washed three times in deionized water. Slides were then washed with 1x PBS and blocked for one hour in 1x PBS + 10% HS at RT. Slides were incubated with primary antibodies as shown in Table 2.1, in 1x PBS + 10% HS overnight at 4°C. The following day, slides were washed with 1x PBS and incubated with secondary antibodies diluted in 1x PBS+10% HS for 1.5 hours at RT. If tyramide and/or streptavidin conjugated fluorophores were utilized, they were diluted in 1x PBS+10% HS and incubated at room temperature for 20 minutes at RT. Slides were washed with 1x PBS and incubated for 15 minutes at RT with DAPI or Sytox Blue to label nuclei. Slides were coverslipped using Vectashield Mounting Media and scanned on Leica SP8 Confocal using LASX software. Primary antibodies used; ckit (R&D Systems, AF1356), Histone H3 (Abcam, Ab5176), BrdU (Abcam, Ab6326), cardiac troponin I (Abcam, Ab47003) and tropomyosin (Sigma, T9283) and WGA 680 (Invitrogen). Secondary antibodies used: DAG HRP (Jackson Immunoresearch), Tyramide Bio (Perkin Elmer), Streptavidin LS490 (Atto tech), DAR 405 (Jackson

Immunoresearch), Donkey anti rat (DARt) Biotin (Jackson Immunoresearch) Streptavidin 700 (Invitrogen) and DAM 633 (Abcam). Dilutions for antibodies can be found on Table 2.1.

Postnatal Developmental Time course

Mice were given a single BrdU injection IP at 150mg/kg two hours prior to harvest. Hearts were excised at postnatal day 0, 2, 7, 10, 14, and 21, 30 and 90 and prepared for histological sections as described above.

Myocardial Infarction Injury

Myocardial Infarction was performed as previously described[100, 117] in 8-12 week old mice. Briefly, mice were subjected to acute myocardial infarction by left anterior descending coronary artery ligation surgery (LAD). Mice were pulsed daily with BrdU at 50mg/kg by intraperitoneal (IP) injection to label DNA synthesis until the day of harvest. Hearts were excised on day 3, 7, 10, 14 and 21 days post-MI and prepared for histological staining as described above.

Cardiotoxic Injury

Cardiotoxic injury was induced in 8-12 week old mice with a single IP bolus injection of isoproterenol at 150mg/kg. Mice were pulsed daily with BrdU at 50mg/kg by IP until day of harvest. Hearts were excised on day 3, 7, 10, 14, 21 and 28dpi and prepared for histological staining as described above.

HeLa FUCCI and Fluorescent Activated Cell Sorting and Cell Cycle Block Treatments

HeLa cells were infected with the FUCCI lentivirus (HeLa-F) generated above. MOI of 1, 5, 10, 50 and 100 were tested with MOI 5 generating the highest efficiency transduction and survival rate. HeLa-F cells were sorted using BD Aria sorter, single mKO, single AzGr and double mKO/AzGr positives were sorted. Only double mKO/AzGr positive cells at the time of sorting were selected for expansion and utilized for subsequent experiments. G1 Blocker, Lovastatin 10 μmol/L, G2 Blocker, Teniposide (VM-26) 0.5μg/mL, and G1/S blockers; Aphidocolin, 10μM, Thymidine, 2mmol/L, and L-mimosine, 400μmol/L were added to media and incubated up to 72 hours at 37°C.

Image Analysis

Nuclei counts for developmental cell cycle oscillation was analyzed using Leica LAS X Suite software. Regions of interest (ROI) of cardiomyocyte nuclei were selected, and exported as excel files containing intensities for AzG, mKO, Sytox, pHH3, and BrdU. Excel macros were written in an effort to eliminate biased analysis. Briefly, the lowest 10 intensities per series per channel where averaged to establish thresholds. A 10% buffer was added to the averaged thresholds to increase values and eliminate borderline positive/negative signals. Positive signals were assigned 1, negative assigned, 0. ROIs with a zero value for Sytox (nuclear stain) were excluded from analysis. ROI with 1, 1, 1 for Sytox, mKO, and AzG where considered mKO^{+}/AzG^{+} respectively. Similarly, ROI

with 1, 1, 0 for Sytox, mKO, and AzG were considered mKO^+ while 1, 0, 1 for Sytox, mKO, AzG were considered AzG^+ nuclei respectively. Additionally, consultation with Dr. Barbara Bailey of SDSU mathematics department was secured to verify analysis. Briefly, to assess accuracy of threshold parameters, histograms for individual channel intensities per section were created. Histograms revealed 1-5 nuclear values at the bottom of the intensity scale were excluded from analysis, thus validating the threshold values generated by the Excel macro. HeLa-F counts for G1/S block experiments were analyzed using Leica LAS X Suite. Briefly, DAPI was utilized to create a reference mask to identify nuclei. The mask was analyzed for the presence of mKO^+ and AzG^+ signal. The images (n=5, per experiment) were batch processed using the same thresholds for all images prior to table export. The presence of AzG or mKO above the set threshold (10%) is assigned a value of 1 by the software. Excel files were then processed for values >0 to be counted for mKO and/or AzG signal and utilized for quantitation.

$BrdU^+$ cardiomyocytes were identified by the presence of BrdU intensity signal in LAS X Suite software. Identified $BrdU^+$ cardiomyocytes were traced to determine area of tissue analyzed within the software.

Statistical Analysis

Data expressed as mean±SEM. Statistical analyses for each figure was performed using GraphPad prism version 5.0 software. Experiments using N=biological replicates were performed in technical triplicates unless otherwise stated. Figures 2.3, 2.5, 2.7, 2.8, 2.10 and 2.11 were assessed by 1-way ANOVA using Tukey's post hoc test. Figures 2.4 and 2.6 were assessed by 1-way ANOVA using Dunnett's post hoc

test. Figure 2.5 was assessed using unpaired t-test. A p-value of less than 0.05 was considered statistically significant.

RESULTS

αMHC-FUCCI expression is specific to cardiomyocytes

The postnatal mammalian heart is a post-mitotic organ with limited cardiomyocyte cell cycle activity shortly after birth[10] yet recent studies place existing cardiomyocytes as the primary source of *de novo* cardiomyogenesis; often utilizing common markers of proliferation[45, 54, 55] found in neonatal development to identify new cells. Given the lack of clarity regarding the mitotic exit of cardiomyocytes and clear identification of *de novo* cardiomyocyte formation, it is difficult to reconcile these two opposing views. Clear and specific cardiomyocyte cell cycle dynamics are currently unavailable in existing FUCCI mouse models [59, 61, 114] and thus prompted the creation of cardiomyocyte specific αMHC-FUCCI reporter. αMHC-mKO2-hCdt1-pA (mKO) and αMHC-Azami Green-hGeminin1-pA (AzG) linearized DNA transgenes were co-injected into 0.5dpc FVB/N J embryos in 1:1 molar ratios **(Figure 2.1A)**. Four potential founders positive for both AzG and mKO by polymerase chain reaction (PCR) resulted from microinjection; germline transmission[91] was verified by backcrossing to FVB/N non-transgenic mice **(Figure 2.1B)**. One validated founder was identified by AzG and mKO protein expression detected exclusively in heart tissue **(Figure 2.1C)**. Validated founder #25 was backcrossed for ten generations into the FVBN/J strain to produce a congenic αMHC-FUCCI line used in experimental procedures. Cardiomyocyte specific expression of AzG and mKO was verified by native fluorescence *in vitro* with neonatal and adult cardiomyocyte cultures **(Figure 2.1D, 2.1E)** and by confocal visualization of cardiomyocyte specific mKO and AzG fluorescence in frozen tissue sections from adult FUCCI hearts *in vivo* **(Figure 2.1F, 2.1G)**. Importantly, AzG and mKO expression were

absent from smooth muscle, endothelial and fibroblast nuclei, further verifying cardiomyocyte specificity in this model **(Figure 2.1F, 2.1G)**. In summary, the creation of αMHC-FUCCI allows direct visualization of cardiomyocyte specific cell cycle dynamics during development through direct detection of green (AzG^+) or red (mKO^+) nuclear fluorescence restricted to the cardiomyocyte population.

Isolated P2 FUCCI cardiomyocytes in culture allow visualization of cell division and binucleation events

Previously existing CAG-FUCCI attempted to demonstrate cardiomyocyte cell cycle activity using whole and thin sliced heart tissue in *ex-vivo* culture methods to observe CM cell cycle activity[118]. Endothelial, smooth muscle, fibroblast and cardiomyocytes within the whole and sliced tissue culture ubiquitously expressed FUCCI and thus complicated analysis *in-vitro*, further requiring immunolabeling to identify cardiomyocytes. To determine if αMHC-FUCCI could serve as a proper tool to analyze stimulation of cardiomyocyte cell cycle activity *in vitro*, P2 neonatal cardiomyocytes were isolated, cultured and imaged for twelve days. Neonatal cardiomyocytes underwent limited normal cell cycle division and endoreduplication events in culture. AzG and mKO fluorescence oscillated accordingly for all events. In a dividing cardiomyocyte, AzG accumulation in nuclei disappeared and was followed by cleavage furrow formation and the creation of two daughter cells, indicative of a full mitotic event **(Figure 2.2A-2.2C)**. Binucleation events showed nuclear envelope breakdown (NEB) accompanied with endomitosis **(**acytokinesis**,** **Figure 2.2D-2.2G)** in culture. Taken together, FUCCI oscillation in these cycling events demonstrate the power of FUCCI for faithful *in vitro*

modeling to assess stimulants and suppressors on neonatal cardiomyocyte cell cycle re-entry.

Proliferation markers BrdU and pHH3 identify cycling myocytes in developing FUCCI hearts

Faithful oscillation of FUCCI in neonatal cardiomyocyte culture provoked the verification of proliferation markers commonly utilized to identify actively cycling cells following neonatal cardiac injury *in vivo*[47, 55, 105, 109]. Thymidine analog BrdU and pHH3 mitotic marker are commonly utilized to identify DNA synthesis and mitosis in active cycling cells and have been utilized to identify *de novo* cardiomyogenesis after injury in both neonatal and adult injury models. Cardiomyocyte specific FUCCI was analyzed in postnatal development to assess the ability of fluorescent probes to accurately identify actively cycling cells. Active cycling in postnatal development was assessed in P2 to P90 FUCCI hearts following intra-peritoneal (IP) administration of BrdU (150mg/kg). In an effort to limit thymidine analog incorporation to S phase events, reported to last eight hours on average in eukaryotic cells[119], BrdU was injected two hours prior to harvest **(Figure 2.3A)**. Cardiomyocytes existing in S/G2/M[120, 121] of the cell cycle were visualized by direct AzG^+ fluorescence and labeled with antibodies against cardiac troponin I (cTnI), BrdU, and pHH3 phosphorylated at serine10 to corroborate fluorescent expression of FUCCI in frozen cardiac tissue sections **(Figure 2.3B-2.3F)**. Cardiomyocytes in G1 phase of the cell cycle were identified by direct visualization of mKO^+ fluorescence and the absence of BrdU and pHH3, respectively. Active cycling

was confirmed in FUCCI cardiomyocytes at P2, P7 and P14 by mKO^+ (G1, Figure 2.3B, 2.3C; white arrows) or AzG^+ (S/G2/M, Figure 2.3B-2.3D; yellow arrows). AzG^+ cardiomyocyte nuclei incorporate BrdU at P2 and P7, as shown in Figure 2B and 2C, respectively. Interestingly, $AzG^+/pHH3^+$ cardiomyocytes representing cardiomyocytes undergoing binucleation prior to mitotic exit or a cellular division[38, 39] were identified in several sections of P14 hearts[3, 56] (Figure 2.3D) [93, 122 93, 122 93, 122 6, 52 6, 52 6, 56]. Oscillation of AzG and mKO resolved by P21 (Figure 2.3E) and was further confirmed by the stark decrease of single labeled cardiomyocyte nuclei expressing AzG^+ or mKO^+ fluorescence at this postnatal age. BrdU incorporation decreased significantly with prolonged postnatal development, undetectable by P90 (Figure 2.3F), consistent with previous observations[9, 15, 52]. Prolonged AzG^+ fluorescence observed in P21 and P90 hearts did not correlate with prior FUCCI studies, fluorescence was expected to decrease as cardiomyocytes exit the cell cycle in accordance with a previous results involving ubiquitously expressed FUCCI and cardiomyocytes[106, 118]. Dual fluorescent AzG^+/mKO^+ cardiomyocyte nuclei accumulated in the αMHC-FUCCI system with age (Figure 2.3E, 2.3F) and prompted immunoblot analysis of whole heart lysates. Continued expression of both AzG and mKO fusion proteins in postnatal FUCCI hearts was confirmed by immunoblot **(Figure 2.3G)**. AzG and mKO protein expression increased significantly as development progressed relative to P2 (**Figure 2.3H**). Observed AzG and mKO expression in whole heart lysates prompted examination of endogenous Geminin and Cdt1 in postnatal cardiomyocyte development revealing previously unreported levels in whole hearts. Non-transgenic FVB/N WT whole heart lysates were analyzed and quantified for endogenous Geminin and Cdt1 at P2, P14 and P30 to substantiate

expression of FUCCI markers in the postnatal heart development (**Figure 2.4A, 2.4B**). Endogenous Geminin (Figure 2.4B, left) significantly increased with age as did endogenous Cdt1(Figure 2.4B, right) showing a 2.6 and 2.4-fold change respectively by P30 relative to P2. Nuclear localization of endogenous Geminin was visualized in ACMs isolated from non-transgenic mice at P30 (data not shown) and P90 (**Figure 2.4C**) as revealed by immunofluorescent labeling **(Figure 2.4C',** geminin=green, **2.4C''**, 4'6-diamindino-2-phenylindole (DAPI)=blue, and **2.4C'''**, αSA=red**)**. These results demonstrate FUCCI probes faithfully identified actively cycling cells, further corroborated by colocalization of BrdU and pHH3. Cardiomyocyte nuclei remain active in the cell cycle through P14, after which cell cycle activity rapidly decreases. Levels of AzG and mKO remain elevated past the proliferative window of murine cardiomyocytes and is consistent with wild type cardiomyocyte endogenous protein expression. Taken together, these results verify the FUCCI probes' ability to faithfully report cardiomyocyte cell cycle dynamics that can be exploited to identify cycling cardiomyocytes.

FUCCI oscillation identifies cardiomyocytes in the cell cycle through P14

Previously unobserved upregulation of both AzG/mKO and endogenous Geminin/Cdt1 protein expression in FUCCI and FVB WT mice, along with dual fluorescence throughout development in cardiomyocyte specific FUCCI, suggested a final resting place of the post-mitotic cardiomyocyte *in vivo*. Examination of cardiomyocyte cell cycle dynamics in postnatal development with αMHC FUCCI provided a unique opportunity to reveal the post-mitotic status of cardiomyocytes. Co-expression of nuclear AzG and mKO has been defined as the G1/S transition in previous

FUCCI reporter systems[59, 61, 72, 123, 124]. The dual AzG^+/mKO^+ fluorescence observed in mature cardiomyocytes suggested arrival to a G1/S stasis condition upon maturation, and not a full mitotic exit as previously reported[9, 108, 125-128]. AzG^+/mKO^+ cardiomyocytes were observed in tissue sections of αMHC-FUCCI hearts between P0 and P90. Single, AzG^+ only nuclei labeling peaked at P2 (9.3%) significantly decreasing to 1% by P21 and maintaining steady thereafter **(Figure 2.5A)**. Single mKO^+ nuclei labeling also peaked at P2 (6.8%) significantly decreasing to 1.1% by P14 and maintained steady through P90. Conversely, the number of cardiomyocytes at the G1/S interface was lowest at P2 (76.5%) reaching a peak over 96% in P90 hearts **(Figure 2.5B)**, suggesting an arrest at the G1/S interface.

Fluorescent proteins such as eGFP have been shown to cause hypertrophic effects if the levels of protein are dysregulated due to the constant activation of the αMHC promoter after birth. Possible dysregulation of the αMHC promoter activity prompted testing for functional ubiquitin/proteasome system (UPS) degradation of FUCCI in cardiomyocytes. Dual fluorescent FUCCI ACMs at P90 and P240 were treated with 10μM MG132, a known UPS inhibitor. FUCCI ACMs exposed to 12hr incubation of MG132 resulted in total ubiquitinated protein accumulation by immunoblot analysis and represented a 2-fold increase vs. untreated (DMSO Ctrl) FUCCI ACMs **(Figure 2.5C**, **2.5D)**. Additionally, AzG protein analysis revealed a 3.6-fold change in upregulated protein accumulation after MG132 treatment and no change in mKO **(Figure 2.5E, 2.5F)** thus suggesting properly regulated FUCCI within cardiomyocytes.

To reconstruct the observed G1/S arrest observed in αMHC FUCCI *in-vivo*, HeLa cells were stably transduced with cytomegalovirus (CMV) driven FUCCI probes. Sorted

ubiquitously expressing dual fluorescent HeLa FUCCI cells (HeLa-F) were expanded **(Figure 2.6A)** and arrested *in vitro* using cell cycle block treatments. HeLa-F arrested in G1 exhibited single fluorescence of nuclear mKO after 24 hours of treatment with Lovastatin[129-131] **(Figure 2.6B)**, consistent with FUCCI readout for G1[59, 72, 112]. HeLa-F arrested in G2/M exhibited AzG^+ fluorescence accumulation as early as 24 hours after Teniposide VM-26[132, 133] treatment **(Figure 2.6C)**. Cell cycle arrest at the G1/S interface was primed with three established G1/S cell cycle blockers; thymidine, Aphidicolin and L-mimosine[132, 134]. AzG fluorescence increased in nuclei treated with 10μM Aphidicolin treatment **(Figure 2.6F)** by 3.5-fold **(Figure 2.6H)** suggesting an S-phase block just past the G1/S interface[134]. Arrest of HeLa-F at the G1/S checkpoint was also absent following a single thymidine block **(Figure 2.6E, 2.6K)**. L-Mimosine[70, 71] treatment resulted in a 6.1-fold increase in double positive nuclei, confirming arrest in G1/S after 72 hours (*Online Figure 3K*)[134, 135] resulting in the AzG^+/mKO^+ co-expression pattern of double positive nuclei similar to αMHC-FUCCI ACM *in vivo*. Taken together, these results demonstrate for the first time that mature cardiomyocytes remain poised at the G1/S interface of the cell cycle and do not undergo a full mitotic exit to G0/G1.

Border zone cardiomyocytes exhibit signs of cell cycle re-entry but fail to show new cardiomyocyte formation

Faithful and functional FUCCI expression in a cardiac specific manner allowed a distinctive ability to validate commonly used proliferation markers as indicators for *de novo* cardiomyogenesis following injury, specifically BrdU and pHH3. Recent studies

suggest existing cardiomyocyte reactivation of the cell cycle and *de novo* cardiomyocyte formation following myocardial infarction (MI)[54, 55]. G1/S arrest in ACMs could indicate a degree of cell cycle plasticity allowing cell cycle re-entry more readily than G0 re-entry after acute injury. Adult αMHC-FUCCI mice subjected to left anterior descending artery (LAD) ligation were pulsed daily with BrdU (50mg/kg) until the day of harvest **(Figure 2.7A)**. BrdU incorporation along the border/infarct zone (BZ/IZ) was assessed in cardiac tissue at 3, 7, 10, 14, and 21dpi. BrdU was not observed in sham operated mice **(Figure 2.7B, 2.7D)**. Bright AzG^+ cardiomyocyte nuclei along the BZ was observed at 14 days post-MI (dpi) **(Figure 2.7C, 2.7C';** yellow arrowhead**)** corroborating possible cardiomyocyte cell cycle re-entry, however, BrdU incorporation was limited to the interstitial population. BrdU incorporation in surviving cardiomyocytes within the BZ/IZ was not detected through 14dpi but incorporated in cycling cardiomyocytes at 21dpi **(Figure 2.7E, 2.7E'; yellow and black arrowheads)**. $BrdU^+$/G0 (n=3), $BrdU^+$/G1(n=12) and $BrdU^+$/G1/S (n=71) cardiomyocyte nuclei were found sporadically throughout at 21dpi over 149 quantified sections containing 6705 nuclei (N=4 hearts) showing extremely low levels of BrdU incorporation as late as 21dpi **(Figure 2.8).** Interestingly, $BrdU^+$ nuclei found within the BZ/IZ as early as 3 days post-MI were restricted to infiltrating or interstitial cells, a possible indication of an immune response after MI **(Figure 2.9)**. pHH3 immunolabeling was undetectable at all tested time points (data not shown) within the cardiomyocyte population.

FUCCI fluorescence in cardiac tissue sections was utilized to identify cell cycle activity in cardiomyocyte nuclei following acute MI and quantified to query injury-induced ACM cell cycle re-entry. Identification of actively cycling cells by AzG and mKO

fluorescence was assessed in the BZ and remote zone (RZ) nuclei of infarcted mice. Interestingly, a small but significant induction of single AzG^+ and mKO^+ myocyte nuclei presents in sham injured hearts that differs from homeostatic adult cardiomyocytes at P90 **(Figure 2.7G,** 2.4% and 2.6% respectively**)**. Similar inductions of cell cycle activity are further observed in the injured myocardium of 7dpi and persisted through 21dpi with the highest induction of single positive nuclei occurring at 10d post-MI (G1; 3.2%, S/G2/M; 3.2%) returning to sham levels by 21dpi. G1/S nuclei inversely correlated with elevated levels of single positive nuclei **(Figure 2.7H)** highlighting the dynamic nature of FUCCI. Interestingly, there was no significant difference between sham and injured hearts thus suggesting the extraction of the myocardium from the chest cavity alone is sufficient to cause a small response in cardiomyocyte cell cycle activity. BrdU and pHH3 immunolabeling in remote zone cardiomyocytes additionally failed to show thymidine analog incorporation or pHH3 upregulation in cardiomyocytes **(Figure 2.10A-2.10E)**. Interestingly, a similar upregulation pattern in cell cycle activity was observed in RZ CMs further corroborating myocardial disruption from the chest cavity is sufficient for a small response in cell cycle activity **(Online Figure 2.10F, 2.10G)**.

Diffuse injury models such as adrenergic stress have been reported to stimulate cardiac regeneration in mammals[99, 136]. Stimulation of cardiomyocyte cell cycle re-entry and induction of a cardiac progenitor response was attempted with a single high dose of isoproterenol (150mg/kg) administered to αMHC-FUCCI mice **(Figure 2.11A)**. c-kit^+ cells were detected as early as 3-7d post injury (dpi) as previously reported[137, 138], however, BrdU incorporation and pHH3 immunolabeling were not detected in CMs at any time-point observed **(Figure 2.11B, 2.11C)**. Similar to myocardial infarction, a small

induction of cell cycle activity was observed at 3dpi that was all but absent by 7dpi **(Figure 2.11D)**, suggesting cardiomyocyte proliferation may not be responsible for regeneration observed in prior studies[99]. These data highlight the existence of a small population of cardiomyocytes capable of re-entering the cell cycle shown by a marked increase in S/G2/M and G1 single fluorescence present in the adult myocardium as result of myocardial disruption. Additionally, BrdU and pHH3 immunolabeling did not coincide with observed FUCCI cell cycle activity in both injury models suggesting a disconnect between cell cycle activity and incorporation of the thymidine analog that may instead be a response to DNA damage[58, 139] ($BrdU^+$/G1/S) or a missed mitotic event ($BrdU^+$/G1). Together these findings further indicate that trauma alone is enough to elicit cell cycle activity however, lack of BrdU and pHH3 immunolabeling suggest surviving cardiomyocytes are limited in their ability to progress through the cell cycle and may be compromised in *de novo* cardiomyocyte formation in response to pathologic challenge[140].

Amplifying cardiac progenitors express αMHC-FUCCI AzGr *in vivo*.

The presence of $cKit^+$ interstitial cells in the isoproterenol study stimulated the thought that cardiac stem/progenitor cells have been shown to contribute to cardiac formation during development and participate in the cardiac regenerative response to injury[96-99, 141, 142]. In an effort to identify early amplifying cardiomyocytes, postnatal FUCCI hearts were probed for expression of cardiac stem cell marker c-Kit and observed for fluorescence. A rare amplifying cardiomyocyte progenitor (N=3 mice, n=1)

was detected within a cluster of c-Kit$^+$ cells at P2, c-Kit$^+$/BrdU$^+$/pHH3$^+$ immune labeled with AzG$^+$ nucleus denoted mitotic activity in a very primitive cardiomyocyte (**Figure 2.12A,** yellow arrowhead). Additionally, a c-Kit$^+$ cluster negative for AzG **(Figure 2.12B)** and an immature cardiomyocyte (N =4 mice, n=2) characterized by AzG$^+$ fluorescence and cTnI expression **(Figure 2.12C,** yellow arrowhead**)** was detected in P7 myocardium. These findings support the concept that a pool of amplifying cardiomyocyte progenitors exist and act as a source for *de novo* cardiomyocyte formation in the myocardium participating in cardiac growth and proliferation in early development.

DISCUSSION

The regenerative response of the post-mitotic mammalian heart is limited at best. Debate over which cell types contribute to *de novo* cardiomyocyte formation following injury falls into two main camps: one advocating for progenitor cell mediated repair, and the other asserting that only pre-existing cardiomyocytes produce new myocardium. The truth probably lies somewhere in between, but regardless, neither cell type effects substantial endogenous repair. Evidence for cell cycle re-entry and cell division in post-proliferative mammalian cardiomyocytes currently relies on assays employing biochemical cell cycle markers that also appear in non-proliferating cardiomyocytes under cellular stress conditions. A clear understanding of the exact stage of cardiomyocyte cell cycle exit also remains elusive, hindering efforts to induce proliferation. The introduction of FUCCI technology has allowed insight into the most intimate workings of cell cycle oscillations without disrupting normal function revolutionizing assessment of cell cycle activity within biological entities[59, 112]. αMHC-FUCCI is a novel mouse model that successfully tracks cardiomyocytes as they oscillate through the cell cycle from G1 to M phase (Figure 2.1). Direct visualization of cardiomyocyte mitosis and endomitosis *in vitro* is now possible in FUCCI cardiomyocytes (Figure 2.2, **Figure 2.13**). Furthermore, visualization of CM specific cell cycle dynamics spanning G1 through M phase in this reporter model circumvents the need for complex breeding schemes utilized in prior studies[53, 91]. Robust and accurate oscillation of AzG^+ and mKO^+ fluorescence allows visualization between the various

phases of the cell cycle *in vivo* during development and after myocardial injury (Figure 2.3, Figure 2.7, Figure 2.8 and Figure 2.10).

During postnatal development, AzG^+ nuclei indicative of S/G2/M phase incorporate BrdU and show pHH3 through P14[9, 93, 106] (Figure 2.3)as previously reported. BrdU incorporation decreases to undetectable levels by P90 as postnatal cardiomyocytes continue to grow in size without dividing. These combined observations correlate with the lack of cell cycle progression observed in models studying cardiomyocyte activity; a switch from proliferation to hypertrophy between one and two weeks after birth[9, 43, 51, 126, 127, 143-145]. A small population of cardiomyocytes showed progression into the cell cycle in response to cardiac trauma (Figure 2.7, Figure 2.8, 2.9) in both border and remote zones of the injured myocardium and perhaps a response to inflammation. Similarly, a likely inflammatory response was observed in diffuse injury model using isoproterenol as an adrenergic stress (Figure 2.10). The lack of a profound upregulation of cell cycle reentry and failure to induce progression through the cell cycle to produce *de novo* cardiomyocytes has been shown in studies involving LAD ligation[48, 56]. Additionally, a lack of pHH3 immunolabeling and the extremely low identification of post-MI BZ/IZ $BrdU^+$ cardiomyocytes (Figure 2.7) at 21dpi further question the validity of these currently utilized markers of proliferation to unequivocally distinguish *de novo* cardiomyogenesis in a post injury model and may instead represent cells undergoing DNA repair or binucleation in response to injury[15].

Moreover, αMHC-FUCCI has identified the cardiomyocyte “mitotic” cell cycle exit as arrest at the G1/S interface (Figure 2.5, Figure 2.6). Over 95% of CMs express both mKO and AzG by P21 in postnatal development indicative of arrest at G1/S. The G1/S

interface is the Restriction point in yeast and mammals[146] at which mitogenic stimuli no longer exert effects on cell cycle progression. Additionally, it has been shown that the G1/S interface is the point of maximal ATP production[147]. The identified arrest at G1/S in this study together with previously reported observations further clarifies and corroborates why mitogenic stimuli fail to have profound effects in post-mitotic cardiomyocytes to induce proliferation. Additionally, the demand of massive ATP production in cardiomyocytes as the primary energy source required for the mechanical pumping action of the heart may further explain arrest at G1/S.

The αMHC-FUCCI model assesses the validity of commonly used markers of proliferation in measuring de novo cardiomyogenesis. Cardiomyocyte specific expression of the FUCCI probes permits direct visualization of cell cycle dynamics in G1 and S/G2/M phase cardiomyocytes. Ubiquitous expression of FUCCI reporters in the original model[59] obscured distinction of cardiomyocytes from other cardiac cell types also expressing FUCCI[118]. Whole and sliced cardiac tissue from CAG-FUCCI in culture exhibited increased mKO^+ fluorescence over time, indicative of the quiescent (G0) or G1 arrested state as previously reported for FUCCI cell lines[68, 72]. The αMHC-FUCCI mouse model circumvents the problem of nonspecific cardiomyocyte labeling and further suggests that cardiomyocytes arrest at the G1/S transition point, not G0 (Figure 2.5). Another cell cycle reporter model, the CyclinA2-eGFP transgenic mouse[107], identifies cycling $eGFP^+$ cardiomyocytes. Detectable eGFP declines in CMs after P15, and no actively cycling $eGFP^+$ CMs were found following injury, consistent with the fact that Cyclin A2 plays a predominant role in S phase[86, 87]. The αMHC-FUCCI system indicates that cardiomyocytes arrest at G1/S and are incapable of significant

progression through the cell cycle following two different myocardial injury stimuli. Recent reports have argued for surviving cardiomyocytes as the only contributors to *de novo* cardiomyocyte formation in postnatal development and following injury[3, 49, 102]. $BrdU^+$ cardiomyocytes spanning the BZ/IZ comprised less than 100 cells in all sections analyzed suggesting re-entry of cardiomyocytes to the cell cycle is limited at best as a source for *de novo* cardiomyocytes in response to injury. Interestingly, a $c\text{-}Kit^+/AzG^+/pHH3^+$ young amplifying progenitor cell was identified in P2 hearts (Figure 2.11), confirming that progenitors can contribute to *de novo* cardiomyogenesis in postnatal development.

A limitation of the αMHC-FUCCI model is that it does not report the final mitotic event, cytokinesis. The loss of AzG^+ fluorescence in late Mitosis before the creation of the cleavage furrow makes it difficult to unambiguously determine if cardiomyocytes undergo this event *in vivo*. Crossing αMHC FUCCI with αMHC-anillin-eGFP mice to observe cytokinesis in ACMs[148] may be a potential alternative. Moreover, it is possible that the BrdU delivery method used in this study underrepresented the number of cycling cardiomyocytes following infarction. The 2 to 4-hour half-life of circulating BrdU could result in discontinuous BrdU incorporation between daily injections. More consistent delivery of BrdU could be achieved in future experiments using osmotic mini pumps.

This is the first study to directly correlate cell cycle activity utilizing FUCCI with markers of proliferation to assess their validity as identifiers *de novo* cardiomyogenesis. Findings presented here indicate that commonly used markers BrdU and pHH3 do not necessarily represent actively cycling cardiomyocytes in response to injury and instead may be labeling cells undergoing DNA repair or endoreplication events as a

consequence of injury[11, 13]. Prior studies have suggested markers such as PCNA and Ki67 may in fact be re-expressed during cardiomyocyte hypertrophy that does not culminate in the formation of new myocytes. Taken together, these results call into question the usability of these markers to identify *de novo* cardiomyogenesis. Furthermore, the αMHC-FUCCI model provides the first direct evidence for G1/S arrest as the point of cell cycle exit in post-mitotic cardiomyocytes. Failure of ACMs stimulated to re-enter the cell cycle may be explained by this observation.

Belief that cardiomyocytes undergo mitotic exit leads to assumed G0/G1 arrest and to some extent, G2, thus studies employing cardiac specific cyclin overexpression focus on Cyclin D and to some extent, Cyclin A. DNA synthesis, binucleation and to a lesser degree re-activation of the cell cycle[23, 103, 128, 149] can be induced by cardiac specific Cyclin D overexpression, targeting quiescent cells receptive to cyclin D stimulation[150, 151]. Cyclin A has also been used to activate the cell cycle[5, 24, 49, 152]. Cyclin A is primarily responsible for S phase progression through the cell cycle, although induction to synthesis has been reported[27]. Aberrant chromosome doubling due to the lack of proper pre-replication complex assembly and improper synthesis is a potential consequence of Cyclin A overexpression[27, 153]. Recently, activators of G2/M cell cycle primarily Cyclin B, Aurora B and Cdk1 have been utilized to force cardiomyocyte cell cycle re-entry[149]. Cell death shortly after mitosis is reported when these genes are overexpressed, a likely byproduct of aberrant chromosome segregation during mitosis. Instead, results presented here demonstrate that ACMs persist at the G1/S transition during postnatal development. Cyclin E is the predominant cyclin of the G1/S transition, however because Cyclin E deletion does not produce an embryonic lethal phenotype,

its function as a potentiator of cardiomyocyte cell cycle re-entry and progression has remained largely uninvestigated [35, 37]. Furthermore, Cyclin E plays a role in endoreplication events, thus the focus of cyclin E has been restricted to this process in somatic cells, trophoblast giant cells (TGC) and megakaryocytes[154]. Unlike TGCs and megakaryocytes, cardiomyocytes arrest in G1/S due to their highly specialized function; typical proliferating cell cycle dynamics do not apply. Hence, Cyclin E may be worth reexamining in the context of its role within the cardiomyocyte cell cycle. Additionally, it is now possible to identify ACMs in G0[68, 155], G1, S/G2/M and G1/S without immunolabeling by identifying mKO^+ and AzG^+ expression patterns indicative of these cell cycle phases within the myocardium. Combining FUCCI with the p27K- cell cycle indicator model to identify cells in G0 and in G0/G1[101] transition together with αMHC-FUCCI would allow isolation of ACMs in all phases of the cell cycle. Sorted cells could then be compared to identify novel chromatin remodeling and/or unique RNA signatures that potentially hold the key to forcing cardiomyocytes cell cycle reentry and completion. As such, Cyclin E along with single cell sorting to identify unique signatures within the existing cardiomyocyte population will be the focus of future studies in our lab utilizing FUCCI.

TABLES

Table 2.1. List of antibodies

Antibody	Vendor	Catalog Number	Dilution IHC-Fr	Dilution Immunoblot
C-Kit (CD117)	R&D systems	AF1356	1:50	
Histone H3 (S10)	Abcam	AB5176	1:200	
BrdU	Abcam	AB6326	1:100	
Cardiac Troponin I	Abcam	AB47003	1:100	
Tropomyosin	Sigma	T9283	1:100	
αSarcomeric Actinin	Sigma	A7811	1:100	
Smooth Muscle 22α	Abcam	AB14106	1:200	
Von Wilebrand Factor	Dako	A0082	1:100	
Geminin (FL-209)	Santa Cruz	SC13015	1:20	
Ubiquitin	Abcam	AB140601		1:500
Vinculin	Sigma	V9131		1:2000
Geminin (F7)	Santa Cruz	SC74456		1:200
Cdt1	Cell Signaling Technology	D10F11		1:1000
Streptavidin 700	Thermo Fisher	S21383	1:100	
Streptavidin LS490	Atto Tech	AD490LS-61	1:100	
WGA 680		W32465	1:200	
Donkey anti goat Biotin	Jackson Immunoresearch	805-065-180	1:200	
Donkey anti goat 680	Jackson Immunoresearch	705-625-147	1:500	
Donkey anti goat HRP	Jackson Immunoresearch	805-035-180	1:100	
Donkey anti goat 633	Abcam	A-21082	1:200	
Donkey anti goat 546	Abcam	A-11056		
Donkey anti rabbit 405	Jackson Immunoresearch	711-475-152	1:200	
Donkey anti rabbit 680 RD	R&D system		1:5000	
Donkey anti rabbit HRP	Jackson Immunoresearch	711-035-152	1:5000	
Donkey anti rabbit 555	Abcam	A-31572	1:5000	
Donkey anti rabbit 488	Abcam	A21206	1:200	
Donkey anti mouse 633	Abcam	A31571	1:200	
Tyramide Biotin	Perkin Elmer	SAT70000	1:75	
Donkey anti Mouse 680	LICOR	P/N 925-68072		1:5000
Donkey anti Goat 680	LICOR	P/N 925-68074		1:5000
Donkey anti Rabbit 680	LICOR	P/N 925-68073		1:5000
Donkey anti Mouse 800	LICOR	P/N 925-32212		1:5000
Donkey anti Rabbit 800	LICOR	P/N 925-32213		1:5000
Donkey anti Goat 800	LICOR	P/N 925-32214		1:5000
Donkey anti rat 594	Abcam	A21209	1:200	
Donkey anti rat 405	Jackson Immunoresearch	712-475-153	1:200	

Table 2.2. List of Reagents

Reagent	Vendor	Catalog Number	Concentration Used
DMSO	Sigma	D2650	0.1%v/v
MG132	Sigma	474787	10μM
Lovastatin	Sigma	1370600	10μM
Thymidine	Sigma	T9250	2mM
Aphidicolin	Sigma	A4487	10μM
L-Mimosine	Sigma	M0253	400μM
Teniposide	Sigma	SML0609	0.5μg/mL

FIGURES

Figure 2.1. αMHC FUCCI expression is specific to cardiomyocytes. Schematic of transgenic mouse production (A). PCR analysis confirm transgene integration in genomic DNA (B). Immunoblot analysis of founder organs; heart, lung, liver, spleen, stomach, and bladder demonstrate cardiac specificity of transgenes (C). Isolated P2 (D) and P90 (E) mouse cardiomyocytes express AzG and mKO *in-vitro* native fluorescence for AzG=green, mKO=red, immunolabeling for α-sarcomeric actinin=blue, DAPI=white. AzG and mKO are visualized in cardiac tissue sections *in-vivo* by confocal microscopy and express faithfully cardiomyocytes (F, G) native fluorescence of AzG=green, mKO=red and immunolabeling for sm22α/von Wilebrand Factor=magenta, Sytox nuclear stain=white, and cardiac Tropomyosin=blue, scale bar 20μm. n=250 embryos injected (A), n=28 pups screened for transgene integration (B), n=1 founder line (C-G).

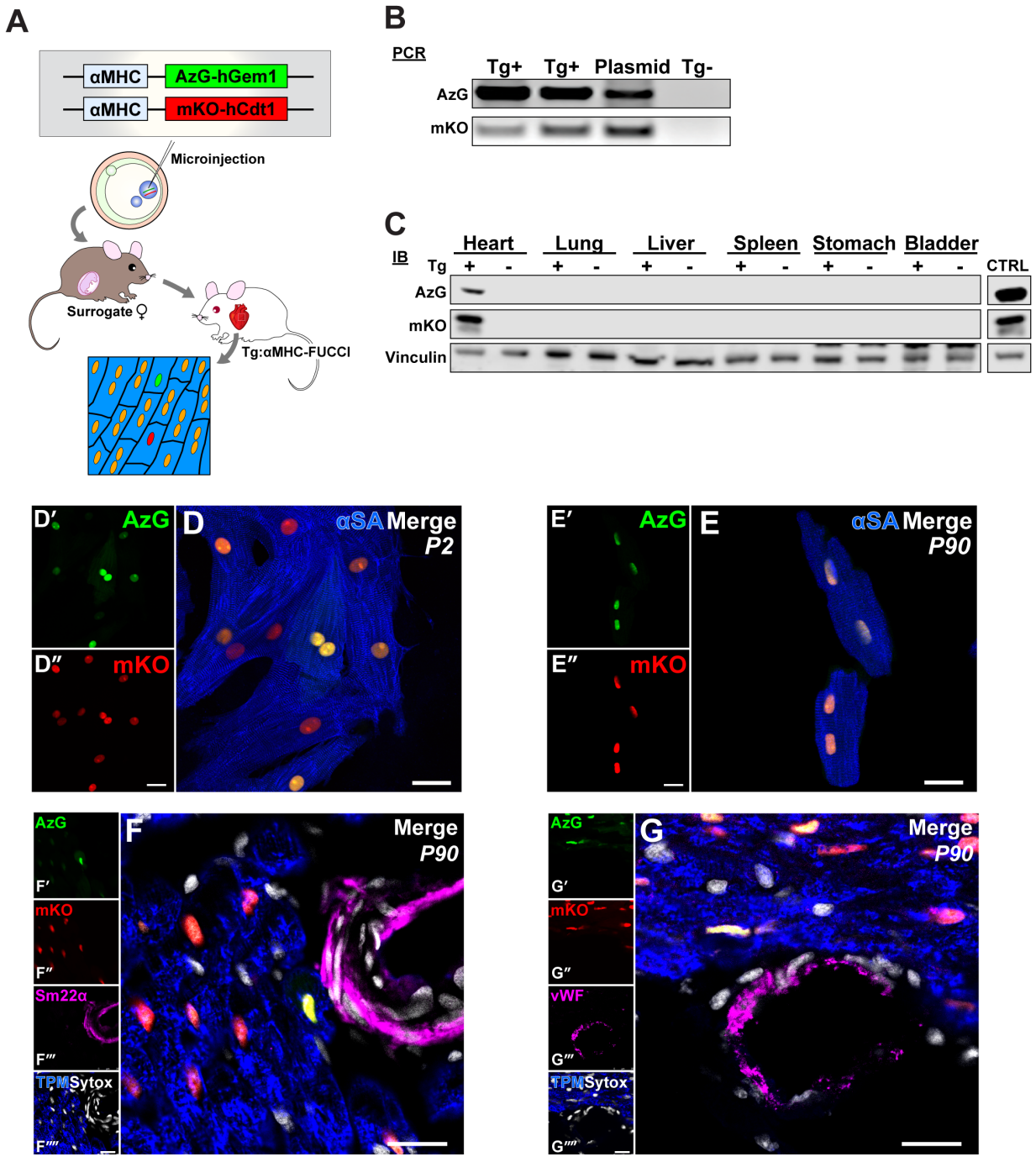
A
αMHC
AzG-hGem1
αMHC
mKO-hCdt1
Microinjection
Surrogate ♀
Tg:αMHC-FUCCI
B
PCR
Tg+ Tg+ Plasmid Tg-
AzG
mKO
C
IB
Heart Lung Liver Spleen Stomach Bladder
Tg + - + - + - + - + - + - CTRL
AzG
mKO
Vinculin
D′ AzG
D″ mKO
D αSA Merge P2
E′ AzG
E″ mKO
E αSA Merge P90
AzG F′
mKO F″
Sm22α F‴
TPM Sytox F⁗
F Merge P90
AzG G′
mKO G″
vWF G‴
TPM Sytox G⁗
G Merge P90

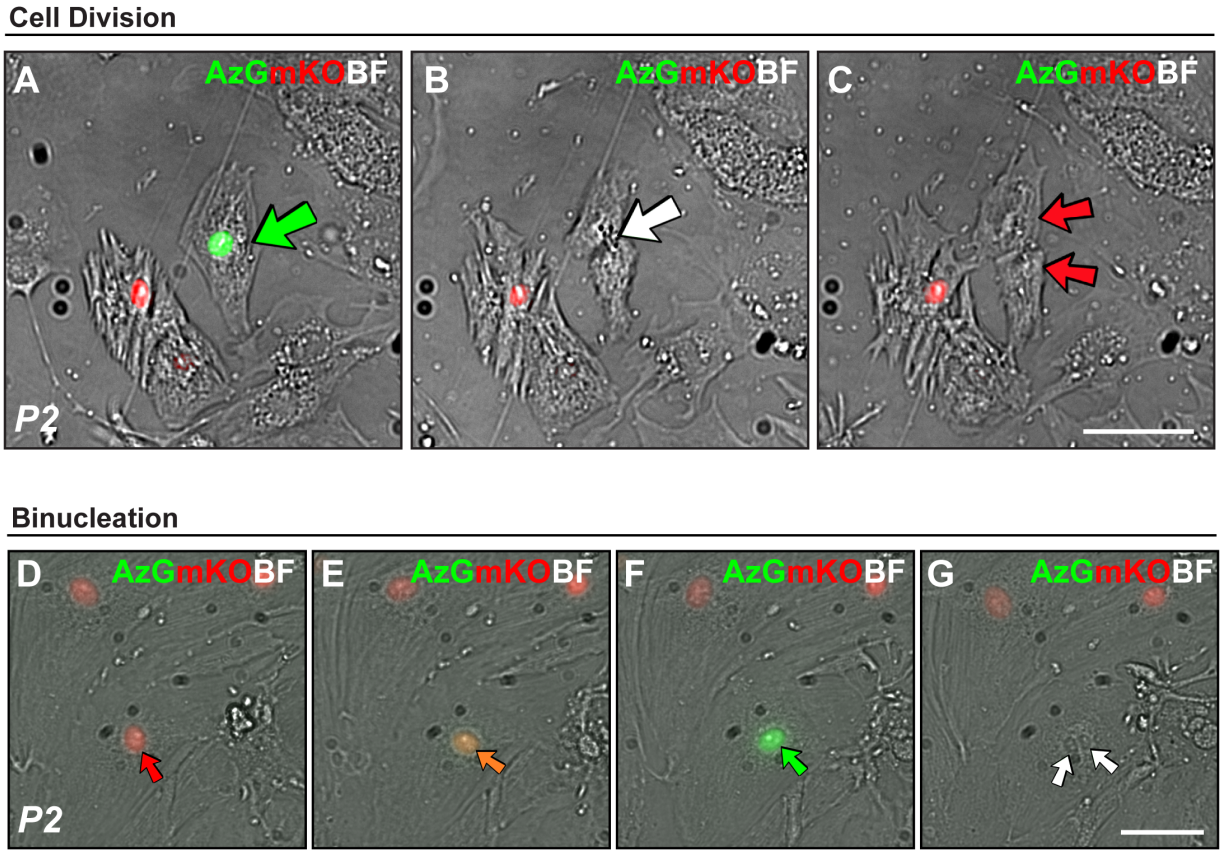

Figure 2.2. Isolated P2 FUCCI cardiomyocytes in culture allow visualization of cell division and binucleation events. Isolated neonatal cardiomyocytes from FUCCI hearts show progression from S/G2/M (green arrow, A) into a cleavage furrow (white arrow, B) ending in two distinct daughter cells (red arrows, C). Neonatal cardiomyocyte culture allows visualization and progression from G1 (red arrow, D), into G1/S (orange arrow, E) and S/G2/M (green arrow, F) before ending in a binucleation event (red arrows, G). Native fluorescence shows AzG=green and mKO=red in brightfield. scale bar 50μm.

Figure 2.3. Proliferation markers BrdU and pHH3 identify cycling myocytes in developing FUCCI hearts. Schematic of developmental time-point isolation, single BrdU injection (150mg/g) given 2 hours prior to harvest (A). Representative AzG and mKO expression in cardiomyocytes during postnatal development visualized by immunostaining and confocal microscopy in cardiac tissue sections at P2 (B), P7 (C), P14 (D), P21 (E), and P90 (F); AzG=green, mKO=red, pHH3=magenta, BrdU=cyan, Sytox=white and cardiac Troponin I=blue, Scale bar 10μm. Representative immunoblot of whole heart lysates indicate AzG/mKO/Vinculin protein expression from P2 to P90 show increased protein expression with age (G). Quantitation of AzG (H, left) and mKO (H, right) protein expression from G whole heart lysates relative own loading vs P2, N=3-5 mice per time point (B-F), N= 6 mice (biological replicates) per time point in (G) analyzed in triplicate. *P<0.05 vs P2, **P<0.001 vs P2, ***P<0.0001 vs P2 in (H). Statistical analysis was performed using 1way ANOVA utilizing Tukey's post hoc test and represented as mean±SEM.

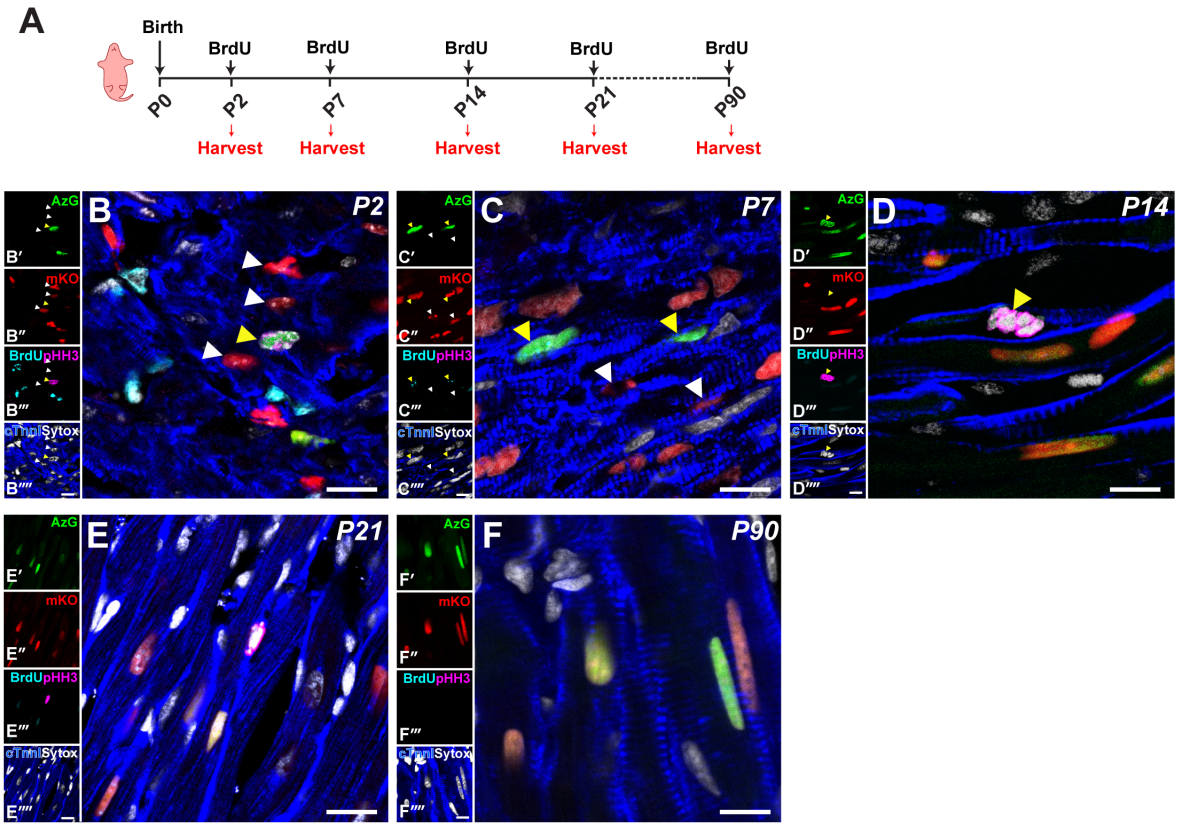
A
Birth
BrdU
BrdU
BrdU
BrdU
BrdU
P0
P2
P7
P14
P21
P90
Harvest
Harvest
Harvest
Harvest
Harvest
B
P2
C
P7
D
P14
E
P21
F
P90
AzG
mKO
BrdUpHH3
cTnnISytox

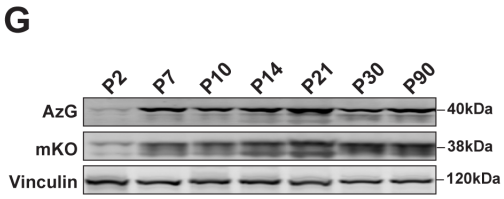
G
P2
P7
P10
P14
P21
P30
P90
AzG
mKO
Vinculin
40kDa
38kDa
120kDa

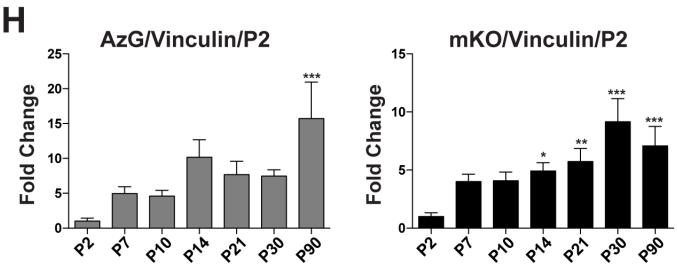
H
AzG/Vinculin/P2
mKO/Vinculin/P2
Fold Change
P2
P7
P10
P14
P21
P30
P90

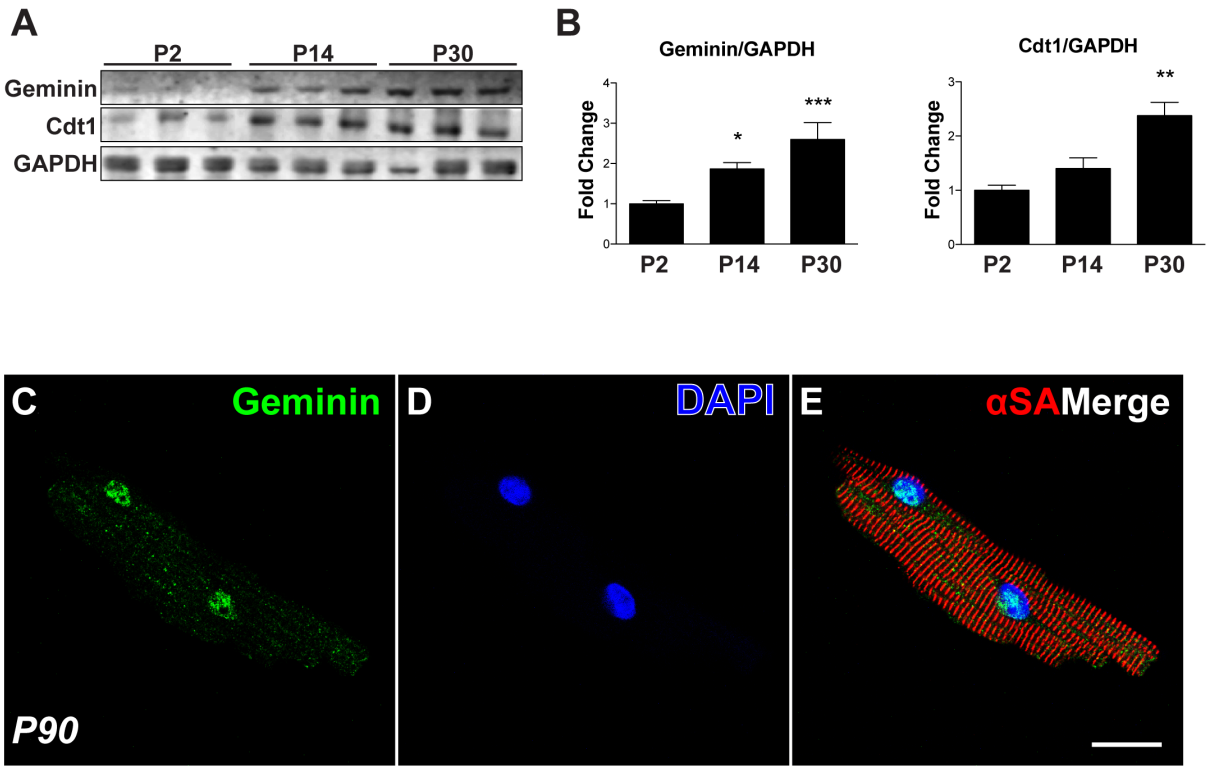

Figure 2.4. FVB non-transgenic hearts show increasing levels of endogenous Geminin and Cdt1. Immunoblot of P2-P30 FVB/N whole heart lysates (A). Quantitated levels of endogenous geminin (B, left) and Cdt1 (B, right) protein expression from A. Isolated P90 FVB/N cardiomyocytes immuno labeled for endogenous Geminin=green, DAPI=blue, and αSA=red, scale bar 20μm. N=3 hearts analyzed in triplicate per time point, *P<0.05, **P<0.001, ***P<0.0001 vs P2 (A, B). Statistical analysis was performed using 1way ANOVA utilizing Dunnett's post hoc test and represented as mean±SEM.

Figure 2.5. FUCCI identifies cardiomyocytes in the cell cycle through P14. Percent of cardiomyocyte nuclei immunolabeled tissue sections in different cell cycle phases show G0(mKO^-/AzG^-), G1(mKO^+) and S/G2/M (AzG^+), G0 quantitation; φP<0.05 P0 vs P21, φφP<0.001 P0 vs P90, φφφP<0.0001 P0 vs P7, P14,* P<0.05 P7 vs P14, *** P<0.001 P7 vs P21, δP<0.05 P21 vs P90; G1 quantitation; ΔP<0.05 P0 vs P90, ### P<0.0001 P2 vs P0, P7, P14, P21, P90, σP<0.05 P7 vs P21, P90; S/G2/M quantification; && P<0.001 P0 vs P21, P90, $$$ P<0.0001 P2 vs P0, P7, P14, P21, P90, ψP<0.05 P7 vs P21, P90 in (A). Percent of cardiomyocyte nuclei immunolabeled tissue sections in G1/S transition of the cell cycle, G1/S quantitation; *** P<0.0001 P2 vs P0, P7, P14, P21, P90 in (B). Representative immunoblot shows increased accumulation of ubiquitinated protein in adult FUCCI ACMs after MG132 treatment (10μM) in (C) and quantified in (D); ***P<=0.0001 vs DMSO Ctrl. Representative immunoblot of AzG-Gem and mKO-Cdt1 accumulation after MG132 proteasome block as in (C). Quantitation of AzG; ***P<0.0001 (F, left) and mKO; NS (F, right) vs DMSO treated samples. N= 3-5 mice per time point analyzed, n=4055, 1953, 7536, 2861, 4765, 3351 nuclei for P0, P2, P7, P14, P21, P90 (A, B). N=5-6 individual CM isolations (biological replicates) analyzed in triplicate (C, E). Statistical analysis was performed using 1way ANOVA utilizing Tukey's post hoc test and represented as mean±SEM (A, B), and unpaired t-test and represented as mean±SEM (D, F).

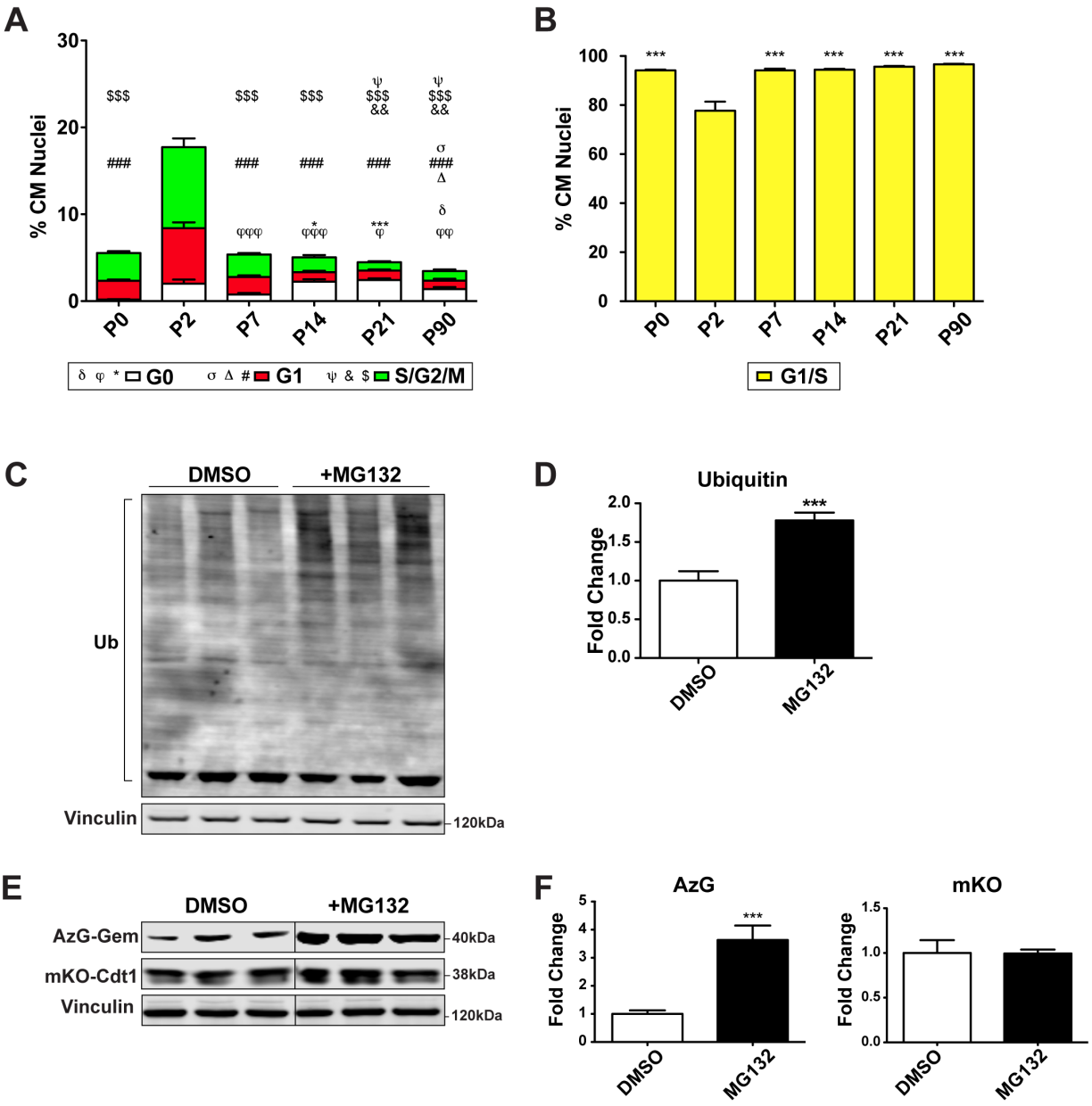
A
% CM Nuclei
30
20
10
0
P0
P2
P7
P14
P21
P90
G0
G1
S/G2/M
B
% CM Nuclei
100
80
60
40
20
0
***
P0
P2
P7
P14
P21
P90
G1/S
C
DMSO
+MG132
Ub
Vinculin
120kDa
D
Ubiquitin
Fold Change
2.0
1.5
1.0
0.5
0.0
***
DMSO
MG132
E
DMSO
+MG132
AzG-Gem
40kDa
mKO-Cdt1
38kDa
Vinculin
120kDa
F
AzG
mKO
Fold Change
5
4
3
2
1
0
1.5
1.0
0.5
0.0
***
DMSO
MG132

Figure 2.6. L-Mimosine increases G1/S block of HeLa FUCCI cells. Representative images of lentiviral transduced HeLa FUCCI Cells showing stable expression (A). Lovastatin G1 block of HeLa-F (B) and teniposide VM-26 G2 block in HeLa-F (C) show proper function of HeLa-F. HeLa cell cycle (CC) block at the G1/S interface using previously published G1/S blockers; DMSO control (D), Thymidine, 2mM (E), Aphidicolin, 10μM (F), and L-mimosine, 400μM (G) showing native fluorescent AzG=green, mKO2=red, and bright field, scale bar 50μm. Quantitation showing fold change of S/G2/M (H), G1 (I), G0 (J), and G1/S (K) vs. DMSO control. Aphidicolin shows largest block of S/G2/M cells (H) while L-mimosine shows the largest G1/S block (K) vs DMSO. *P<0.05, **P<0.001, ***P<0.0001 vs. DMSO controls. N= 3 independent culture treatments (biological replicates), n=5 sections (technical replicates) per treatment, n= 461, 132, 574, and 313 total cells for NT, Aphid, Thym and L-Mim respectively. Statistical analysis was performed using 1way ANOVA utilizing Dunnett's post hoc test and represented as mean±SEM.

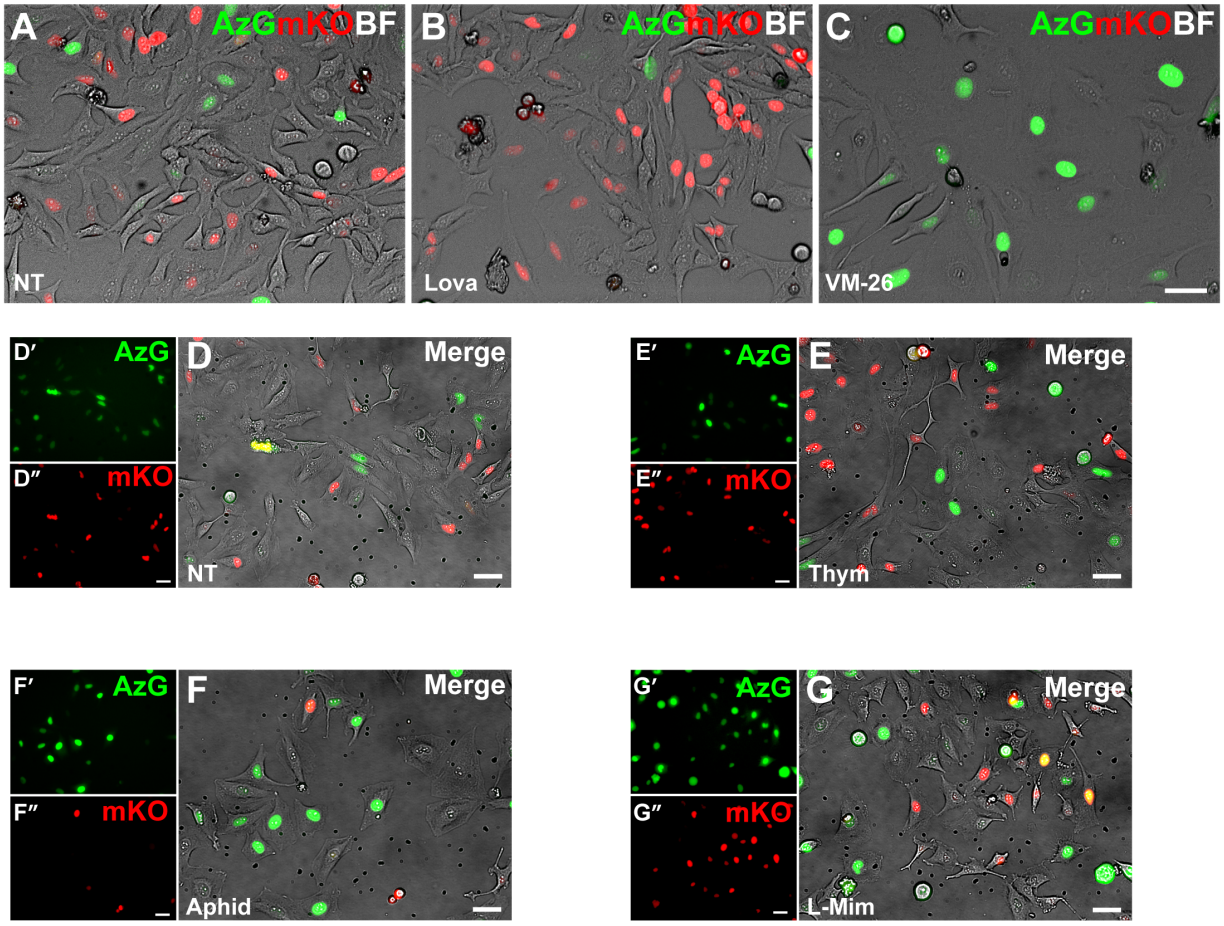
A
AzGmKOBF
NT
B
AzGmKOBF
Lova
C
AzGmKOBF
VM-26
D′
AzG
D″
mKO
D
Merge
NT
E′
AzG
E″
mKO
E
Merge
Thym
F′
AzG
F″
mKO
F
Merge
Aphid
G′
AzG
G″
mKO
G
Merge
L-Mim
H
S/G2/M
Fold Change
NT
Aphid
Thym
L-Mim
I
G1
Fold Change
NT
Aphid
Thym
L-Mim
J
G0
Fold Change
NT
Aphid
Thym
L-Mim
K
G1/S
Fold Change
NT
Aphid
Thym
L-Mim

Figure 2.7. Border zone cardiomyocytes exhibit signs of cell cycle re-entry but fail to show new cardiomyocyte formation. Schematic timeline showing cardiac infarction and daily BrdU pulse (50mg/kg) in (A). Representative sham tissue sections showing native AzG and mKO fluorescence and immunolabeled at 10 days post MI injury (dpi) and 21 dpi in (B) and (D). Border zone (BZ) cardiomyocytes at 14 dpi show AzG expression (n=4 total cells over 27 sections analyzed), yellow arrowhead; BrdU incorporation is restricted to interstitial population (C). BZ cardiomyocytes at 21 dpi show $mKO^+/AzG^+/BrdU^+$, yellow arrowhead and $mKO^+/BrdU^+$ black arrowhead (E); Native fluorescence for AzG=green, mKO=red, and immunolabeled for cardiac Troponin I=blue, BrdU=magenta, and Sytox=white in (B-E) scale bar 20μm. (F) Average $BrdU^+$ myocyte nuclei per mm2 of tissue in G0, G1, S/G2/M and G1/S phase of the cell cycle. Percent CM nuclei at G0, G1, S/G2/M phase in tissue sections at 7, 10, 14 and 21dpi; quantitation of G0; ns, G1; ##P<0.001 P90 vs 7dpi, ###P<0.0001 P90 vs Sham, 10dpi and S/G2/M; *P<0.05 P90 vs Sham, **P<0.001 vs 10dpi (G). Percent CM nuclei at G1/S interface; *P<0.05 P90 vs 14dpi, **P<0.001 P90 vs Sham, 7dpi and ***P<0.0001 P90 vs 10dpi quantitated in (H). N=4 hearts (biological replicates), n = 149 sections and over 6700 nuclei analyzed for F. N=3-5 hearts per time point (biological replicates) (G, H) n=3351, 2116, 987, 936, 1299, 1235 nuclei for P90, sham, 7, 10, 14, 21dpi and 9 sections along IZ/BZ for each heart. Statistical analysis was performed using 1way ANOVA utilizing Tukey's post hoc test and represented as mean±SEM.

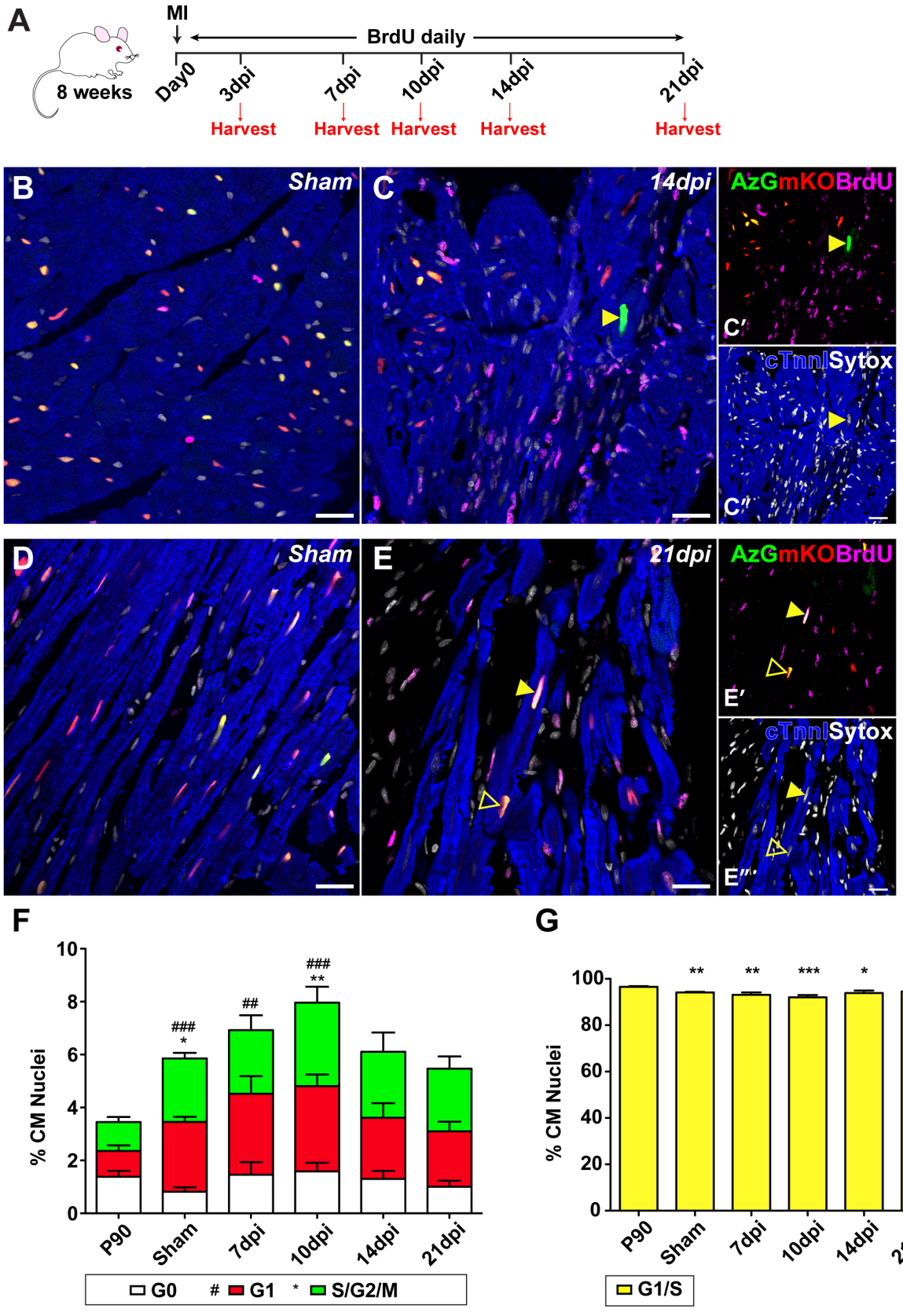
A
MI
BrdU daily
8 weeks
Day0
3dpi
7dpi
10dpi
14dpi
21dpi
Harvest
B
Sham
C
14dpi
AzGmKOBrdU
C′
cTnnISytox
C″
D
Sham
E
21dpi
AzGmKOBrdU
E′
cTnnISytox
E″
F
% CM Nuclei
P90
Sham
7dpi
10dpi
14dpi
21dpi
G0
G1
S/G2/M
G
% CM Nuclei
G1/S

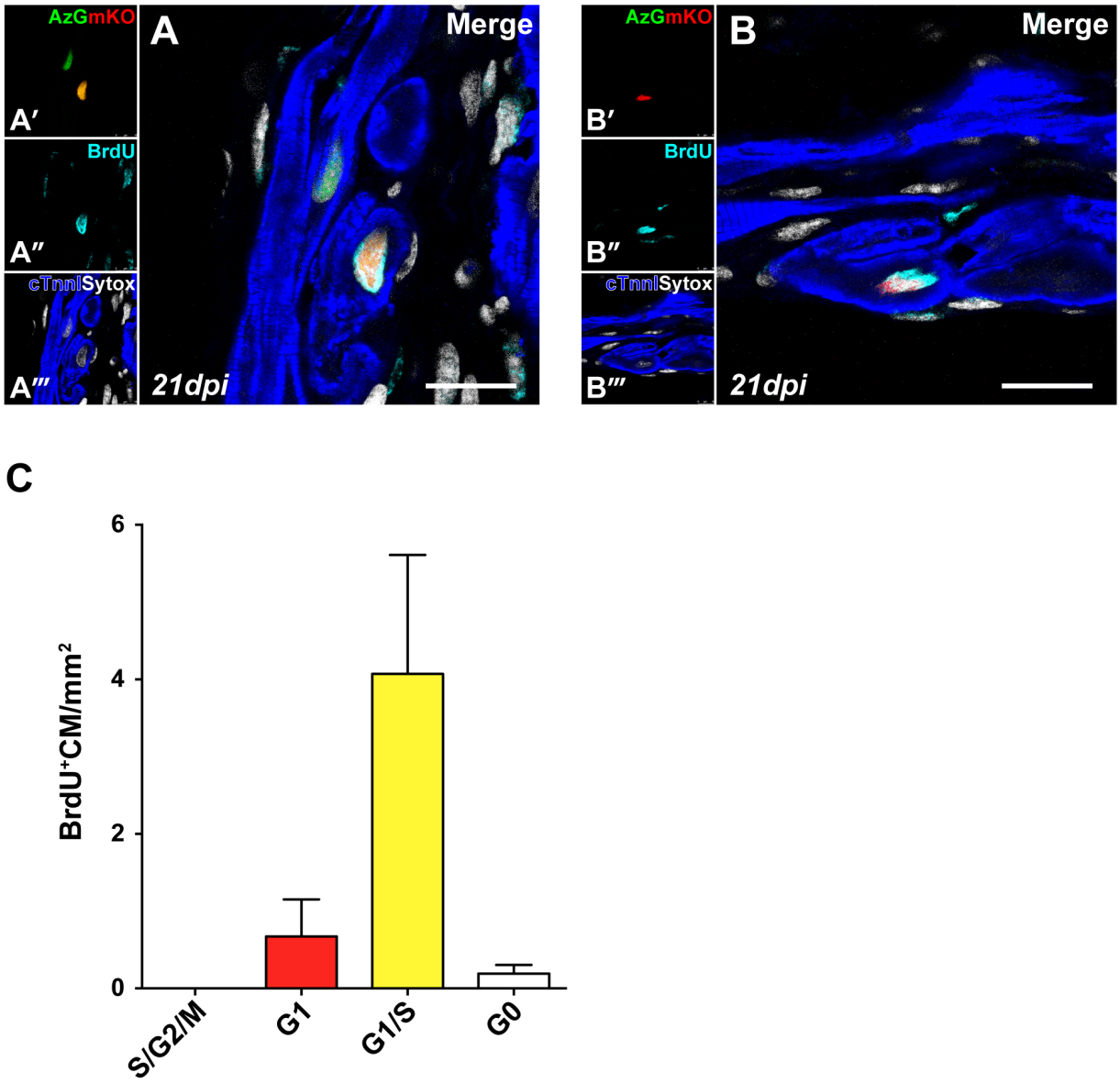

Figure 2.8. Border zone cardiomyocytes exhibit limited BrdU integration at 21dpi. Representative images of sporadic IZ/BZ CMs showing BrdU incorporation $BrdU^+$/G1/S (A), $BrdU^+$/G1 (B). BrdU+ FUCCI cardiomyocytes per unit area(mm^2) in S/G2/M, G1, G1/S and G0. Native fluorescence shows AzG=green, mKO=red, immunostaining shows BrdU=cyan, sytox=white, and cTnI=blue. Scale bar 20μm. N=4 hearts (biological replicates), n=149 tissue sections, and n=6705 individual nuclei. Statistical analysis was performed using 1way ANOVA utilizing Tukey post hoc test and represented as mean±SEM.

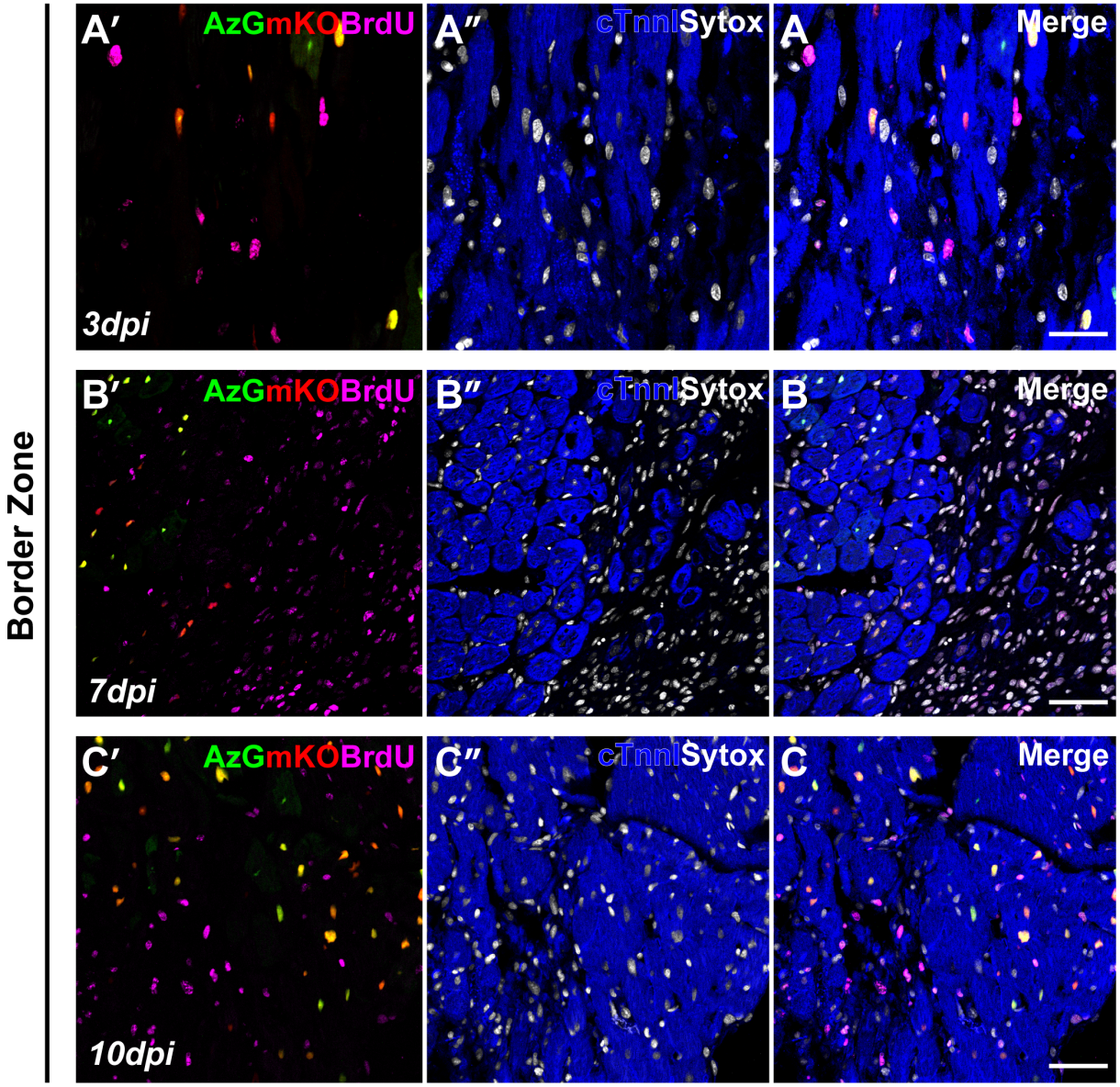

Figure 2.9. Border zone cardiomyocytes fail to incorporate BrdU through 10 dpi. Representative images of IZ/BZ showing BrdU incorporation in interstitial population, not cardiomyocytes at 3 (A), 7 (B) and 10dpi (C) respectively. Native fluorescence shows AzG=green, mKO=red, immunostaining shows BrdU=magenta, sytox=white, and cTnI=blue. Scale bar 50μm. N= 3-4 hearts per time point.

Figure 2.10. Remote Zone FUCCI cardiomyocytes fail to incorporate BrdU through 21 days post MI. Representative images of remote zone cardiomyocytes from 3 (A), 7 (B), 10 (C), 14 (D) and 21 dpi (E) tissue sections show lack of BrdU incorporation in cardiomyocytes. Native fluorescence for AzG=green, mKO=red immunofluorescence for BrdU=magenta, sytox=white and cTnI=blue. Percent cardiomyocyte nuclei at G0; ns, G1; ###P<0.0001 P90 vs sham, p14dpi, S/G2/M, **P<0.001 P90 vs 10dpi, ***P<0.0001 P90 vs sham, 14dpi (F) and G1/S interface; **P<0.001 P90 vs 10dpi, ***P<0.0001 P90 vs sham, 14, 21dpi (G). Scale bar 50μm, N= 3-4 (biological replicates) hearts per time point. Statistical analysis was performed using 1way ANOVA utilizing Tukey's post hoc test and represented as mean±SEM.

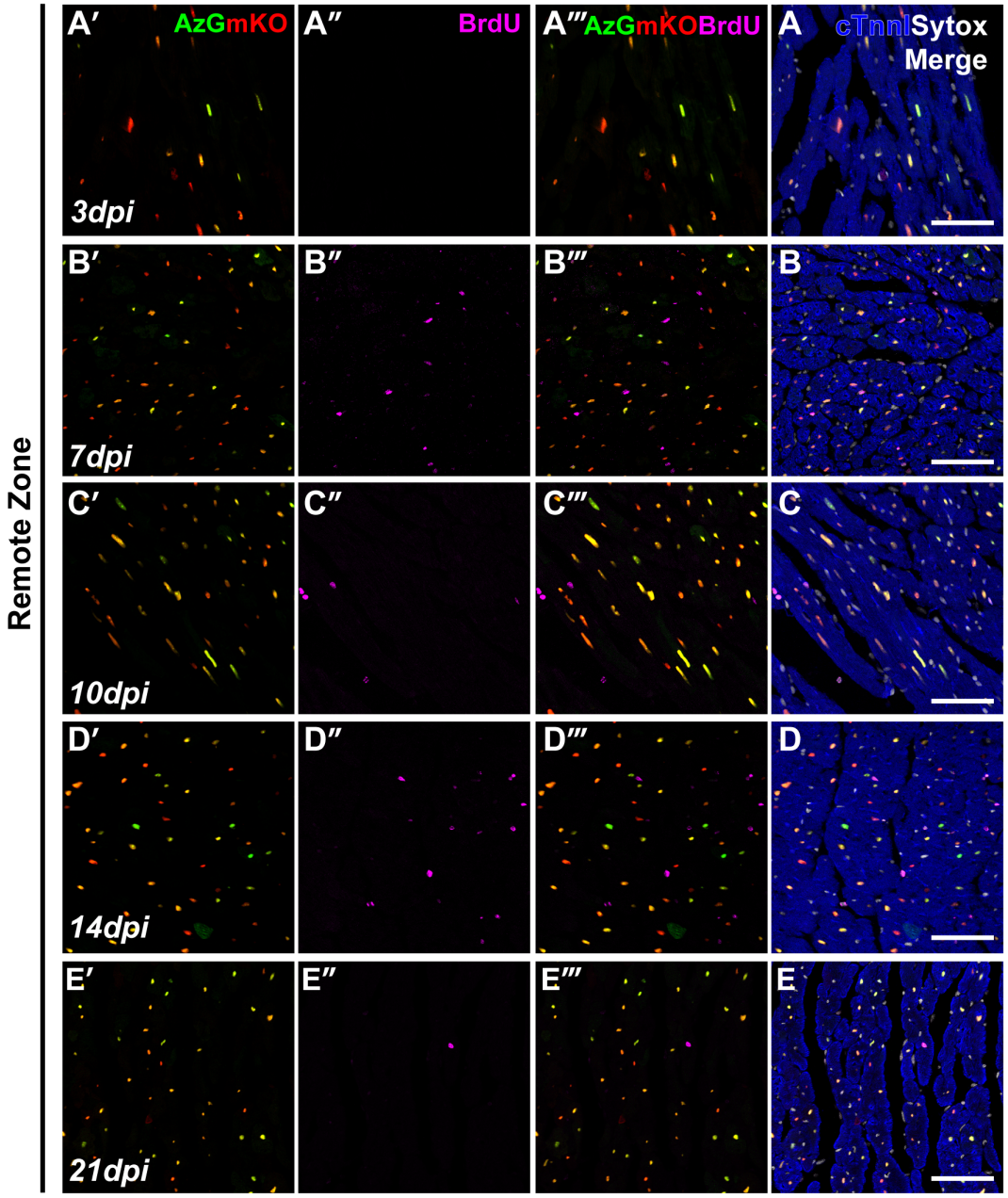
Remote Zone
A′ AzGmKO
A″ BrdU
A‴AzGmKOBrdU
A cTnnISytox Merge
3dpi
B′
B″
B‴
B
7dpi
C′
C″
C‴
C
10dpi
D′
D″
D‴
D
14dpi
E′
E″
E‴
E
21dpi

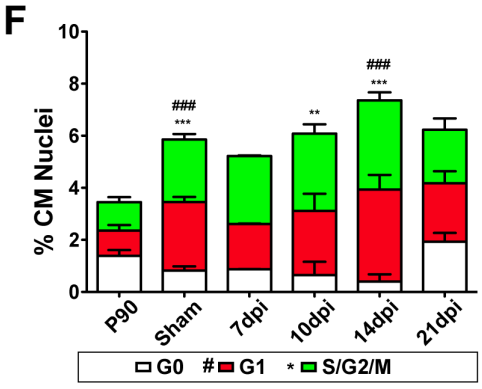
F
% CM Nuclei
10
8
6
4
2
0
###
***
**
P90
Sham
7dpi
10dpi
14dpi
21dpi
G0
G1
* S/G2/M

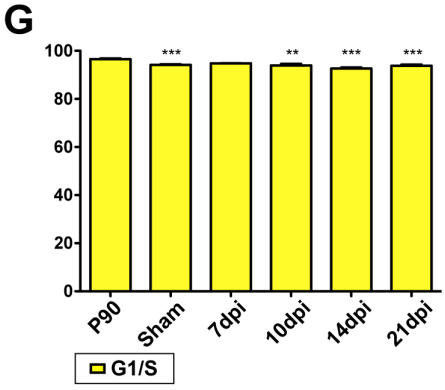
G
100
80
60
40
20
0
***
**
P90
Sham
7dpi
10dpi
14dpi
21dpi
G1/S

Figure 2.11. Isoproterenol induced cardiotoxic injury fails to force cardiomyocyte cell cycle re-entry through 28 days post injury. Schematic of Isoproterenol (single dose, 150mg/kg) injury and daily BrdU (50mg/kg) pulse (A). Representative confocal images of isoproterenol induced cardiotoxic injury at 3 and 7 days post injury (dpi, B, C). Native fluorescence for AzG=green, mKO=red and immunolabeling of BrdU=magenta, ckit=cyan, sytox=white, and cTnI=blue. Percent cardiomyocyte nuclei at G0; *P<0.05 P90 vs 7dpi, G1; #P<0.05 P90 vs 3dpi, and S/G2/M; $P<0.05 P90 vs 3dpi in (D) and G1/S; ns (E). N =3-4 (biological replicates) hearts per time point, n= 3351, 1707, 1344, 1027, 839, 937 nuclei counted utilizing 9 sections per time point at P90, 3, 7, 14, 21, and 28dpi. Statistical analysis was performed using 1way ANOVA utilizing Tukey's post hoc test and represented as mean±SEM.

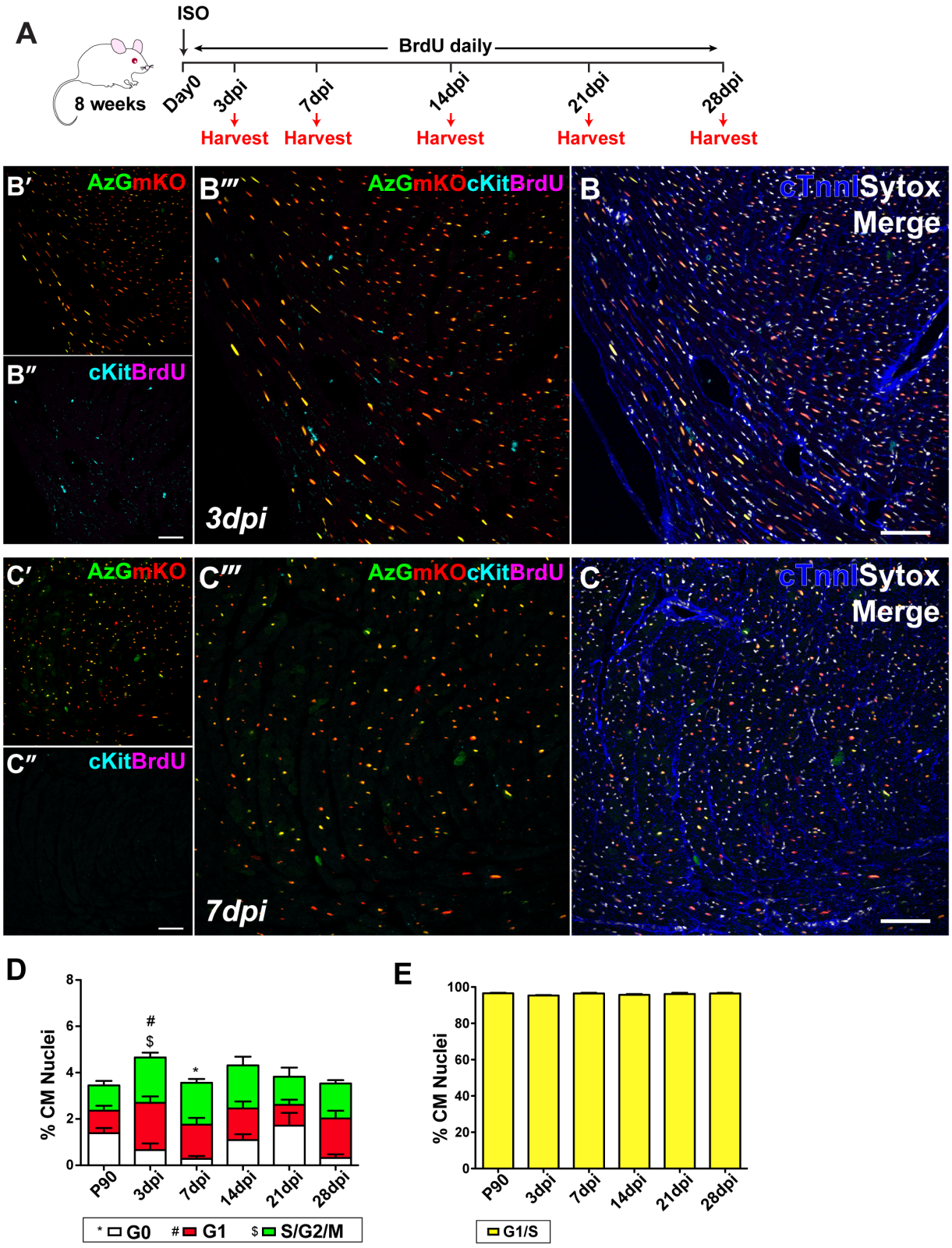
A
ISO
BrdU daily
8 weeks
Day0
3dpi
7dpi
14dpi
21dpi
28dpi
Harvest
B′ AzGmKO
B″ cKitBrdU
B‴ AzGmKOcKitBrdU
3dpi
B cTnnISytox Merge
C′ AzGmKO
C″ cKitBrdU
C‴ AzGmKOcKitBrdU
7dpi
C cTnnISytox Merge
D
% CM Nuclei
P90
3dpi
7dpi
14dpi
21dpi
28dpi
* G0 # G1 $ S/G2/M
E
% CM Nuclei
G1/S

Figure 2.12. Amplifying progenitors express AzG *in vivo*. Representative images of early postnatal development tissue sections P2 (A) and P7 (B, C) respectively, showing native fluorescence of AzG=green, mKO=red, and immunolabeling for ckit=cyan, pHH3=magenta, sytox=white and tropomyosin=blue, scale bar 25μm. Yellow arrow shows c-kit^{+}/AzG^{+}/pHH3^{+} amplifying cardiac progenitor in P2 cardiac sections (A), and AzG^{+}/cTnI^{+} immature cardiomyocyte in P7 section (C).

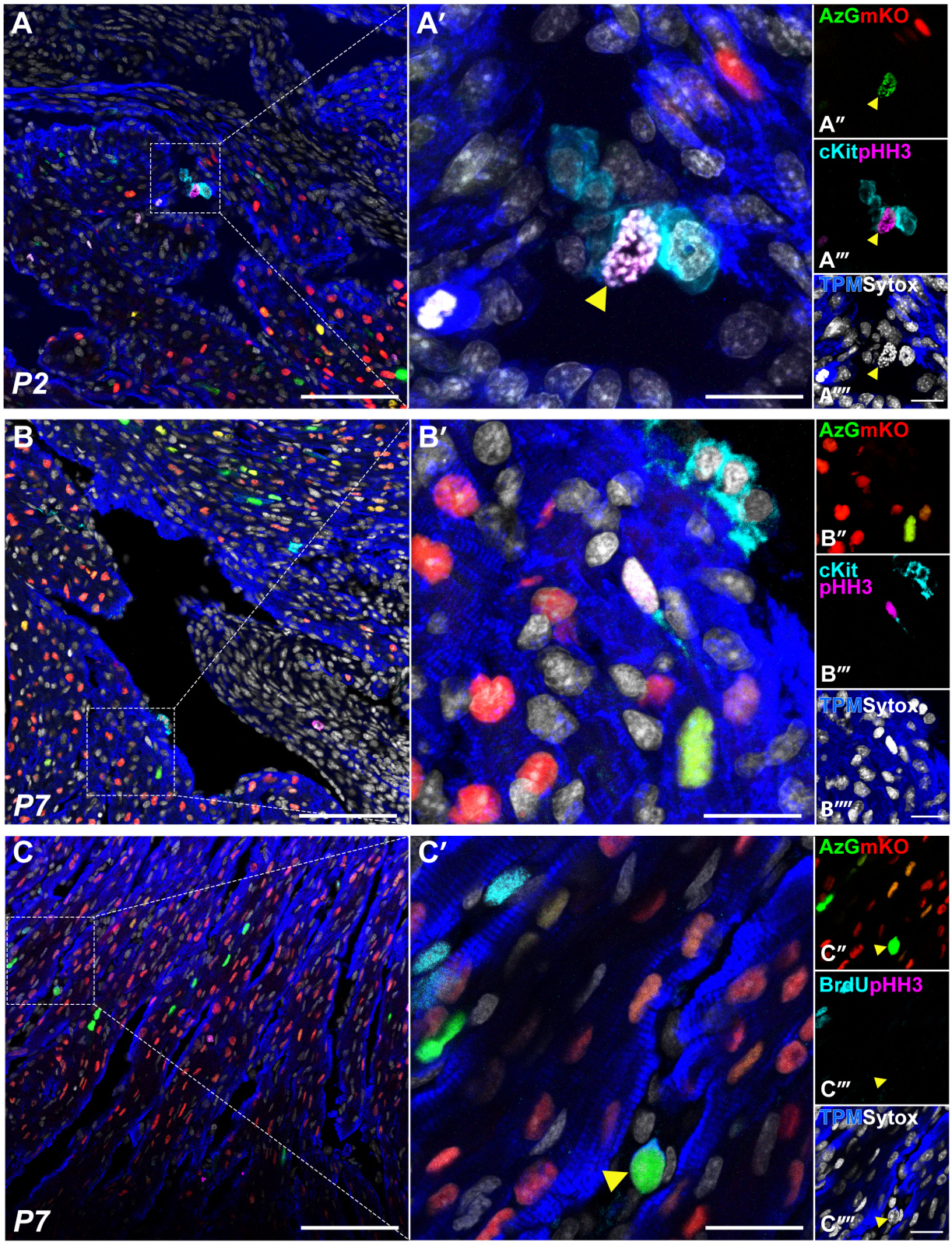
A
A′
AzGmKO
A″
cKitpHH3
A‴
TPMSytox
A⁗
P2
B
B′
AzGmKO
B″
cKit
pHH3
B‴
TPMSytox
B⁗
P7
C
C′
AzGmKO
C″
BrdUpHH3
C‴
TPMSytox
C⁗
P7

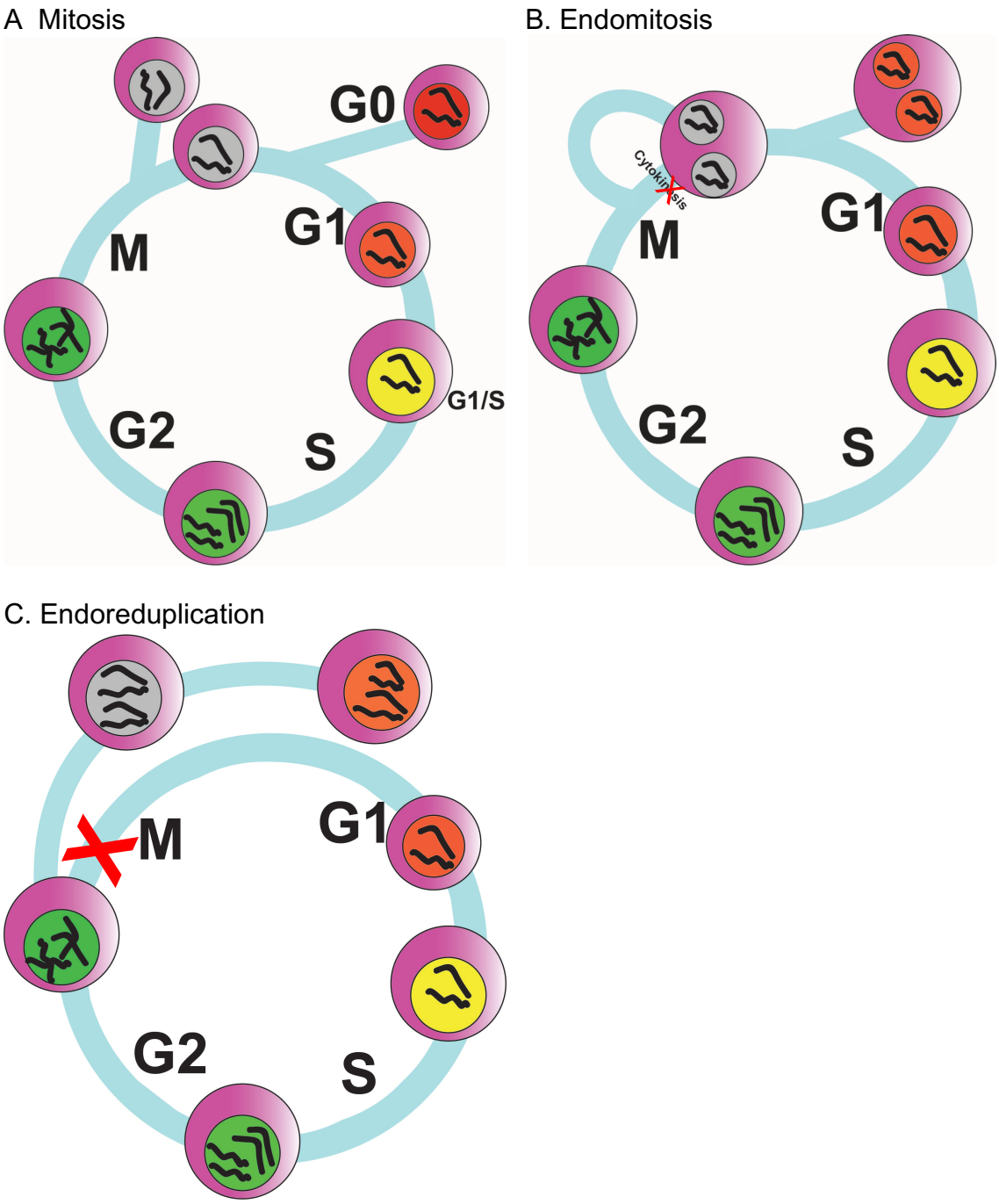

Figure 2.13. αMHC FUCCI myocyte cell cycle observations. A) Normal mitosis B) Endomitosis, C) Endoreduplication as observed in Figure 2.2.

Chapter 2, in full, is prepared for submission. I would like to thank all the co-authors who contributed to this work; Bingyan J. Wang, Natalie Gude, Fareheh Firouzi, David Ebeid, and Mark Sussman. Thank you all for your participation. The dissertation author was the primary author and investigator of this manuscript.

CHAPTER 3

CONCLUSION OF THE DISSERTATION

The heart has long been considered a post mitotic organ incapable of regeneration after injury[143]. As such, methods to stimulate proliferation in post-mitotic cardiomyocytes have looked for ways to increase *de novo* cardiomyocyte formation. Resident cardiac progenitor cells and existing cardiomyocyte reentry into the cell cycle to generate *de novo* cardiomyocytes after acute myocardial injury is still a hotly contested matter of investigation[97]. During the 1990s a plethora of studies concentrated their efforts to forcing reactivation of the postnatal cardiomyocyte cell cycle with little success[8, 22, 33, 103]. By the early 2000s cardiac regeneration and repair in the form of resident cardiac progenitor cells peaked as a potential source of new myocyte formation[7, 117, 156]. However, cardiac progenitors as a viable source of *de novo* cardiomyogenesis has recently come under severe scrutiny due to the limited regenerative effects obtained using these cells[101, 120]. Recent reports have reopened investigation into cardiomyocyte driven regeneration arising from existing myocytes[47, 54, 55, 97]. Interestingly, the use of neonatal injury models showing cardiomyocyte proliferation are utilized as proof of concept[47, 51, 55, 157, 158] for adult cardiomyocyte regenerative potential. These studies circle back to the underlying issue: how do you get cardiomyocytes to proliferate? Buried deep within this question is a lack of understanding of the postnatal cardiomyocyte cell cycle. As such, the focus of this dissertation is to elucidate the validity of commonly used markers for proliferation to adequately identify *de novo* cardiomyogenesis after injury and to provide insight into the cardiomyocyte cell cycle using a cardiomyocyte specific FUCCI reporter model. Improved knowledge of the perceived terminal differentiation state allows future studies to focus on methods necessary to push past the current cell cycle block experienced by

the majority of cardiomyocytes and provide insight necessary to close the existing knowledge gap preventing cardiomyocyte division necessary to regenerate the damaged myocardium.

Cardiomyocytes proliferative potential is high in embryonic development but is lost shortly before birth. Embryonic cardiomyocyte cell cycle activity is highest between E10.5 to E12.5[14]. A limited number of cardiomyocytes retain the ability to actively progress through the cell cycle shortly after birth reaching levels as high as 19% which diminish to less than 4% by P21 (Figure 2.3, 2.5). This finding is in concert with reports citing mononucleated myocytes as a potential source of proliferating myocytes after birth[50] which show inherent variability dependent on strain. This dissertation along with prior studies[107, 140], show that adult cardiomyocytes predominantly fail to progress through the perceived cell cycle block, defined as the G1/S interface, after induced injury (Figure 2.7, 2.11). Thus, re-activating proliferation in cardiomyocytes to replace the lost myocardium is an ongoing research strategy to preserve cardiac function and prevent remodeling following pathologic challenge.

In an effort to re-activate proliferation, mitogenic genes have been utilized to induce cardiomyocyte growth and proliferation following injury, targeting overexpression in a cardiac specific manner. Pro-survival genes such as Myc, AKT, Pim1, IGF-1, TERT, and YAP1 have all been shown to induce DNA synthesis when overexpressed in cardiac specific models[22, 159-161]. Unfortunately, the effects perceived as existing cardiomyocyte proliferation fail to unequivocally show *de novo* cardiomyocyte formation, relying heavily on markers of DNA synthesis (BrdU, PCNA, Ki67) and/or mitotic markers (pHH3 and Aurora Kinase B). However, these markers have also been utilized to show DNA

damage response after injury and cells in G2 phase[120, 162] and could account for the presence of these markers after injury. The lack of *de novo* cardiomyocyte formation is further corroborated by the modest effects observed in the level of myocardial regeneration; insufficient to ameliorate conditions long term. Interestingly, these pro-survival genes share one commonality targeting specific aspects of the cell cycle machinery, primarily G1 phase genes Cyclin D and Cdk4/6[163-165]. Stimulating postnatal cardiomyocyte cell cycle reentry using cell cycle machinery genes, specifically Cyclin D isoforms and kinase Cdk4/6, has also been attempted.

Cardiomyocyte specific overexpression of Cyclin D isoforms[23, 103, 166] have been shown to increase the rate of DNA synthesis under normal conditions. After injury, Cyclin D overexpression in cardiomyocytes show an increase in DNA synthesis and increased mitotic events, evidenced by increased immunolabeling of BrdU and/or pHH3[23, 166]. *De novo* cardiomyocyte formation is not discernable in these models, but the regressed remodeling observed makes this a plausible speculation. The reported increases in DNA synthesis may be attributed to a shortened G1 phase regulated in part by Cyclin D[23, 30, 103, 166].

Additionally, targeting the G1 phase of the cell cycle by Cyclin D overexpression allows for the activation of cells in G0 (quiescent)[150]. Elevated levels of Cyclin D-Cdk4/6 complex phosphorylates Rb, freeing E2F transcription factor for progressive cell cycle signaling. A small cohort of mononucleated cardiomyocytes resident to the postnatal myocardium have been reported[10, 50]. This subset of cardiomyocytes is shown to be smaller, exhibit an immature phenotype and presumed responsible for *de novo* cardiomyocyte formation[10, 94]. It is conceivable that targeting the G1 phase of the cell

cycle in turn activates this small population of mononucleated myocytes. In fact, recent studies show Cyclin D1/Cdk4 overexpression results in a 20% increase of cardiomyocyte proliferation[149]; the same number of mononucleated cells postulated to reside within the mouse myocyardium[10, 149]. However, the majority of postnatal cardiomyocytes are poised at the G1/S interface (Figure 2.3, 2.5) and Cyclin D overexpression may be insufficient to achieve the robust *de novo* cardiomyocyte formation necessary for regeneration after injury.

Interestingly, cardiomyocyte specific Cyclin A overexpression has also been attempted[24, 49] resulting in comparable outcomes as cardiomyocyte specific Cyclin D overexpression. Indeed, studies involved in cyclin A overexpression have demonstrated elevated levels of DNA synthesis and mitotic events, evidenced by increased proliferating cell nuclear antigen (PCNA) and pHH3 positive nuclei within the myocardium[5, 24, 49, 152]. Targeting the cell cycle S phase via Cyclin A stimulates reentry into S/G2 in cardiomyocytes[27]. However, pre-mature expression of CyclinA-Cdk2 complex may result in anomalous DNA synthesis due to a premature start[26, 27]. Altered downstream cell cycle activity may result in arrested cells in G2/M prior to karyokinesis and cytokinesis, still showing BrdU and pHH3 staining[167]. Cyclin A overexpression may induce cell cycle progression but fail to result in *de novo* cardiomyocyte formation in part due to the G1/S arrest of over 95% of adult cardiomyocytes by P21 (Figure 2.5). These two approaches, targeting the G1 and S phase of the cardiomyocyte cell cycle, fall short in re-activating the level of cardiomyocyte proliferation necessary to produce significant benefits.

Targeting other phases of the cell cycle, primarily G2/M phase has led to Cyclin B, Aurora kinase B and Cdk1 overexpression in a cardiomyocyte specific fashion in the postnatal heart[149, 168]. Postnatal cardiomyocyte cultures induced to express these genes resulted in mitotic catastrophe shortly after division as a result of dysregulated chromosome alignment[149]. Forced overexpression of G2/M phase cell cycle genes in cardiomyocyte specific fashion may result in premature alignment of chromosomes to the mitotic spindle and aberrant chromatin redistribution. Without DNA synthesis necessary to provide an exact copy of genes to the resulting daughter cells, aneuploidy is probable; increasing the chance of mitotic catastrophe[168, 169]. Thus, genes targeting G2/M phase of the cardiomyocyte cell cycle also fail to induce *de novo* cardiomyocyte formation.

The central dogma establishes cardiomyocytes as terminally differentiated cells that undergo a full mitotic “exit” shortly after birth. A “full mitotic exit” would presume cells exit and arrest in G0/G1 immediately following mitosis; this terminology may account for the number of studies that focus on mitotic stimulation of postnatal cardiomyocytes in an attempt to induce proliferation and ultimately, de novo cardiomyogenesis. Studies to stimulate cardiomyocyte cell cycle re-entry have focused their efforts in *de novo* cardiomyocyte formation by G1 and to a lesser extent, S/G2/M phase cyclin stimulation. Unfortunately, there has been a lack of focus on Cyclin E, the fourth major cyclin of the cell cycle machinery.

Cyclin E is activated in late G1, in part by Cyclin D-Cdk4/6 phosphorylation of Rb[25, 26, 30, 103]. It has been suggested that the primary role of Cyclin D is to activate Cyclin E[170]. So why has Cyclin E been overlooked? The answer may lie in prior experimental

observations regarding global Cyclin E ablation. Ablation of Cyclin E in the mouse model failed to produce embryonic lethal phenotypes[35]. As a result of these observations, this cyclin has been overlooked in its role during cell cycle progression. Nonetheless Cyclin E, together with Cdk2, is responsible for transitioning a cell from growth to synthesis, G1 to S phase.

This dissertation shows the majority of cardiomyocytes arrest at the G1/S transition[59, 112]; shown by the accumulation of mKO (orange) and AzGr (green) fluorescence (Figure 2.3). Double fluorescent nuclei in cardiomyocytes strengthen this observation and make a case against terminal differentiation or cell cycle exit at G0 or G1. Successful progression from G1 to S phase requires the activation of E2F transcription factor. E2F is necessary to activate Cyclin E in late G1 phase. E2F overexpression in cardiomyocytes has been shown to induce proliferation of arrested cells[33, 171], primarily by activating Cyclin E, forcing progression of cardiomyocytes through the G1/S transition. Furthermore, Cyclin E targets the Cdk2 suppressor p27. Cdk2 is necessary for progression through S phase. Taken together, these observations and the findings within this dissertation elucidate the understanding of the existing cardiomyocyte cell cycle fate, G1/S and place a focus on Cyclin E (Figure 3.1). Given this new information, prior studies regarding G1 and S phase stimulation now fall into place; lack of amelioration and unequivocal *de novo* myocyte formation comes into focus.

The FUCCI probes specific to cardiomyocytes express as intended, making this model ideal for the study of cell cycle dynamics in postnatal cardiomyocytes. To our knowledge, this is the first model that allows for the visualization of postnatal cardiac

myocytes in different phases of the cell cycle, particularly, G1 and S/G2/M after birth. The use of FUCCI to visualize the cell cycle in cardiomyocytes now allows us to identify the terminal differentiation state of cardiomyocytes. We now know cells arrest at the G1/S interface, unable to progress further. Manipulation of the G1/S interface will become the focus of future studies to induce cardiomyocyte proliferation *in vivo*. Additionally, we can utilize isolated cardiomyocytes *in vitro* to study effects on cardiomyocyte cell cycle progression induced by different stimuli (Figure 2.2). Furthermore, FUCCI allows the identification of cells in G0[68] and can now be unequivocally corroborated with mono-nucleated cells to test the postulate of mononuclear cardiomyocyte division. Moreover, single cell sequencing technology is gaining steam and affordability. This technology can be utilized to study the various cardiomyocyte populations within the myocardium to determine transcriptional differences between G0, G1/S and S/G2/M myocytes to further elucidate *de novo* cardiomyocyte formation in an effort to regenerate the heart after injury.

In conclusion, the creation of the FUCCI model described in this dissertation allows further insight into the cardiomyocyte cell cycle machinery. Future experiments will focus on forcing the transition from the G1/S interface through a full mitotic event, resulting in two functional daughter cells. However, it is plausible that even with new knowledge regarding the cell cycle arrest of postnatal cardiomyocytes, *de novo* cardiomyocyte formation to the extent necessary to ameliorate damage after cardiac injury may be an unattainable endeavor. This may require devising additional strategies involving all cyclins within the cell cycle machinery. Tactics to regulate forced cyclin

expression in a spatiotemporal fashion in all phases of the cell cycle may be a way to overcome the many checkpoints inherent in the cell cycle.

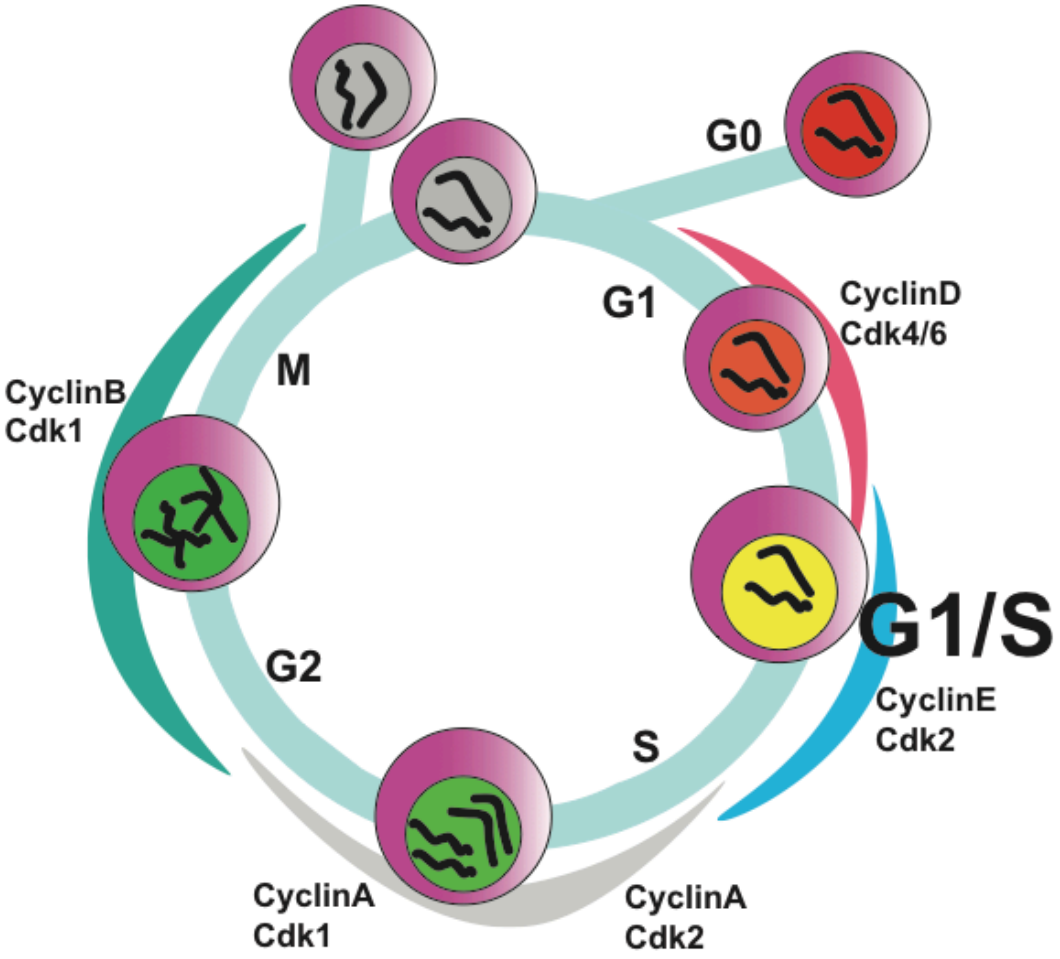

Figure 3.1. The Mammalian Cell Cycle; FUCCI and Cyclins. Gap1 (G1: mKO^{+}): Growth phase of a new cell. Cyclin D-Cdk4/6**.** G1-S ($mKO^{+}/AzGr^{+}$): Transition from Growth (G1) to Synthesis (S). Cyclin E-Cdk2. Synthesis (S: $AzGr^{+}$): DNA content is duplicated 2n→4n. Cyclin A-Cdk2. Gap 2 (G2: $AzGr^{+}$): DNA integrity check. Cyclin A-Cdk1. Mitosis (M: $AzGr^{+}$): Distribution of DNA and cytoplasmic contents to two daughter cells ($mKO^{-}/AzGr^{-}$) 4n→ 2n + 2n. CyclinB-Cdk1

REFERENCES

1. Benjamin EJ, Blaha MJ, Chiuve SE, Cushman M, Das SR, Deo R, de Ferranti SD, Floyd J, Fornage M, Gillespie C, Isasi CR, Jimenez MC, Jordan LC, Judd SE, Lackland D, Lichtman JH, Lisabeth L, Liu S, Longenecker CT, Mackey RH, Matsushita K, Mozaffarian D, Mussolino ME, Nasir K, Neumar RW, Palaniappan L, Pandey DK, Thiagarajan RR, Reeves MJ, Ritchey M, Rodriguez CJ, Roth GA, Rosamond WD, Sasson C, Towfighi A, Tsao CW, Turner MB, Virani SS, Voeks JH, Willey JZ, Wilkins JT, Wu JH, Alger HM, Wong SS, Muntner P, American Heart Association Statistics C and Stroke Statistics S. Heart Disease and Stroke Statistics-2017 Update: A Report From the American Heart Association. *Circulation*. 2017;135:e146-e603.

2. Benjamin EJ, Virani SS, Callaway CW, Chamberlain AM, Chang AR, Cheng S, Chiuve SE, Cushman M, Delling FN, Deo R, de Ferranti SD, Ferguson JF, Fornage M, Gillespie C, Isasi CR, Jimenez MC, Jordan LC, Judd SE, Lackland D, Lichtman JH, Lisabeth L, Liu S, Longenecker CT, Lutsey PL, Mackey JS, Matchar DB, Matsushita K, Mussolino ME, Nasir K, O'Flaherty M, Palaniappan LP, Pandey A, Pandey DK, Reeves MJ, Ritchey MD, Rodriguez CJ, Roth GA, Rosamond WD, Sampson UKA, Satou GM, Shah SH, Spartano NL, Tirschwell DL, Tsao CW, Voeks JH, Willey JZ, Wilkins JT, Wu JH, Alger HM, Wong SS, Muntner P, American Heart Association Council on E, Prevention Statistics C and Stroke Statistics S. Heart Disease and Stroke Statistics-2018 Update: A Report From the American Heart Association. *Circulation*. 2018;137:e67-e492.

3. Senyo SE, Steinhauser ML, Pizzimenti CL, Yang VK, Cai L, Wang M, Wu TD, Guerquin-Kern JL, Lechene CP and Lee RT. Mammalian heart renewal by pre-existing cardiomyocytes. *Nature*. 2013;493:433-6.

4. Malliaras K, Zhang Y, Seinfeld J, Galang G, Tseliou E, Cheng K, Sun B, Aminzadeh M and Marban E. Cardiomyocyte proliferation and progenitor cell recruitment underlie therapeutic regeneration after myocardial infarction in the adult mouse heart. *EMBO Mol Med*. 2013;5:191-209.

5. Cheng RK, Asai T, Tang H, Dashoush NH, Kara RJ, Costa KD, Naka Y, Wu EX, Wolgemuth DJ and Chaudhry HW. Cyclin A2 induces cardiac regeneration after myocardial infarction and prevents heart failure. *Circ Res*. 2007;100:1741-8.

6. Taniyama Y, Ito M, Sato K, Kuester C, Veit K, Tremp G, Liao R, Colucci WS, Ivashchenko Y, Walsh K and Shiojima I. Akt3 overexpression in the heart results in progression from adaptive to maladaptive hypertrophy. *J Mol Cell Cardiol*. 2005;38:375-85.

7. Beltrami AP, Barlucchi L, Torella D, Baker M, Limana F, Chimenti S, Kasahara H, Rota M, Musso E, Urbanek K, Leri A, Kajstura J, Nadal-Ginard B and Anversa

P. Adult cardiac stem cells are multipotent and support myocardial regeneration. *Cell*. 2003;114:763-76.

8. Reiss K, Cheng W, Ferber A, Kajstura J, Li P, Li B, Olivetti G, Homcy CJ, Baserga R and Anversa P. Overexpression of insulin-like growth factor-1 in the heart is coupled with myocyte proliferation in transgenic mice. *Proc Natl Acad Sci U S A*. 1996;93:8630-5.

9. Soonpaa MH, Kim KK, Pajak L, Franklin M and Field LJ. Cardiomyocyte DNA synthesis and binucleation during murine development. *Am J Physiol*. 1996;271:H2183-9.

10. Paradis AN, Gay MS and Zhang L. Binucleation of cardiomyocytes: the transition from a proliferative to a terminally differentiated state. *Drug Discov Today*. 2014;19:602-9.

11. Zebrowski DC and Engel FB. The cardiomyocyte cell cycle in hypertrophy, tissue homeostasis, and regeneration. *Rev Physiol Biochem Pharmacol*. 2013;165:67-96.

12. Leone M, Magadum A and Engel FB. Cardiomyocyte proliferation in cardiac development and regeneration: a guide to methodologies and interpretations. *Am J Physiol Heart Circ Physiol*. 2015;309:H1237-50.

13. Zebrowski DC, Becker R and Engel FB. Towards regenerating the mammalian heart: challenges in evaluating experimentally induced adult mammalian cardiomyocyte proliferation. *Am J Physiol Heart Circ Physiol*. 2016;310:H1045-54.

14. Ikenishi A, Okayama H, Iwamoto N, Yoshitome S, Tane S, Nakamura K, Obayashi T, Hayashi T and Takeuchi T. Cell cycle regulation in mouse heart during embryonic and postnatal stages. *Dev Growth Differ*. 2012;54:731-8.

15. Soonpaa MH and Field LJ. Assessment of cardiomyocyte DNA synthesis in normal and injured adult mouse hearts. *Am J Physiol*. 1997;272:H220-6.

16. Garbern JC and Lee RT. Cardiac stem cell therapy and the promise of heart regeneration. *Cell Stem Cell*. 2013;12:689-98.

17. Kajstura J, Gurusamy N, Ogorek B, Goichberg P, Clavo-Rondon C, Hosoda T, D'Amario D, Bardelli S, Beltrami AP, Cesselli D, Bussani R, del Monte F, Quaini F, Rota M, Beltrami CA, Buchholz BA, Leri A and Anversa P. Myocyte turnover in the aging human heart. *Circ Res*. 2010;107:1374-86.

18. Kajstura J, Rota M, Cappetta D, Ogorek B, Arranto C, Bai Y, Ferreira-Martins J, Signore S, Sanada F, Matsuda A, Kostyla J, Caballero MV, Fiorini C, D'Alessandro DA, Michler RE, del Monte F, Hosoda T, Perrella MA, Leri A, Buchholz BA, Loscalzo J and Anversa P. Cardiomyogenesis in the aging and failing human heart. *Circulation*. 2012;126:1869-81.

19. Walsh S, Ponten A, Fleischmann BK and Jovinge S. Cardiomyocyte cell cycle control and growth estimation in vivo--an analysis based on cardiomyocyte nuclei. *Cardiovasc Res*. 2010;86:365-73.

20. Condorelli G, Drusco A, Stassi G, Bellacosa A, Roncarati R, Iaccarino G, Russo MA, Gu Y, Dalton N, Chung C, Latronico MV, Napoli C, Sadoshima J, Croce CM and Ross J, Jr. Akt induces enhanced myocardial contractility and cell size in vivo in transgenic mice. *Proc Natl Acad Sci U S A*. 2002;99:12333-8.

21. Gude N, Muraski J, Rubio M, Kajstura J, Schaefer E, Anversa P and Sussman MA. Akt promotes increased cardiomyocyte cycling and expansion of the cardiac progenitor cell population. *Circ Res*. 2006;99:381-8.

22. Jackson T, Allard MF, Sreenan CM, Doss LK, Bishop SP and Swain JL. The c-myc proto-oncogene regulates cardiac development in transgenic mice. *Mol Cell Biol*. 1990;10:3709-16.

23. Pasumarthi KB, Nakajima H, Nakajima HO, Soonpaa MH and Field LJ. Targeted expression of cyclin D2 results in cardiomyocyte DNA synthesis and infarct regression in transgenic mice. *Circ Res*. 2005;96:110-8.

24. Chaudhry HW, Dashoush NH, Tang H, Zhang L, Wang X, Wu EX and Wolgemuth DJ. Cyclin A2 mediates cardiomyocyte mitosis in the postmitotic myocardium. *J Biol Chem*. 2004;279:35858-66.

25. Fu M, Wang C, Li Z, Sakamaki T and Pestell RG. Minireview: Cyclin D1: normal and abnormal functions. *Endocrinology*. 2004;145:5439-47.

26. Schafer KA. The cell cycle: a review. *Vet Pathol*. 1998;35:461-78.

27. Yam CH, Fung TK and Poon RY. Cyclin A in cell cycle control and cancer. *Cell Mol Life Sci*. 2002;59:1317-26.

28. Law ME, Corsino PE, Narayan S and Law BK. Cyclin-Dependent Kinase Inhibitors as Anticancer Therapeutics. *Mol Pharmacol*. 2015;88:846-52.

29. Tane S, Ikenishi A, Okayama H, Iwamoto N, Nakayama KI and Takeuchi T. CDK inhibitors, p21(Cip1) and p27(Kip1), participate in cell cycle exit of mammalian cardiomyocytes. *Biochem Biophys Res Commun*. 2014;443:1105-9.

30. Dong P, Zhang C, Parker BT, You L and Mathey-Prevot B. Cyclin D/CDK4/6 activity controls G1 length in mammalian cells. *PLoS One*. 2018;13:e0185637.

31. Barnum KJ and O'Connell MJ. Cell cycle regulation by checkpoints. *Methods Mol Biol*. 2014;1170:29-40.

32. Roccio M, Schmitter D, Knobloch M, Okawa Y, Sage D and Lutolf MP. Predicting stem cell fate changes by differential cell cycle progression patterns. *Development*. 2013;140:459-70.

33. Kirshenbaum LA, Abdellatif M, Chakraborty S and Schneider MD. Human E2F-1 reactivates cell cycle progression in ventricular myocytes and represses cardiac gene transcription. *Dev Biol*. 1996;179:402-11.

34. Parisi T, Beck AR, Rougier N, McNeil T, Lucian L, Werb Z and Amati B. Cyclins E1 and E2 are required for endoreplication in placental trophoblast giant cells. *EMBO J*. 2003;22:4794-803.

35. Geng Y, Yu Q, Sicinska E, Das M, Schneider JE, Bhattacharya S, Rideout WM, Bronson RT, Gardner H and Sicinski P. Cyclin E ablation in the mouse. *Cell*. 2003;114:431-43.

36. Sheaff RJ, Groudine M, Gordon M, Roberts JM and Clurman BE. Cyclin E-CDK2 is a regulator of p27Kip1. *Genes Dev*. 1997;11:1464-78.

37. Hwang HC and Clurman BE. Cyclin E in normal and neoplastic cell cycles. *Oncogene*. 2005;24:2776-86.

38. Gavet O and Pines J. Progressive activation of CyclinB1-Cdk1 coordinates entry to mitosis. *Dev Cell*. 2010;18:533-43.

39. Gavet O and Pines J. Activation of cyclin B1-Cdk1 synchronizes events in the nucleus and the cytoplasm at mitosis. *J Cell Biol*. 2010;189:247-59.

40. Ahuja P, Sdek P and MacLellan WR. Cardiac myocyte cell cycle control in development, disease, and regeneration. *Physiol Rev*. 2007;87:521-44.

41. Bergmann O, Zdunek S, Felker A, Salehpour M, Alkass K, Bernard S, Sjostrom SL, Szewczykowska M, Jackowska T, Dos Remedios C, Malm T, Andra M, Jashari R, Nyengaard JR, Possnert G, Jovinge S, Druid H and Frisen J. Dynamics of Cell Generation and Turnover in the Human Heart. *Cell*. 2015;161:1566-75.

42. Jopling C, Sleep E, Raya M, Marti M, Raya A and Izpisua Belmonte JC. Zebrafish heart regeneration occurs by cardiomyocyte dedifferentiation and proliferation. *Nature*. 2010;464:606-9.

43. Puente BN, Kimura W, Muralidhar SA, Moon J, Amatruda JF, Phelps KL, Grinsfelder D, Rothermel BA, Chen R, Garcia JA, Santos CX, Thet S, Mori E, Kinter MT, Rindler PM, Zacchigna S, Mukherjee S, Chen DJ, Mahmoud AI, Giacca M, Rabinovitch PS, Aroumougame A, Shah AM, Szweda LI and Sadek HA. The oxygen-rich postnatal environment induces cardiomyocyte cell-cycle arrest through DNA damage response. *Cell*. 2014;157:565-79.

44. Bryant DM, O'Meara CC, Ho NN, Gannon J, Cai L and Lee RT. A systematic analysis of neonatal mouse heart regeneration after apical resection. *J Mol Cell Cardiol*. 2015;79:315-8.

45. Darehzereshki A, Rubin N, Gamba L, Kim J, Fraser J, Huang Y, Billings J, Mohammadzadeh R, Wood J, Warburton D, Kaartinen V and Lien CL. Differential regenerative capacity of neonatal mouse hearts after cryoinjury. *Dev Biol*. 2015;399:91-9.

46. Sturzu AC, Rajarajan K, Passer D, Plonowska K, Riley A, Tan TC, Sharma A, Xu AF, Engels MC, Feistritzer R, Li G, Selig MK, Geissler R, Robertson KD, Scherrer-Crosbie M, Domian IJ and Wu SM. Fetal Mammalian Heart Generates a Robust Compensatory Response to Cell Loss. *Circulation*. 2015;132:109-21.

47. Polizzotti BD, Ganapathy B, Haubner BJ, Penninger JM and Kuhn B. A cryoinjury model in neonatal mice for cardiac translational and regeneration research. *Nat Protoc*. 2016;11:542-52.

48. Reuter S, Soonpaa MH, Firulli AB, Chang AN and Field LJ. Recombinant neuregulin 1 does not activate cardiomyocyte DNA synthesis in normal or infarcted adult mice. *PLoS One*. 2014;9:e115871.

49. Shapiro SD, Ranjan AK, Kawase Y, Cheng RK, Kara RJ, Bhattacharya R, Guzman-Martinez G, Sanz J, Garcia MJ and Chaudhry HW. Cyclin A2 induces cardiac regeneration after myocardial infarction through cytokinesis of adult cardiomyocytes. *Sci Transl Med*. 2014;6:224ra27.

50. Patterson M, Barske L, Van Handel B, Rau CD, Gan P, Sharma A, Parikh S, Denholtz M, Huang Y, Yamaguchi Y, Shen H, Allayee H, Crump JG, Force TI, Lien CL, Makita T, Lusis AJ, Kumar SR and Sucov HM. Frequency of mononuclear diploid cardiomyocytes underlies natural variation in heart regeneration. *Nat Genet*. 2017;49:1346-1353.

51. Mahmoud AI, Kocabas F, Muralidhar SA, Kimura W, Koura AS, Thet S, Porrello ER and Sadek HA. Meis1 regulates postnatal cardiomyocyte cell cycle arrest. *Nature*. 2013;497:249-253.

52. Soonpaa MH, Rubart M and Field LJ. Challenges measuring cardiomyocyte renewal. *Biochim Biophys Acta*. 2013;1833:799-803.

53. Engel FB, Schebesta M and Keating MT. Anillin localization defect in cardiomyocyte binucleation. *J Mol Cell Cardiol*. 2006;41:601-12.

54. Porrello ER, Mahmoud AI, Simpson E, Johnson BA, Grinsfelder D, Canseco D, Mammen PP, Rothermel BA, Olson EN and Sadek HA. Regulation of neonatal and adult mammalian heart regeneration by the miR-15 family. *Proc Natl Acad Sci U S A*. 2013;110:187-92.

55. Porrello ER and Olson EN. A neonatal blueprint for cardiac regeneration. *Stem Cell Res*. 2014;13:556-70.

56. Zebrowski DC, Vergarajauregui S, Wu CC, Piatkowski T, Becker R, Leone M, Hirth S, Ricciardi F, Falk N, Giessl A, Just S, Braun T, Weidinger G and Engel FB. Developmental alterations in centrosome integrity contribute to the post-mitotic state of mammalian cardiomyocytes. *Elife*. 2015;4.

57. Yuan X and Braun T. Multimodal Regulation of Cardiac Myocyte Proliferation. *Circ Res*. 2017;121:293-309.

58. Muskhelishvili L, Latendresse JR, Kodell RL and Henderson EB. Evaluation of cell proliferation in rat tissues with BrdU, PCNA, Ki-67(MIB-5) immunohistochemistry and in situ hybridization for histone mRNA. *J Histochem Cytochem*. 2003;51:1681-8.

59. Sakaue-Sawano A, Kurokawa H, Morimura T, Hanyu A, Hama H, Osawa H, Kashiwagi S, Fukami K, Miyata T, Miyoshi H, Imamura T, Ogawa M, Masai H and Miyawaki A. Visualizing spatiotemporal dynamics of multicellular cell-cycle progression. *Cell*. 2008;132:487-98.

60. Sakaue-Sawano A, Hoshida T, Yo M, Takahashi R, Ohtawa K, Arai T, Takahashi E, Noda S, Miyoshi H and Miyawaki A. Visualizing developmentally programmed endoreplication in mammals using ubiquitin oscillators. *Development*. 2013;140:4624-32.

61. Bouldin CM and Kimelman D. Dual fucci: a new transgenic line for studying the cell cycle from embryos to adults. *Zebrafish*. 2014;11:182-3.

62. Shirakawa J, Ezura Y, Moriya S, Kawasaki M, Yamada T, Notomi T, Nakamoto T, Hayata T, Miyawaki A, Omura K and Noda M. Migration linked to FUCCI-indicated cell cycle is controlled by PTH and mechanical stress. *J Cell Physiol*. 2014;229:1353-8.

63. Yano S, Li S, Han Q, Tan Y, Bouvet M, Fujiwara T and Hoffman RM. Selective methioninase-induced trap of cancer cells in S/G2 phase visualized by FUCCI imaging confers chemosensitivity. *Oncotarget*. 2014;5:8729-36.

64. Yano S, Miwa S, Mii S, Hiroshima Y, Uehara F, Yamamoto M, Kishimoto H, Tazawa H, Bouvet M, Fujiwara T and Hoffman RM. Invading cancer cells are predominantly in G0/G1 resulting in chemoresistance demonstrated by real-time FUCCI imaging. *Cell Cycle*. 2014;13:953-60.

65. Yo M, Sakaue-Sawano A, Noda S, Miyawaki A and Miyoshi H. Fucci-guided purification of hematopoietic stem cells with high repopulating activity. *Biochem Biophys Res Commun*. 2015;457:7-11.

66. Caillat C and Perrakis A. Cdt1 and geminin in DNA replication initiation. *Subcell Biochem*. 2012;62:71-87.

67. Xouri G, Dimaki M, Bastiaens PI and Lygerou Z. Cdt1 interactions in the licensing process: a model for dynamic spatiotemporal control of licensing. *Cell Cycle*. 2007;6:1549-52.

68. Tomura M, Sakaue-Sawano A, Mori Y, Takase-Utsugi M, Hata A, Ohtawa K, Kanagawa O and Miyawaki A. Contrasting quiescent G0 phase with mitotic cell cycling in the mouse immune system. *PLoS One*. 2013;8:e73801.

69. Honda-Uezono A, Kaida A, Michi Y, Harada K, Hayashi Y, Hayashi Y and Miura M. Unusual expression of red fluorescence at M phase induced by anti-microtubule agents in HeLa cells expressing the fluorescent ubiquitination-based cell cycle indicator (Fucci). *Biochem Biophys Res Commun*. 2012;428:224-9.

70. Nishitani H, Taraviras S, Lygerou Z and Nishimoto T. The human licensing factor for DNA replication Cdt1 accumulates in G1 and is destabilized after initiation of S-phase. *J Biol Chem*. 2001;276:44905-11.

71. Kaida A and Miura M. Visualizing the effect of hypoxia on fluorescence kinetics in living HeLa cells using the fluorescent ubiquitination-based cell cycle indicator (Fucci). *Exp Cell Res*. 2012;318:288-97.

72. Kaida A, Sawai N, Sakaguchi K and Miura M. Fluorescence kinetics in HeLa cells after treatment with cell cycle arrest inducers visualized with Fucci (fluorescent ubiquitination-based cell cycle indicator). *Cell Biol Int*. 2011;35:359-63.

73. Nakayama M, Kaida A, Deguchi S, Sakaguchi K and Miura M. Radiosensitivity of early and late M-phase HeLa cells isolated by a combination of fluorescent ubiquitination-based cell cycle indicator (Fucci) and mitotic shake-off. *Radiat Res*. 2011;176:407-11.

74. Sakaue-Sawano A, Kobayashi T, Ohtawa K and Miyawaki A. Drug-induced cell cycle modulation leading to cell-cycle arrest, nuclear mis-segregation, or endoreplication. *BMC Cell Biol*. 2011;12:2.

75. Choi WY, Gemberling M, Wang J, Holdway JE, Shen MC, Karlstrom RO and Poss KD. In vivo monitoring of cardiomyocyte proliferation to identify chemical modifiers of heart regeneration. *Development*. 2013;140:660-6.

76. Zielke N, Korzelius J, van Straaten M, Bender K, Schuhknecht GF, Dutta D, Xiang J and Edgar BA. Fly-FUCCI: A versatile tool for studying cell proliferation in complex tissues. *Cell Rep*. 2014;7:588-98.

77. Hoffman RM and Yano S. In Vivo-Like Cell-Cycle Phase Distribution of Cancer Cells in Gelfoam((R)) Histoculture Observed in Real Time by FUCCI Imaging. *Methods Mol Biol*. 2018;1760:109-123.

78. Tomura M. New Tools for Imaging of Immune Systems: Visualization of Cell Cycle, Cell Death, and Cell Movement by Using the Mice Lines Expressing Fucci, SCAT3.1, and Kaede and KikGR. *Methods Mol Biol*. 2018;1763:165-174.

79. Chicheportiche A, Ruat M, Boussin FD and Daynac M. Isolation of Neural Stem and Progenitor Cells from the Adult Brain and Live Imaging of Their Cell Cycle with the FUCCI System. *Methods Mol Biol*. 2018;1686:69-78.

80. Bechard ME, Bankaitis ED, Ustione A, Piston DW, Magnuson MA and Wright CVE. FUCCI tracking shows cell-cycle-dependent Neurog3 variation in pancreatic progenitors. *Genesis*. 2017;55.

81. Yano S, Takehara K, Tazawa H, Kishimoto H, Urata Y, Kagawa S, Fujiwara T and Hoffman RM. Cell-cycle-dependent drug-resistant quiescent cancer cells induce tumor angiogenesis after chemotherapy as visualized by real-time FUCCI imaging. *Cell Cycle*. 2017;16:406-414.

82. Yano S, Takehara K, Tazawa H, Kishimoto H, Urata Y, Kagawa S, Fujiwara T and Hoffman RM. Efficacy of a Cell-Cycle Decoying Killer Adenovirus on 3-D Gelfoam(R)-Histoculture and Tumor-Sphere Models of Chemo-Resistant Stomach Carcinomatosis Visualized by FUCCI Imaging. *PLoS One*. 2016;11:e0162991.

83. Wang D, Lu P, Liu Y, Chen L, Zhang R, Sui W, Dumitru AG, Chen X, Wen F, Ouyang HW and Ji J. Isolation of Live Premature Senescent Cells Using FUCCI Technology. *Sci Rep*. 2016;6:30705.

84. Prasedya ES, Miyake M, Kobayashi D and Hazama A. Carrageenan delays cell cycle progression in human cancer cells in vitro demonstrated by FUCCI imaging. *BMC Complement Altern Med*. 2016;16:270.

85. Yano S, Takehara K, Tazawa H, Kishimoto H, Urata Y, Kagawa S, Fujiwara T and Hoffman RM. Therapeutic Cell-Cycle-Decoy Efficacy of a Telomerase-Dependent Adenovirus in an Orthotopic Model of Chemotherapy-Resistant Human Stomach Carcinomatosis Peritonitis Visualized With FUCCI Imaging. *J Cell Biochem*. 2017;118:3635-3642.

86. Yano S, Takehara K, Zhao M, Tan Y, Han Q, Li S, Bouvet M, Fujiwara T and Hoffman RM. Tumor-specific cell-cycle decoy by Salmonella typhimurium A1-R combined with tumor-selective cell-cycle trap by methioninase overcome tumor intrinsic chemoresistance as visualized by FUCCI imaging. *Cell Cycle*. 2016;15:1715-23.

87. Saitou T and Imamura T. Quantitative imaging with Fucci and mathematics to uncover temporal dynamics of cell cycle progression. *Dev Growth Differ*. 2016;58:6-15.

88. Roccio M, Hahnewald S, Perny M and Senn P. Cell cycle reactivation of cochlear progenitor cells in neonatal FUCCI mice by a GSK3 small molecule inhibitor. *Sci Rep*. 2015;5:17886.

89. Goto T, Kaida A and Miura M. Visualizing cell-cycle kinetics after hypoxia/reoxygenation in HeLa cells expressing fluorescent ubiquitination-based cell cycle indicator (Fucci). *Exp Cell Res*. 2015;339:389-96.

90. Subramaniam A, Jones WK, Gulick J, Wert S, Neumann J and Robbins J. Tissue-specific regulation of the alpha-myosin heavy chain gene promoter in transgenic mice. *J Biol Chem*. 1991;266:24613-20.

91. Davis J, Maillet M, Miano JM and Molkentin JD. Lost in transgenesis: a user's guide for genetically manipulating the mouse in cardiac research. *Circ Res*. 2012;111:761-77.

92. Mollova M, Bersell K, Walsh S, Savla J, Das LT, Park SY, Silberstein LE, Dos Remedios CG, Graham D, Colan S and Kuhn B. Cardiomyocyte proliferation contributes to heart growth in young humans. *Proc Natl Acad Sci U S A*. 2013;110:1446-51.

93. Naqvi N, Li M, Calvert JW, Tejada T, Lambert JP, Wu J, Kesteven SH, Holman SR, Matsuda T, Lovelock JD, Howard WW, Iismaa SE, Chan AY, Crawford BH, Wagner MB, Martin DI, Lefer DJ, Graham RM and Husain A. A proliferative burst during preadolescence establishes the final cardiomyocyte number. *Cell*. 2014;157:795-807.

94. Senyo SE, Lee RT and Kuhn B. Cardiac regeneration based on mechanisms of cardiomyocyte proliferation and differentiation. *Stem Cell Res*. 2014;13:532-41.

95. Takeuchi T. Regulation of cardiomyocyte proliferation during development and regeneration. *Dev Growth Differ*. 2014;56:402-9.

96. Zhang Y, Mignone J and MacLellan WR. Cardiac Regeneration and Stem Cells. *Physiol Rev*. 2015;95:1189-204.

97. Eschenhagen T, Bolli R, Braun T, Field LJ, Fleischmann BK, Frisen J, Giacca M, Hare JM, Houser S, Lee RT, Marban E, Martin JF, Molkentin JD, Murry CE, Riley PR, Ruiz-Lozano P, Sadek HA, Sussman MA and Hill JA. Cardiomyocyte Regeneration: A Consensus Statement. *Circulation*. 2017;136:680-686.

98. Urbanek K, Quaini F, Tasca G, Torella D, Castaldo C, Nadal-Ginard B, Leri A, Kajstura J, Quaini E and Anversa P. Intense myocyte formation from cardiac stem cells in human cardiac hypertrophy. *Proc Natl Acad Sci U S A*. 2003;100:10440-5.

99. Angert D, Berretta RM, Kubo H, Zhang H, Chen X, Wang W, Ogorek B, Barbe M and Houser SR. Repair of the injured adult heart involves new myocytes potentially derived from resident cardiac stem cells. *Circ Res*. 2011;108:1226-37.

100. Mohsin S, Siddiqi S, Collins B and Sussman MA. Empowering adult stem cells for myocardial regeneration. *Circ Res*. 2011;109:1415-28.

101. Malliaras K and Terrovitis J. Cardiomyocyte proliferation vs progenitor cells in myocardial regeneration: The debate continues. *Glob Cardiol Sci Pract*. 2013;2013:303-15.

102. Oyama K, El-Nachef D and MacLellan WR. Regeneration potential of adult cardiac myocytes. *Cell Res*. 2013;23:978-9.

103. Soonpaa MH, Koh GY, Pajak L, Jing S, Wang H, Franklin MT, Kim KK and Field LJ. Cyclin D1 overexpression promotes cardiomyocyte DNA synthesis and multinucleation in transgenic mice. *J Clin Invest*. 1997;99:2644-54.

104. Tschen SI, Zeng C, Field L, Dhawan S, Bhushan A and Georgia S. Cyclin D2 is sufficient to drive beta cell self-renewal and regeneration. *Cell Cycle*. 2017;16:2183-2191.

105. Porrello ER, Mahmoud AI, Simpson E, Hill JA, Richardson JA, Olson EN and Sadek HA. Transient regenerative potential of the neonatal mouse heart. *Science*. 2011;331:1078-80.

106. Hashimoto H, Yuasa S, Tabata H, Tohyama S, Seki T, Egashira T, Hayashiji N, Hattori F, Kusumoto D, Kunitomi A, Takei M, Kashimura S, Yozu G, Shimojima M, Motoda C, Muraoka N, Nakajima K, Sakaue-Sawano A, Miyawaki A and Fukuda K. Analysis of cardiomyocyte movement in the developing murine heart. *Biochem Biophys Res Commun*. 2015;464:1000-7.

107. Hirai M, Chen J and Evans SM. Tissue-Specific Cell Cycle Indicator Reveals Unexpected Findings for Cardiac Myocyte Proliferation. *Circ Res*. 2016;118:20-8.

108. Siddiqi S and Sussman MA. The heart: mostly postmitotic or mostly premitotic? Myocyte cell cycle, senescence, and quiescence. *Can J Cardiol*. 2014;30:1270-8.

109. Mahmoud AI, Porrello ER, Kimura W, Olson EN and Sadek HA. Surgical models for cardiac regeneration in neonatal mice. *Nat Protoc*. 2014;9:305-11.

110. Fukuhara S, Zhang J, Yuge S, Ando K, Wakayama Y, Sakaue-Sawano A, Miyawaki A and Mochizuki N. Visualizing the cell-cycle progression of endothelial cells in zebrafish. *Dev Biol*. 2014;393:10-23.

111. Sakaue-Sawano A and Miyawaki A. Visualizing spatiotemporal dynamics of multicellular cell-cycle progressions with fucci technology. *Cold Spring Harb Protoc*. 2014;2014.

112. Newman RH and Zhang J. Fucci: street lights on the road to mitosis. *Chem Biol*. 2008;15:97-8.

113. Abe T, Sakaue-Sawano A, Kiyonari H, Shioi G, Inoue K, Horiuchi T, Nakao K, Miyawaki A, Aizawa S and Fujimori T. Visualization of cell cycle in mouse embryos with Fucci2 reporter directed by Rosa26 promoter. *Development*. 2013;140:237-46.

114. Mort RL, Ford MJ, Sakaue-Sawano A, Lindstrom NO, Casadio A, Douglas AT, Keighren MA, Hohenstein P, Miyawaki A and Jackson IJ. Fucci2a: a bicistronic cell cycle reporter that allows Cre mediated tissue specific expression in mice. *Cell Cycle*. 2014;13:2681-96.

115. Ng WA, Grupp IL, Subramaniam A and Robbins J. Cardiac myosin heavy chain mRNA expression and myocardial function in the mouse heart. *Circ Res*. 1991;68:1742-50.

116. Ehler E, Moore-Morris T and Lange S. Isolation and culture of neonatal mouse cardiomyocytes. *J Vis Exp*. 2013.

117. Fischer KM, Cottage CT, Wu W, Din S, Gude NA, Avitabile D, Quijada P, Collins BL, Fransioli J and Sussman MA. Enhancement of myocardial regeneration through genetic engineering of cardiac progenitor cells expressing Pim-1 kinase. *Circulation*. 2009;120:2077-87.

118. Hashimoto H, Yuasa S, Tabata H, Tohyama S, Hayashiji N, Hattori F, Muraoka N, Egashira T, Okata S, Yae K, Seki T, Nishiyama T, Nakajima K, Sakaue-Sawano A, Miyawaki A and Fukuda K. Time-lapse imaging of cell cycle dynamics during development in living cardiomyocyte. *J Mol Cell Cardiol*. 2014;72:241-9.

119. Weber TS, Jaehnert I, Schichor C, Or-Guil M and Carneiro J. Quantifying the length and variance of the eukaryotic cell cycle phases by a stochastic model and dual nucleoside pulse labelling. *PLoS Comput Biol*. 2014;10:e1003616.

120. Hendzel MJ, Wei Y, Mancini MA, Van Hooser A, Ranalli T, Brinkley BR, Bazett-Jones DP and Allis CD. Mitosis-specific phosphorylation of histone H3 initiates primarily within pericentromeric heterochromatin during G2 and spreads in an ordered fashion coincident with mitotic chromosome condensation. *Chromosoma*. 1997;106:348-60.

121. Van Hooser A, Goodrich DW, Allis CD, Brinkley BR and Mancini MA. Histone H3 phosphorylation is required for the initiation, but not maintenance, of mammalian chromosome condensation. *J Cell Sci*. 1998;111 (Pt 23):3497-506.

122. Zacchigna S and Giacca M. Extra- and intracellular factors regulating cardiomyocyte proliferation in postnatal life. *Cardiovasc Res*. 2014;102:312-20.

123. Sugiyama M, Sakaue-Sawano A, Iimura T, Fukami K, Kitaguchi T, Kawakami K, Okamoto H, Higashijima S and Miyawaki A. Illuminating cell-cycle progression in the developing zebrafish embryo. *Proc Natl Acad Sci U S A*. 2009;106:20812-7.

124. Abe T and Fujimori T. Reporter mouse lines for fluorescence imaging. *Dev Growth Differ*. 2013;55:390-405.

125. Crescenzi M, Soddu S and Tato F. Mitotic cycle reactivation in terminally differentiated cells by adenovirus infection. *J Cell Physiol*. 1995;162:26-35.

126. Li F, Wang X, Capasso JM and Gerdes AM. Rapid transition of cardiac myocytes from hyperplasia to hypertrophy during postnatal development. *J Mol Cell Cardiol*. 1996;28:1737-46.

127. Li F, Wang X, Bunger PC and Gerdes AM. Formation of binucleated cardiac myocytes in rat heart: I. Role of actin-myosin contractile ring. *J Mol Cell Cardiol*. 1997;29:1541-51.

128. Latella L, Sacco A, Pajalunga D, Tiainen M, Macera D, D'Angelo M, Felici A, Sacchi A and Crescenzi M. Reconstitution of cyclin D1-associated kinase activity drives terminally differentiated cells into the cell cycle. *Mol Cell Biol*. 2001;21:5631-43.

129. Keyomarsi K, Sandoval L, Band V and Pardee AB. Synchronization of tumor and normal cells from G1 to multiple cell cycles by lovastatin. *Cancer Res*. 1991;51:3602-9.

130. Rao S, Lowe M, Herliczek TW and Keyomarsi K. Lovastatin mediated G1 arrest in normal and tumor breast cells is through inhibition of CDK2 activity and redistribution of p21 and p27, independent of p53. *Oncogene*. 1998;17:2393-402.

131. Rao S, Porter DC, Chen X, Herliczek T, Lowe M and Keyomarsi K. Lovastatin-mediated G1 arrest is through inhibition of the proteasome, independent of hydroxymethyl glutaryl-CoA reductase. *Proc Natl Acad Sci U S A*. 1999;96:7797-802.

132. Borel F, Lacroix FB and Margolis RL. Prolonged arrest of mammalian cells at the G1/S boundary results in permanent S phase stasis. *J Cell Sci*. 2002;115:2829-38.

133. Li J, Chen W, Zhang P and Li N. Topoisomerase II trapping agent teniposide induces apoptosis and G2/M or S phase arrest of oral squamous cell carcinoma. *World J Surg Oncol*. 2006;4:41.

134. Watson PA, Hanauske-Abel HH, Flint A and Lalande M. Mimosine reversibly arrests cell cycle progression at the G1-S phase border. *Cytometry*. 1991;12:242-6.

135. Galgano PJ and Schildkraut CL. G1/S phase synchronization using mimosine arrest. *CSH Protoc*. 2006;2006.

136. Wallner M, Duran JM, Mohsin S, Troupes CD, Vanhoutte D, Borghetti G, Vagnozzi RJ, Gross P, Yu D, Trappanese DM, Kubo H, Toib A, Sharp TE, 3rd, Harper SC, Volkert MA, Starosta T, Feldsott EA, Berretta RM, Wang T, Barbe MF, Molkentin JD and Houser SR. Acute Catecholamine Exposure Causes

Reversible Myocyte Injury Without Cardiac Regeneration. *Circ Res*. 2016;119:865-79.

137. Saroff J and Wexler BC. Isoproterenol-induced myocardial infarction in rats. Distribution of corticosterone. *Circ Res*. 1970;27:1101-9.

138. Lobo Filho HG, Ferreira NL, Sousa RB, Carvalho ER, Lobo PL and Lobo Filho JG. Experimental model of myocardial infarction induced by isoproterenol in rats. *Rev Bras Cir Cardiovasc*. 2011;26:469-76.

139. Hesse M, Raulf A, Pilz GA, Haberlandt C, Klein AM, Jabs R, Zaehres H, Fugemann CJ, Zimmermann K, Trebicka J, Welz A, Pfeifer A, Roll W, Kotlikoff MI, Steinhauser C, Gotz M, Scholer HR and Fleischmann BK. Direct visualization of cell division using high-resolution imaging of M-phase of the cell cycle. *Nat Commun*. 2012;3:1076.

140. Quaife-Ryan GA, Sim CB, Ziemann M, Kaspi A, Rafehi H, Ramialison M, El-Osta A, Hudson JE and Porrello ER. Multicellular Transcriptional Analysis of Mammalian Heart Regeneration. *Circulation*. 2017;136:1123-1139.

141. Chong JJ and Murry CE. Cardiac regeneration using pluripotent stem cells--progression to large animal models. *Stem Cell Res*. 2014;13:654-65.

142. Sadek HA, Martin CM, Latif SS, Garry MG and Garry DJ. Bone-marrow-derived side population cells for myocardial regeneration. *J Cardiovasc Transl Res*. 2009;2:173-81.

143. Rumyantsev PP. Interrelations of the proliferation and differentiation processes during cardiact myogenesis and regeneration. *Int Rev Cytol*. 1977;51:186-273.

144. Pasumarthi KB and Field LJ. Cardiomyocyte cell cycle regulation. *Circ Res*. 2002;90:1044-54.

145. Sedmera D and Thompson RP. Myocyte proliferation in the developing heart. *Dev Dyn*. 2011;240:1322-34.

146. Blagosklonny MV and Pardee AB. The Restriction Point of the Cell Cycle. *Cell Cycle*. 2014;1:102-109.

147. Finkel T and Hwang PM. The Krebs cycle meets the cell cycle: mitochondria and the G1-S transition. *Proc Natl Acad Sci U S A*. 2009;106:11825-6.

148. Raulf A, Horder H, Tarnawski L, Geisen C, Ottersbach A, Roll W, Jovinge S, Fleischmann BK and Hesse M. Transgenic systems for unequivocal identification

of cardiac myocyte nuclei and analysis of cardiomyocyte cell cycle status. *Basic Res Cardiol*. 2015;110:33.

149. Mohamed TMA, Ang YS, Radzinsky E, Zhou P, Huang Y, Elfenbein A, Foley A, Magnitsky S and Srivastava D. Regulation of Cell Cycle to Stimulate Adult Cardiomyocyte Proliferation and Cardiac Regeneration. *Cell*. 2018;173:104-116 e12.

150. Ladha MH, Lee KY, Upton TM, Reed MF and Ewen ME. Regulation of exit from quiescence by p27 and cyclin D1-CDK4. *Mol Cell Biol*. 1998;18:6605-15.

151. Yang K, Hitomi M and Stacey DW. Variations in cyclin D1 levels through the cell cycle determine the proliferative fate of a cell. *Cell Div*. 2006;1:32.

152. Woo YJ, Panlilio CM, Cheng RK, Liao GP, Atluri P, Hsu VM, Cohen JE and Chaudhry HW. Therapeutic delivery of cyclin A2 induces myocardial regeneration and enhances cardiac function in ischemic heart failure. *Circulation*. 2006;114:I206-13.

153. Handa K, Yamakawa M, Takeda H, Kimura S and Takahashi T. Expression of cell cycle markers in colorectal carcinoma: superiority of cyclin A as an indicator of poor prognosis. *Int J Cancer*. 1999;84:225-33.

154. Zielke N, Edgar BA and DePamphilis ML. Endoreplication. *Cold Spring Harb Perspect Biol*. 2013;5:a012948.

155. Oki T, Nishimura K, Kitaura J, Togami K, Maehara A, Izawa K, Sakaue-Sawano A, Niida A, Miyano S, Aburatani H, Kiyonari H, Miyawaki A and Kitamura T. A novel cell-cycle-indicator, mVenus-p27K-, identifies quiescent cells and visualizes G0-G1 transition. *Sci Rep*. 2014;4:4012.

156. Leri A, Hosoda T, Rota M, Kajstura J and Anversa P. Myocardial Regeneration by Exogenous and Endogenous Progenitor Cells. *Drug Discov Today Dis Mech*. 2007;4:197-203.

157. Foglia MJ and Poss KD. Building and re-building the heart by cardiomyocyte proliferation. *Development*. 2016;143:729-40.

158. Smart N, Bollini S, Dube KN, Vieira JM, Zhou B, Davidson S, Yellon D, Riegler J, Price AN, Lythgoe MF, Pu WT and Riley PR. De novo cardiomyocytes from within the activated adult heart after injury. *Nature*. 2011;474:640-4.

159. Tsujita Y, Muraski J, Shiraishi I, Kato T, Kajstura J, Anversa P and Sussman MA. Nuclear targeting of Akt antagonizes aspects of cardiomyocyte hypertrophy. *Proc Natl Acad Sci U S A*. 2006;103:11946-51.

160. Zhou J. An emerging role for Hippo-YAP signaling in cardiovascular development. *J Biomed Res*. 2014;28:251-4.

161. Richardson GD, Breault D, Horrocks G, Cormack S, Hole N and Owens WA. Telomerase expression in the mammalian heart. *FASEB J*. 2012;26:4832-40.

162. Engel FB. Cardiomyocyte proliferation: a platform for mammalian cardiac repair. *Cell Cycle*. 2005;4:1360-3.

163. Shimura T, Noma N, Oikawa T, Ochiai Y, Kakuda S, Kuwahara Y, Takai Y, Takahashi A and Fukumoto M. Activation of the AKT/cyclin D1/Cdk4 survival signaling pathway in radioresistant cancer stem cells. *Oncogenesis*. 2012;1:e12.

164. Hong J, Lee JH and Chung IK. Telomerase activates transcription of cyclin D1 gene through an interaction with NOL1. *J Cell Sci*. 2016;129:1566-79.

165. von Gise A, Lin Z, Schlegelmilch K, Honor LB, Pan GM, Buck JN, Ma Q, Ishiwata T, Zhou B, Camargo FD and Pu WT. YAP1, the nuclear target of Hippo signaling, stimulates heart growth through cardiomyocyte proliferation but not hypertrophy. *Proc Natl Acad Sci U S A*. 2012;109:2394-9.

166. Tamamori-Adachi M, Takagi H, Hashimoto K, Goto K, Hidaka T, Koshimizu U, Yamada K, Goto I, Maejima Y, Isobe M, Nakayama KI, Inomata N and Kitajima S. Cardiomyocyte proliferation and protection against post-myocardial infarction heart failure by cyclin D1 and Skp2 ubiquitin ligase. *Cardiovasc Res*. 2008;80:181-90.

167. Nielsen PS, Riber-Hansen R, Jensen TO, Schmidt H and Steiniche T. Proliferation indices of phosphohistone H3 and Ki67: strong prognostic markers in a consecutive cohort with stage I/II melanoma. *Mod Pathol*. 2013;26:404-13.

168. Mc Gee MM. Targeting the Mitotic Catastrophe Signaling Pathway in Cancer. *Mediators Inflamm*. 2015;2015:146282.

169. Gonzalez-Loyola A, Fernandez-Miranda G, Trakala M, Partida D, Samejima K, Ogawa H, Canamero M, de Martino A, Martinez-Ramirez A, de Carcer G, Perez de Castro I, Earnshaw WC and Malumbres M. Aurora B Overexpression Causes Aneuploidy and p21Cip1 Repression during Tumor Development. *Mol Cell Biol*. 2015;35:3566-78.

170. Keenan SM, Lents NH and Baldassare JJ. Expression of cyclin E renders cyclin D-CDK4 dispensable for inactivation of the retinoblastoma tumor suppressor protein, activation of E2F, and G1-S phase progression. *J Biol Chem*. 2004;279:5387-96.

171. Ebelt H, Zhang Y, Kampke A, Xu J, Schlitt A, Buerke M, Muller-Werdan U, Werdan K and Braun T. E2F2 expression induces proliferation of terminally differentiated cardiomyocytes in vivo. *Cardiovasc Res*. 2008;80:219-26.